Supporting Information

Bisarylthiourea comprising cycloalkyl-thiophene-3-carboxylate derivatives as potential Human Toll-Like Receptor (TLR)2 Agonists: Design, Synthesis, and Structure–Activity Relationship Enabling the Switch from TLR2/1 to TLR2/6 Activation

Munugala Chandrakanth,[a] Yoshikazu Honda-Okubo,[b,c,d] Arya C G,[a] Deepak B. Salunke,[b,e,f] Nikolai Petrovsky,[b,c,d]* Janardhan Banothu[a]*

[a]Department of Chemistry, National Institute of Technology Calicut, Kozhikode – 673601, Kerala, India.

[b]National Interdisciplinary Centre of Vaccine, Immunotherapeutics and Antimicrobials (NICOVIA), Panjab University, Chandigarh - 160014, India.

[c]Vaxine Pty Ltd., 11 Walkley Avenue, Warradale, South Australia 5046, Australia.

[d]Australian Respiratory and Sleep Medicine Institute, Bedford Park, South Australia 5042, Australia.

[e]Department of Medicinal Chemistry, National Institute of Pharmaceutical Education and Research, Sector 67, S.A.S. Nagar, Mohali 160 062, Punjab, India.

[f]Department of Chemistry and Centre of Advanced Studies in Chemistry, Panjab University, Chandigarh - 160014, India.

Corresponding Authors:

***Dr. Janardhan Banothu**: Room No. 210(C), Department of Chemistry, NIT Calicut, Kozhikode, Kerala-673601, India, Email: janardhan@nitc.ac.in; ORCID: 0000-0002-2449-1647

***Dr. Nikolai Petrovsky**: Vaxine Pty Ltd, Warradale, South Australia 5046, Australia; Australian Respiratory and Sleep Medicine Institute, Bedford Park, South Australia 5042, Australia; National Interdisciplinary Centre of Vaccine, Immunotherapeutics and Antimicrobials (NICOVIA), Panjab University, Chandigarh-160014, India; Email: nikolai.petrovsky@vaxine.net

List of Contents

1. Single Crystal XRD Data

1.1. Single crystal preparation: Single crystals of compounds **8d** and **9f** suitable for X-ray crystallographic analysis were obtained using a slow evaporation technique. Each compound was dissolved in absolute ethanol at room temperature, and the solvent was allowed to evaporate gradually under ambient conditions. After 4–5 days, high-quality, defect-free, translucent rectangular crystals formed and were carefully isolated from the mother liquor. The crystals were immediately preserved in paraffin oil to maintain their integrity prior to single-crystal X-ray diffraction (SCXRD) studies.

***1.2. Single crystal X-ray diffraction studies*:** X-ray crystallographic measurements for **8d** and **9f** were conducted at 298 K using a Bruker D8 VENTURE diffractometer equipped with Mo(Kα) and Cu(Kα) microsource (λ = 0.7107 Å) and a PHOTON-100 CMOS detector. Data reduction and absorption correction were managed through the Bruker Apex 3 software suite.[1] Crystal structures were determined by intrinsic phasing, with final full-matrix least-squares refinements on F^2 executed using SHELXTL.[2] Molecular geometry and thermal ellipsoid plots were generated in ORTEP3,[3] and materials for publication were prepared using Mercury 3.8. Crystallographic data files (CIF) were submitted to the Cambridge Crystallographic Data Centre under accession numbers 2495663 for **8d** and 2495664 for **9f**. For **8d**, refinement included 4,476 variables and converged with R1 = 0.0473 for observed reflections, wR2 = 0.1233 for all data, a goodness-of-fit of 1.036, and 99.7% completeness. For **9f**, refinement over 4,394 variables yielded R1 = 0.0531, wR2 = 0.1555, a goodness-of-fit of 1.058, and 99.8% completeness.

***1.3. Crystal structure of compounds 8d and 9f*:** Single-crystal X-ray diffraction analysis demonstrated that compounds **8d** and **9f** crystallize in a triclinic crystal system with space group P-1, containing a single molecule in the asymmetric unit. The crystallographic parameters and refinement details are summarized in **Table 1**, while the ORTEP diagrams depicting the molecular structures are presented in **Figure 2**.

For compound **8d**, the crystallographic data indicate that the cyclopentyl-fused thiophene and ester moieties lie approximately in the same plane as the thiourea fragment, whereas the benzene ring deviates from this plane, showing non-coplanarity with the thiourea group. This spatial arrangement is confirmed by the torsion angles of S(1)−C(8)−N(1)−C(7) = 5.9(4)° and S(1)−C(8)−N(2)−C(9) = −174.11(19)°. The bond length C(8)−S(1) = 1.679(2) Å supports the presence of a characteristic C=S double bond, while the C(8)−N(1) = 1.349(3) Å and

C(8)−N(2) = 1.346(3) Å distances are consistent with C–N single bonds, collectively confirming the incorporation of a thiourea functionality. The morpholine ring in **8d** adopts a chair conformation, as evidenced by bond angles that fall within the expected range of 108–113°. Specifically, the measured bond angles include N(3)−C(15)−C(16) = 109.6(2)°, O(3)−C(16)−C(15) = 111.8(2)°, O(3)−C(17)−C(18) = 111.4(2)°, N(3)−C(18)−C(17) = 109.9(2)°, C(18)−N(3)−C(15) = 110.34(19)° and C(16)−O(3)−C(17) = 109.2(2)°, thereby confirming the stable chair geometry. The molecular conformation is stabilized by intramolecular hydrogen bonding of the type N—H•••O with parameters {d(H···A)/Å, d(D···A), <(DHA)/°: 1.96(2) Å, 2.677(2) Å, 142(2)°} interactions. The overall crystal packing is further reinforced by intermolecular N—H•••S hydrogen bonding with {d(H···A)/Å, d(D···A), <(DHA)/°: 2.521(18) Å, 3.3487(19) Å, 163(2)°}. The crystal packing features of **8d** along the crystallographic axes are illustrated in **Figure S1**.

In the case of **9f**, an analogous structural pattern to that of **8d** is observed, with only minor deviations in bond parameters and torsion angles. The crystal packing arrangement of **9f** along the three axes is shown in **Figure S2**.

These data can be obtained free of charge at www.ccdc.cam.ac.uk/conts/retrieving.html [or from the Cambridge Crystallographic Data Centre (CCDC), 12 Union Road, Cambridge CB2 1EZ, UK; fax: +44(0) 1223 336 033; email: deposit@ccdc.cam.ac.uk].

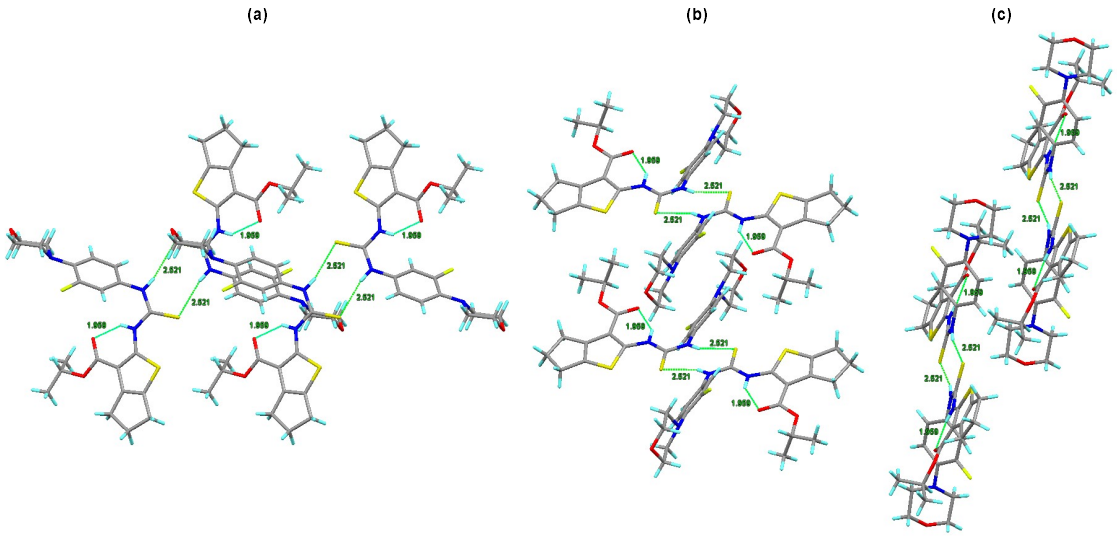

Figure S1. The overall crystal packing of compound **8d** along the a-axis (**a**), along the b-axis (**b**), and along the c-axis (**c**).

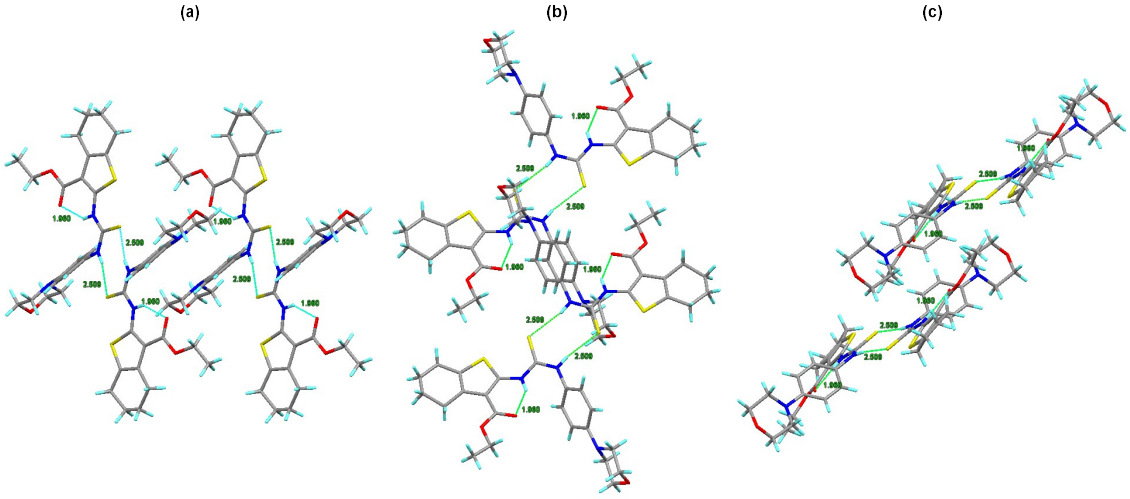

Figure S2. The overall crystal packing of compound **9f** along the a-axis (**a**), along the b-axis (**b**), and along the c-axis (**c**).

2. Spectral Characterization (HRMS, ^{1}H NMR, and ^{13}C NMR)

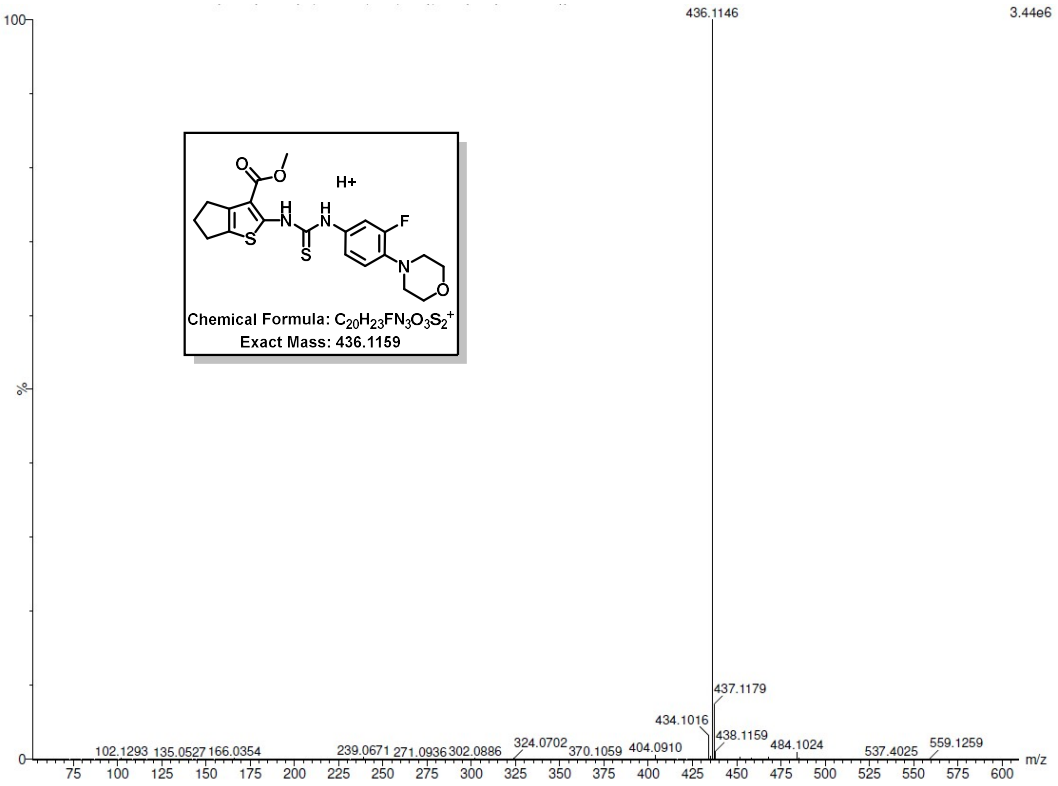

Figure S3. HRMS spectrum of **8a**.

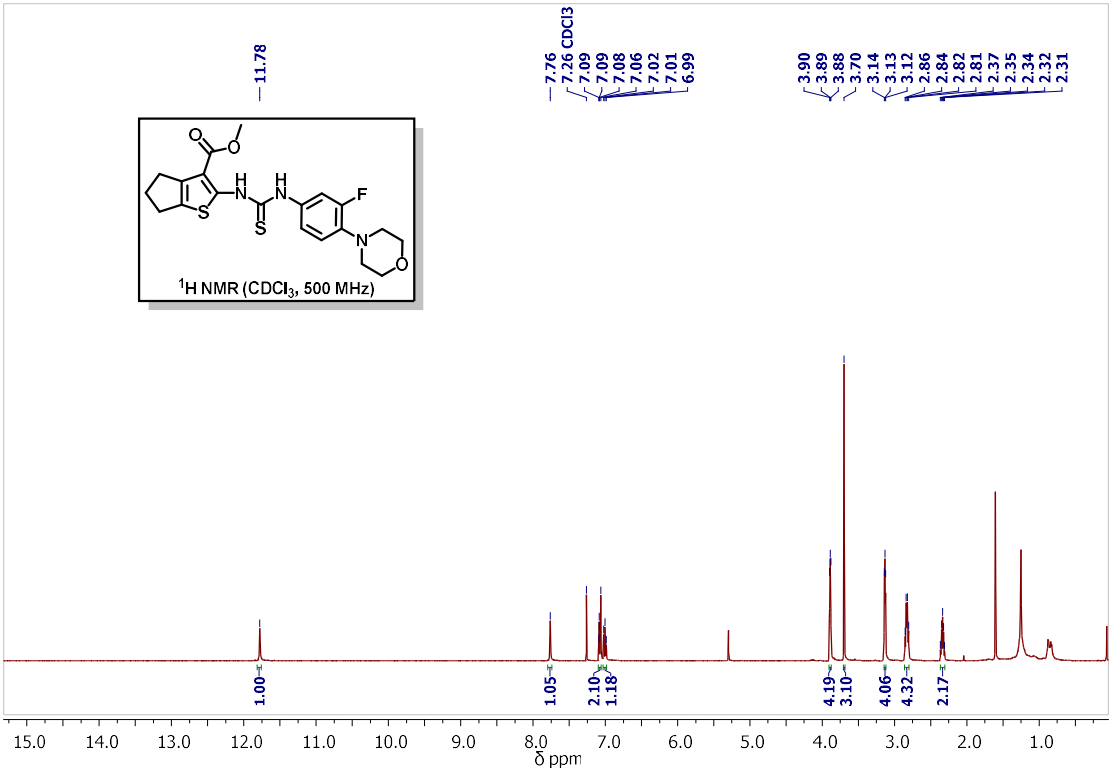

Figure S4. ^{1}H NMR spectra (500 MHz, RT) of compound **8a** in $CDCl_3$.

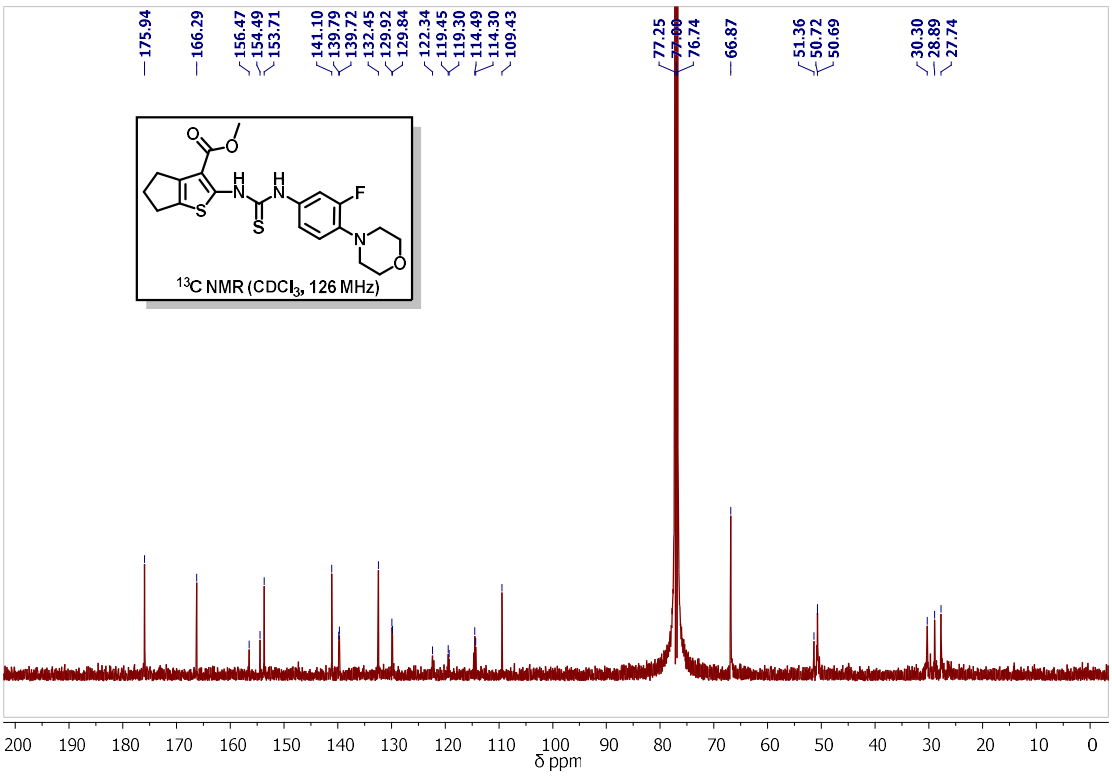

Figure S5. $^{13}C\{^{1}H\}$ NMR spectra (126 MHz, RT) of compound **8a** in $CDCl_3$.

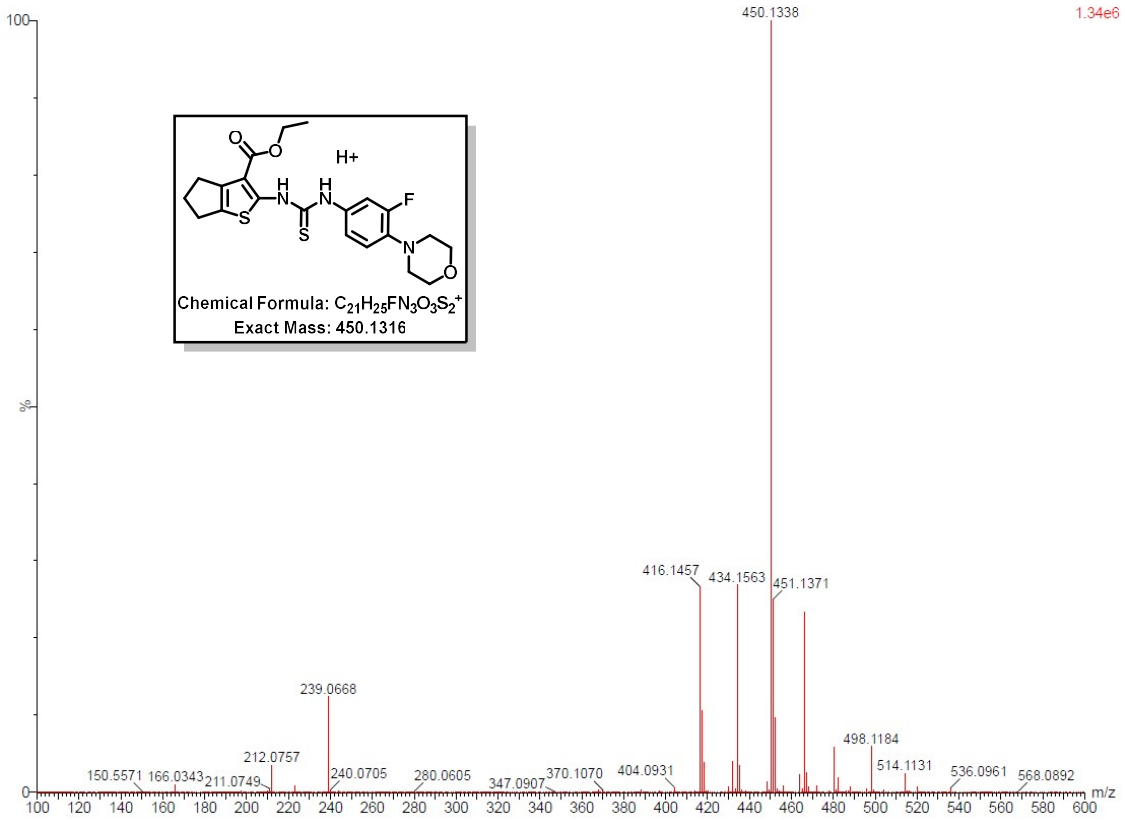

Figure S6. HRMS spectrum of **8b**.

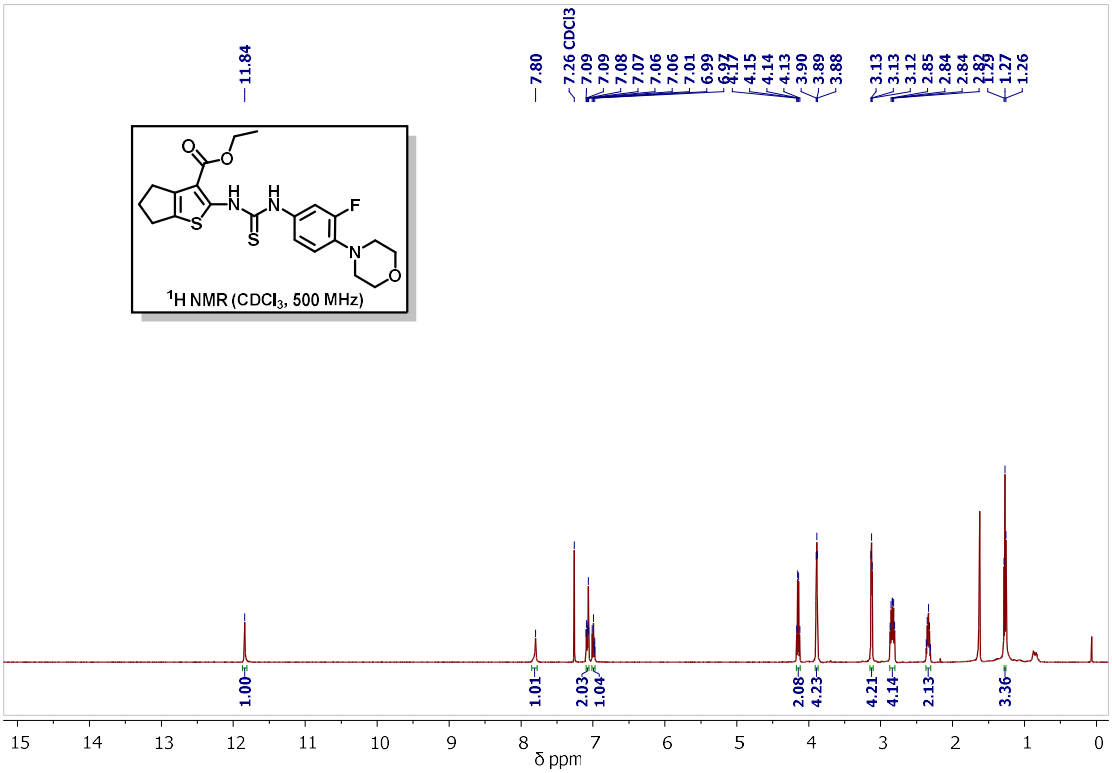

Figure S7. ^{1}H NMR spectra (500 MHz, RT) of compound **8b** in $CDCl_3$.

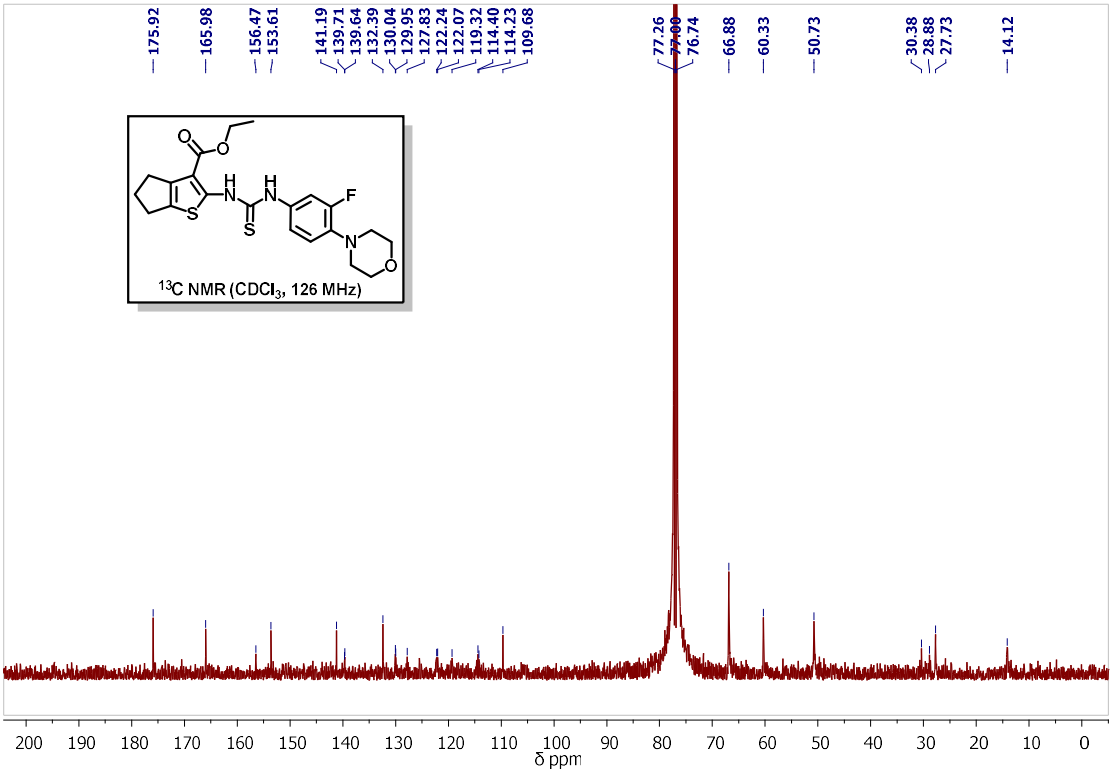

Figure S8. $^{13}C\{^{1}H\}$ NMR spectra (126 MHz, RT) of compound **8b** in $CDCl_3$.

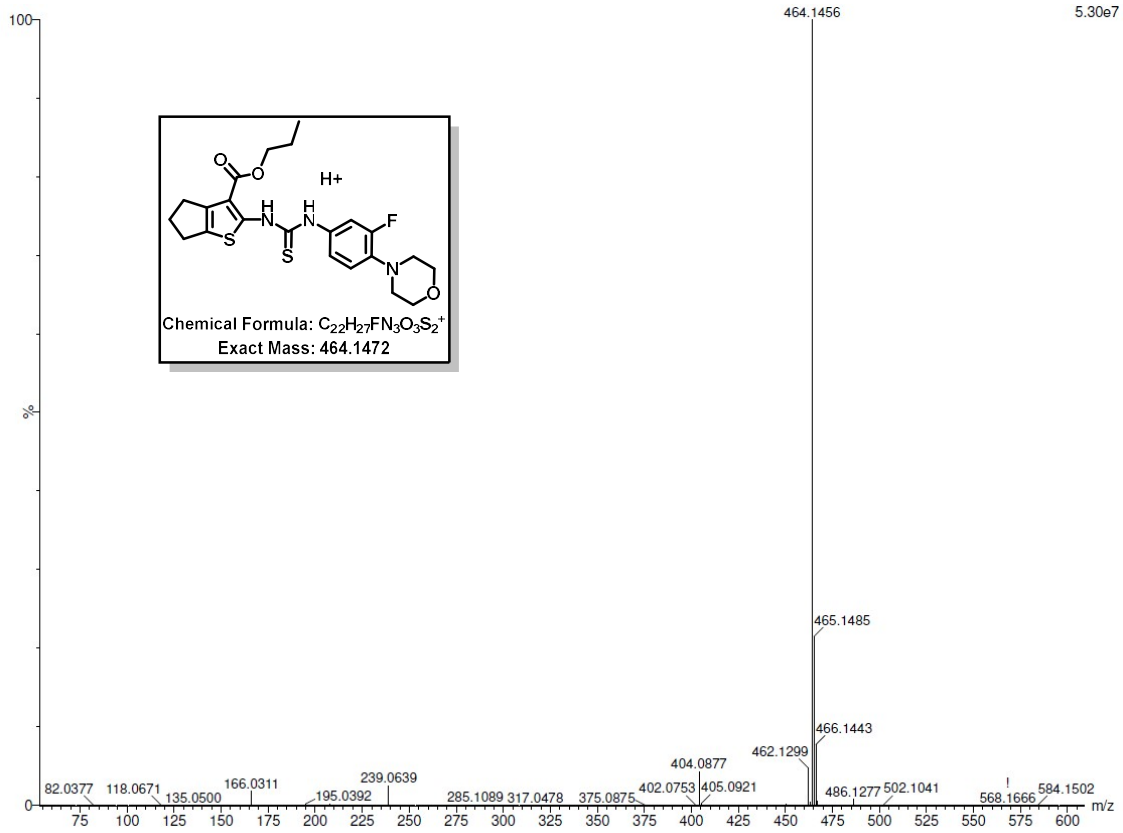

Figure S9. HRMS spectrum of **8c**.

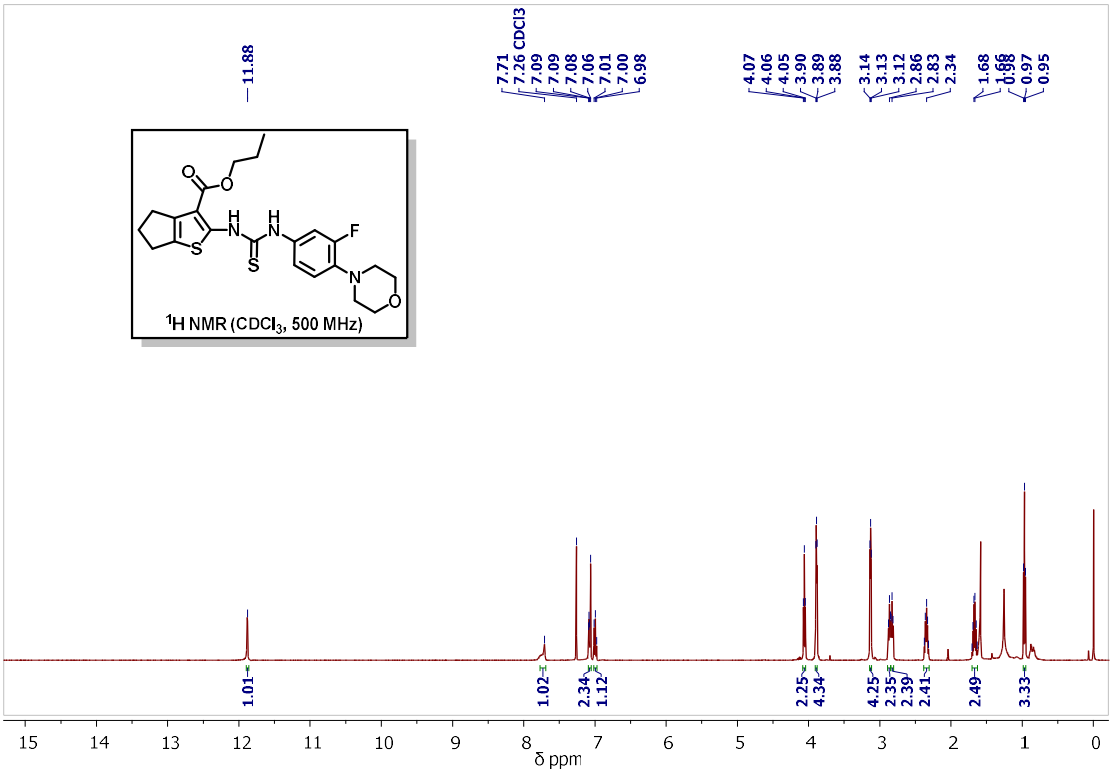

Figure S10. ^{1}H NMR spectra (500 MHz, RT) of compound **8c** in $CDCl_3$.

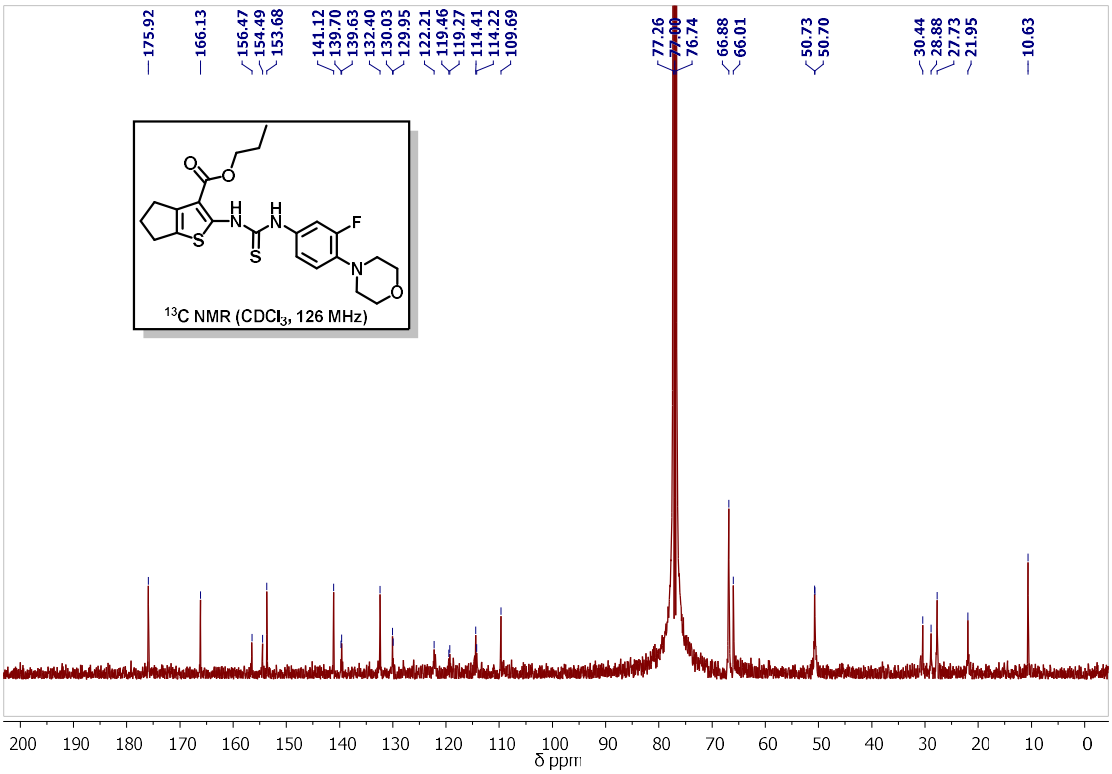

Figure S11. $^{13}C\{^{1}H\}$ NMR spectra (126 MHz, RT) of compound **8c** in $CDCl_3$.

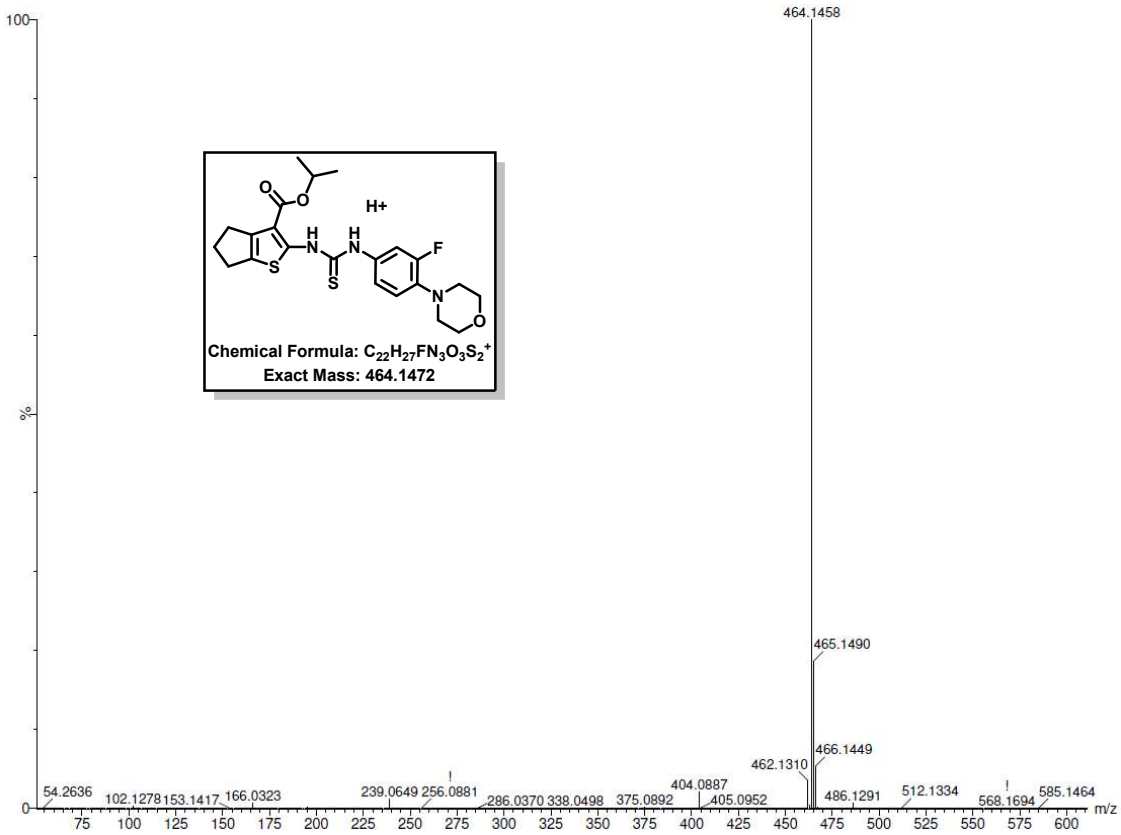

Figure S12. HRMS spectrum of **8d**.

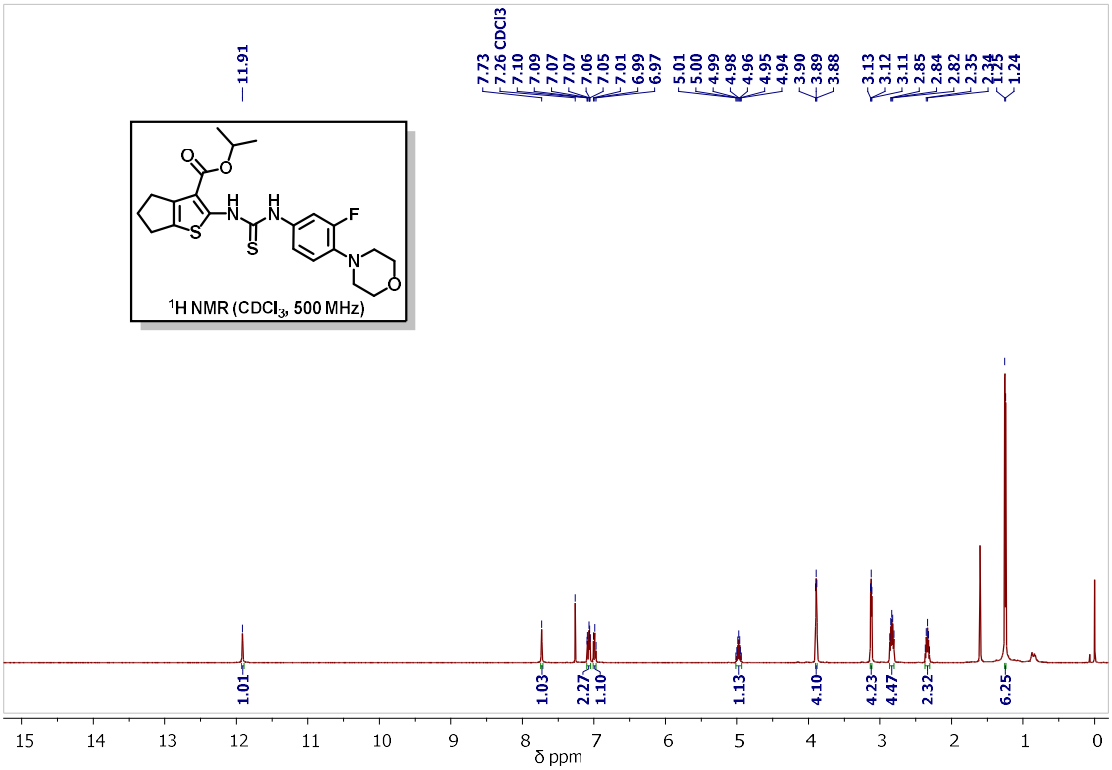

Figure S13. ^{1}H NMR spectra (500 MHz, RT) of compound **8d** in $CDCl_3$.

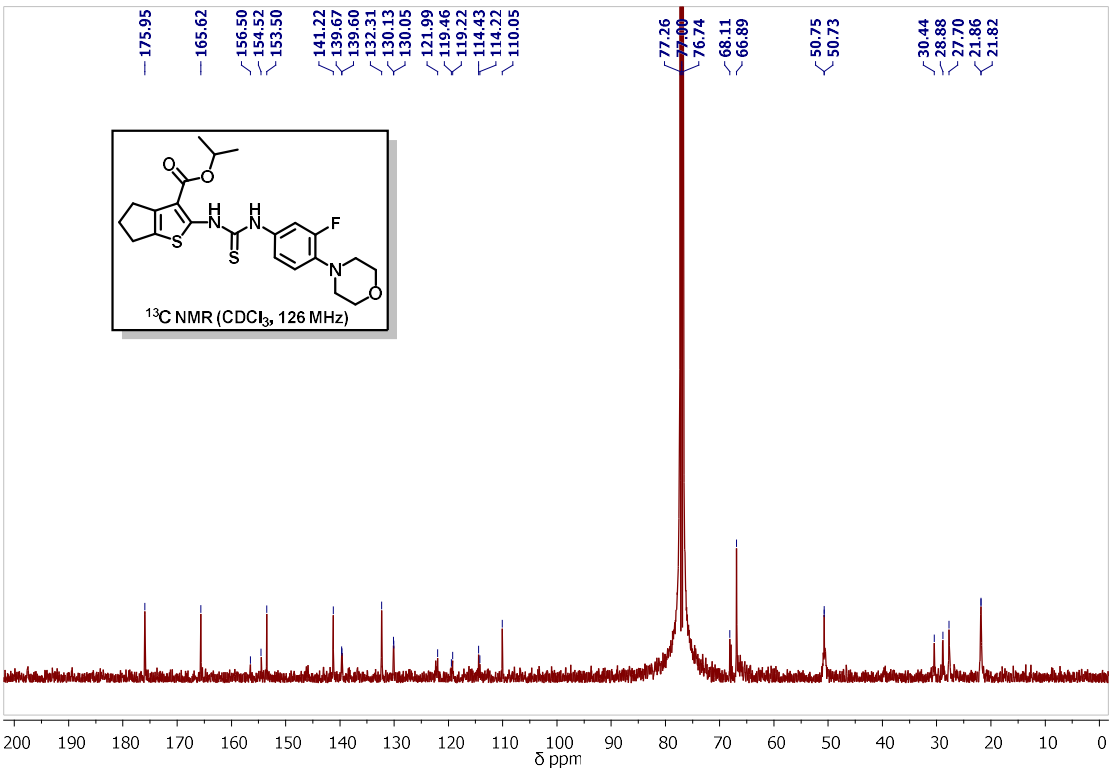

Figure S14. $^{13}C\{^{1}H\}$ NMR spectra (126 MHz, RT) of compound **8d** in $CDCl_3$.

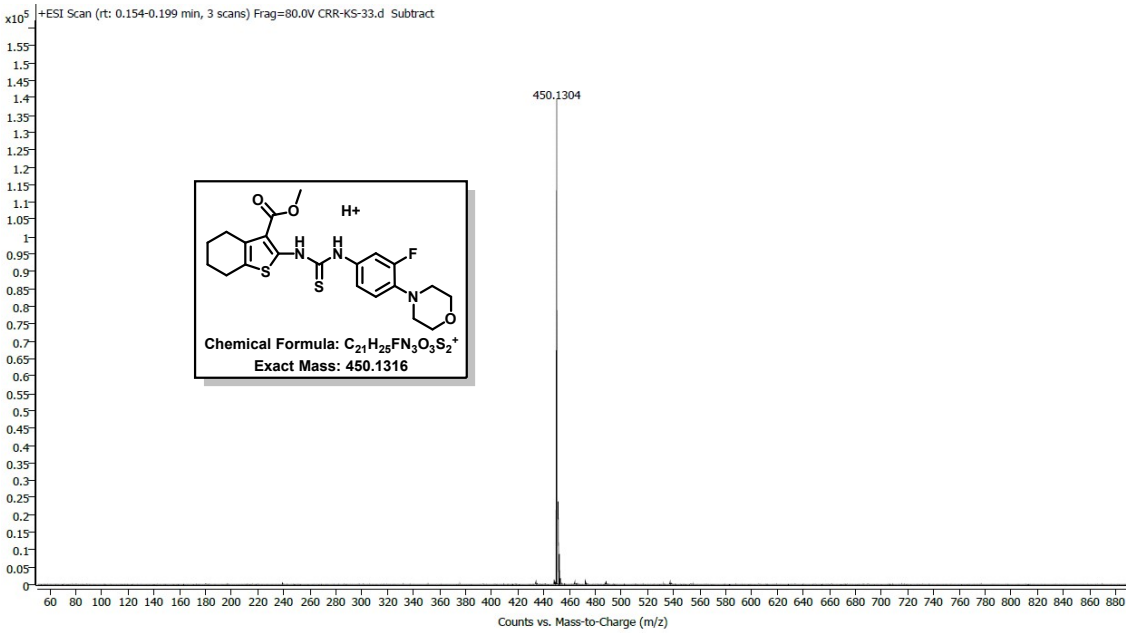

Figure S15. HRMS spectrum of **8e**.

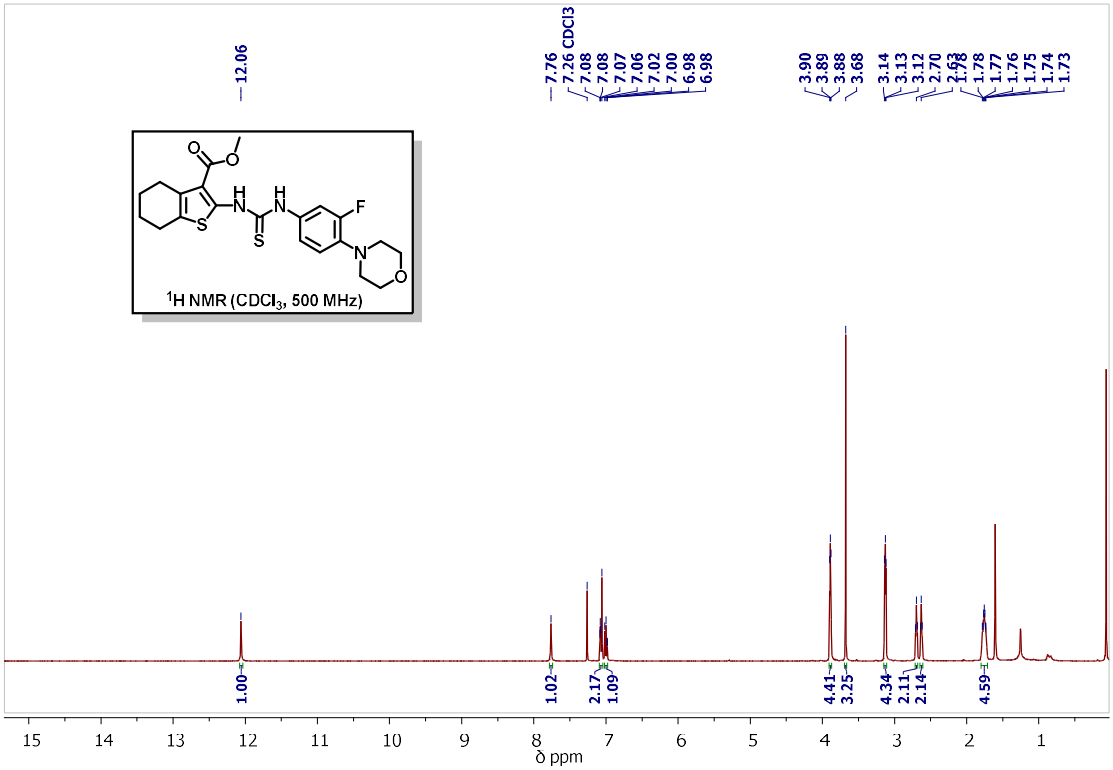

Figure S16. ^{1}H NMR spectra (500 MHz, RT) of compound **8e** in $CDCl_3$.

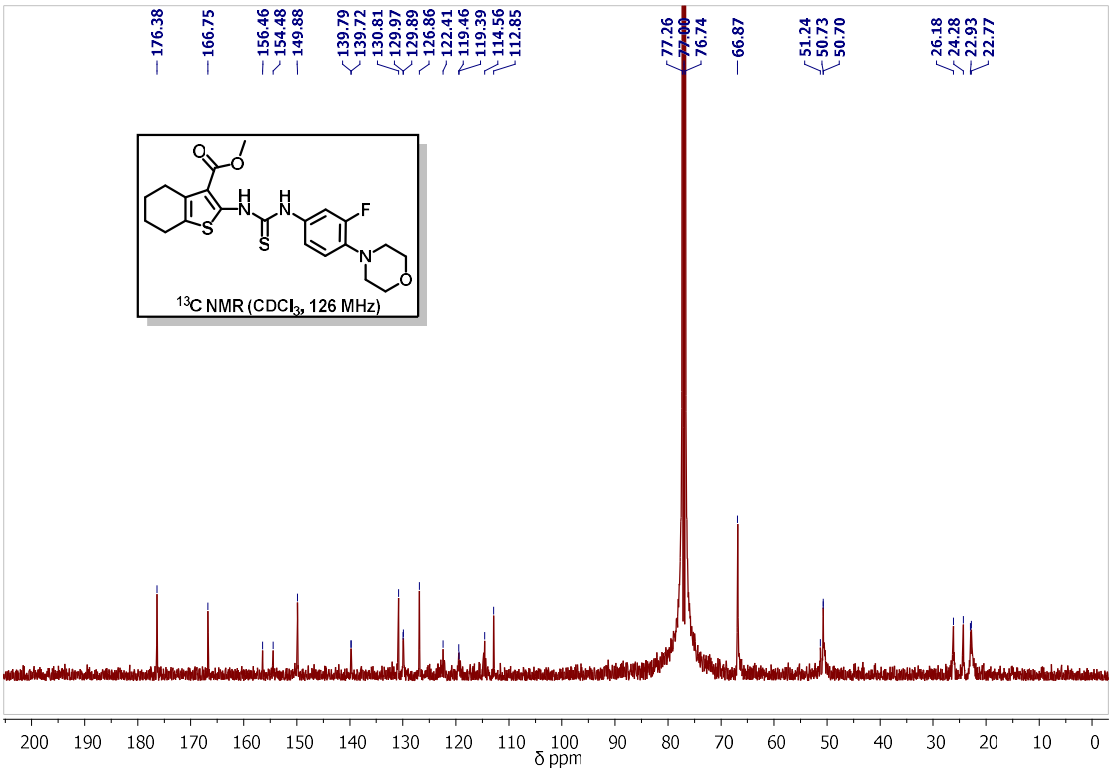

Figure S17. $^{13}C\{^{1}H\}$ NMR spectra (126 MHz, RT) of compound **8e** in $CDCl_3$.

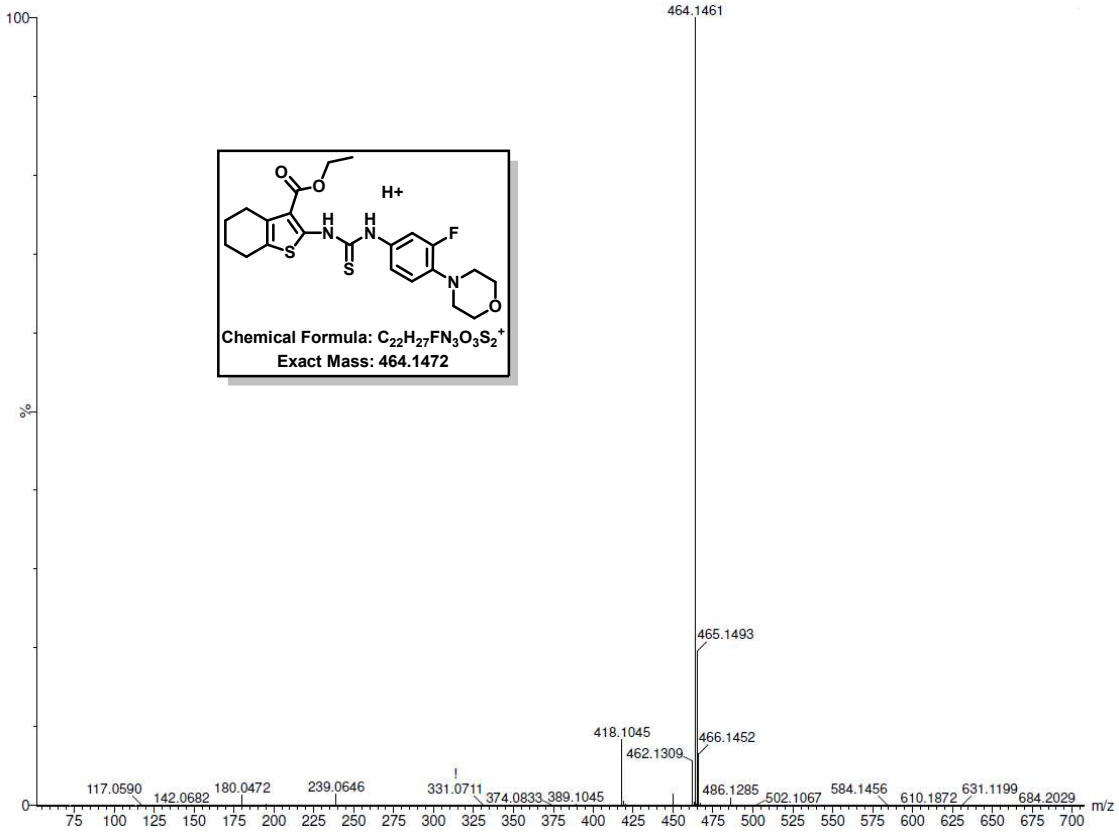

Figure S18. HRMS spectrum of **8f**.

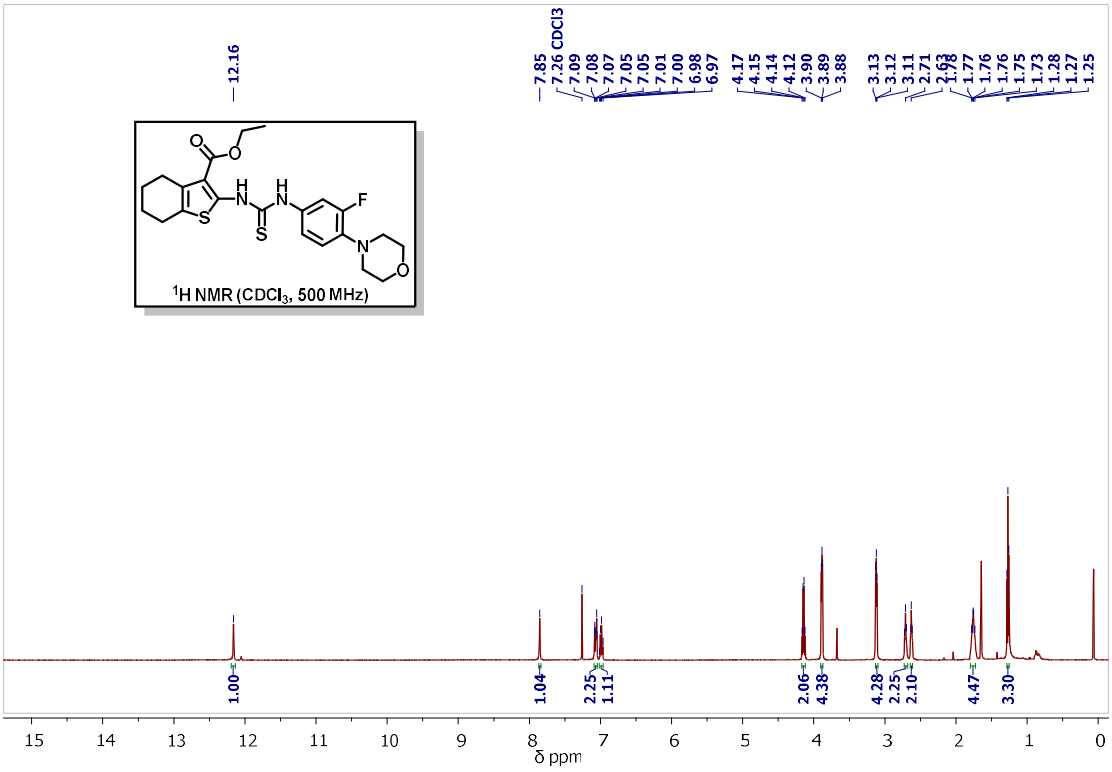

Figure S19. ^{1}H NMR spectra (500 MHz, RT) of compound **8f** in $CDCl_3$.

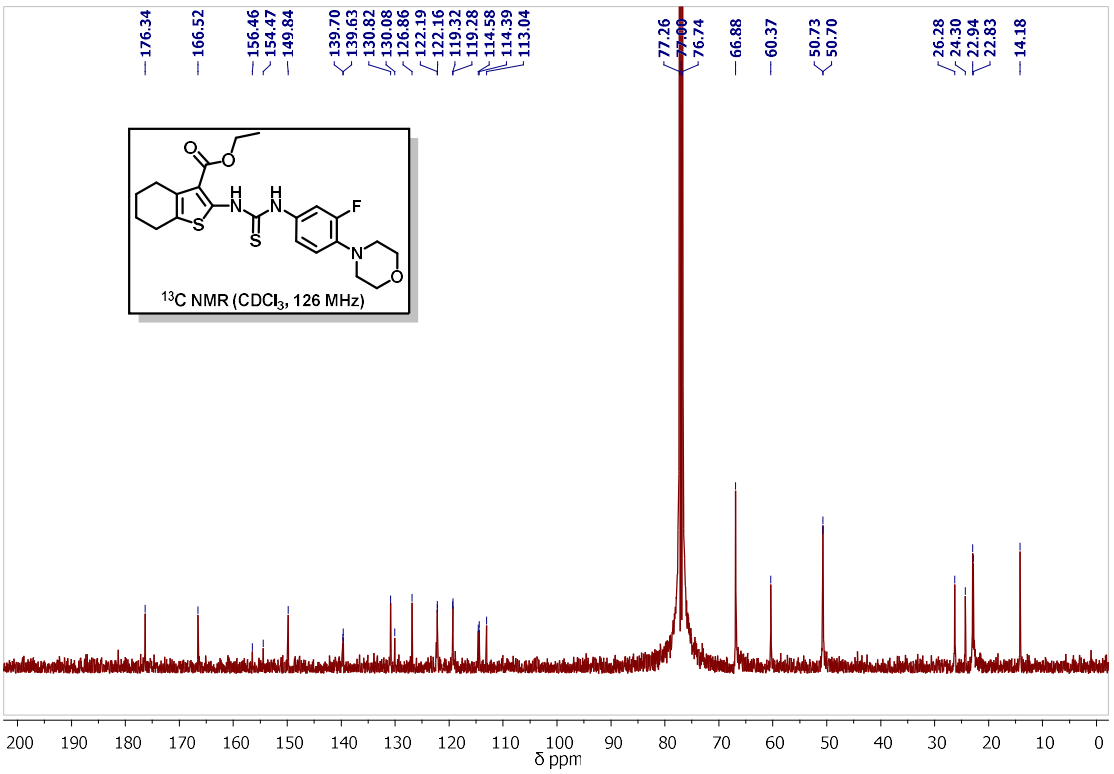

Figure S20. $^{13}C\{^{1}H\}$ NMR spectra (126 MHz, RT) of compound **8f** in $CDCl_3$.

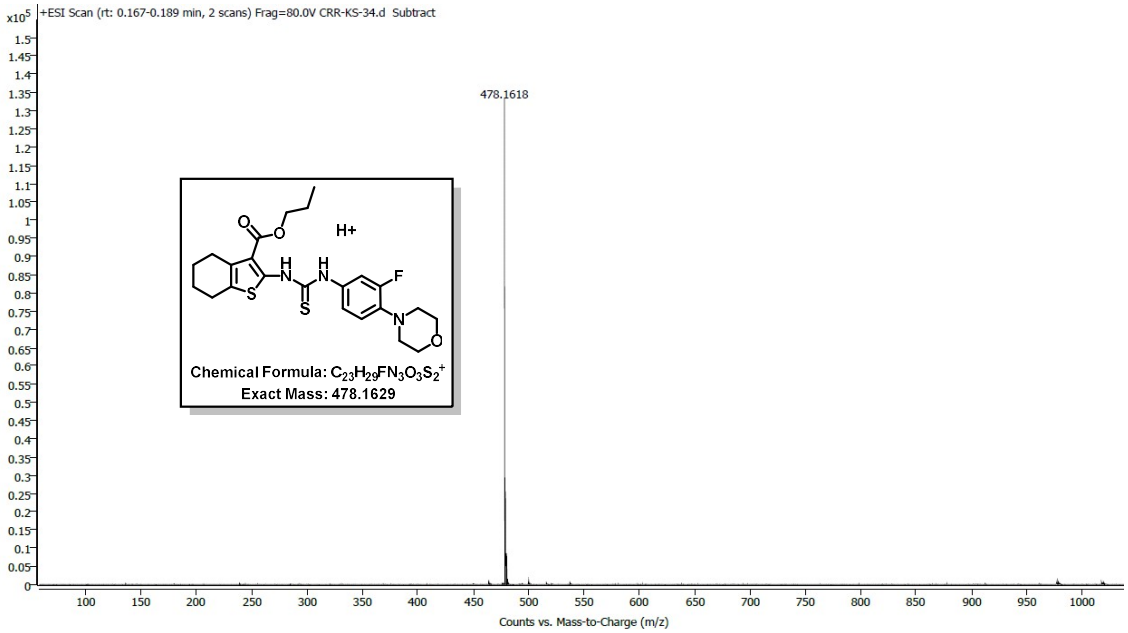

Figure S21. HRMS spectrum of **8g**.

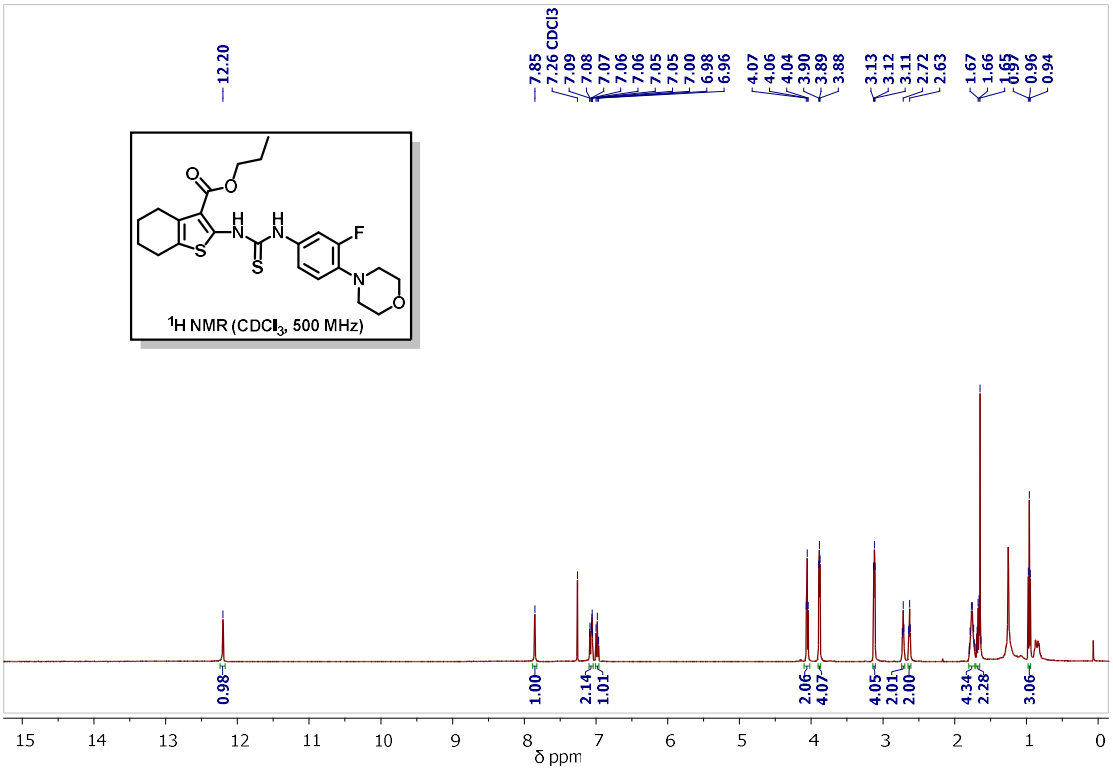

Figure S22. ^{1}H NMR spectra (500 MHz, RT) of compound **8g** in $CDCl_3$.

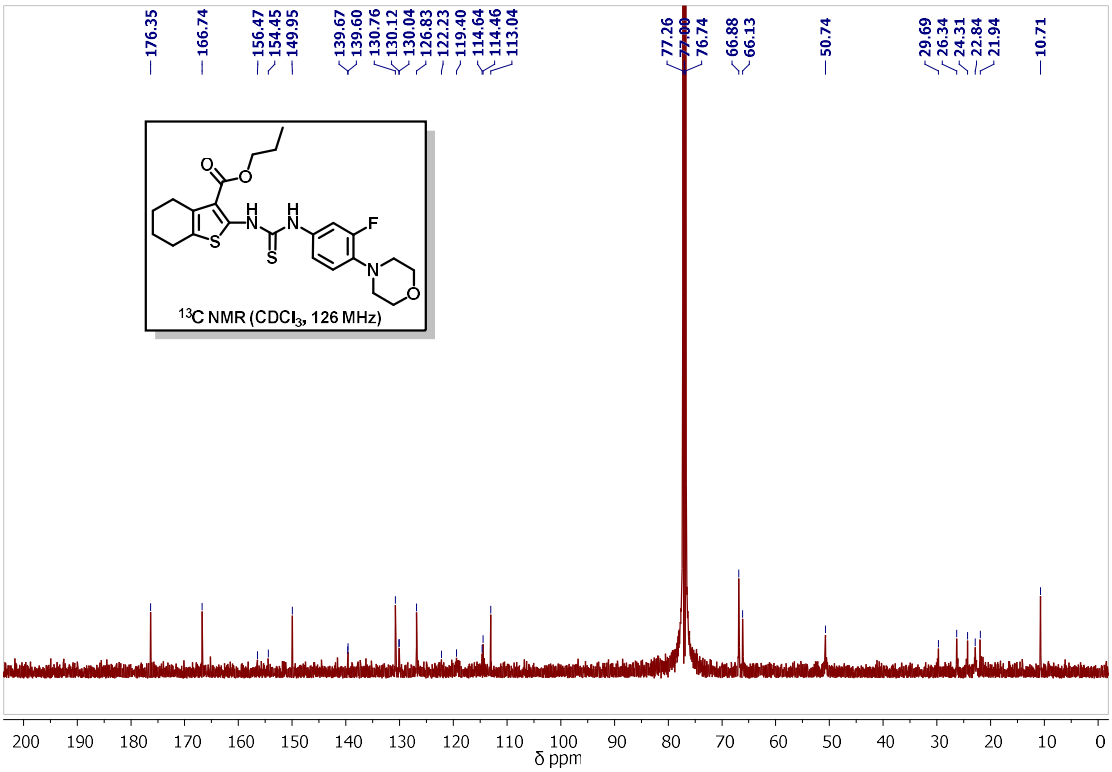

Figure S23. $^{13}C\{^{1}H\}$ NMR spectra (126 MHz, RT) of compound **8g** in $CDCl_3$.

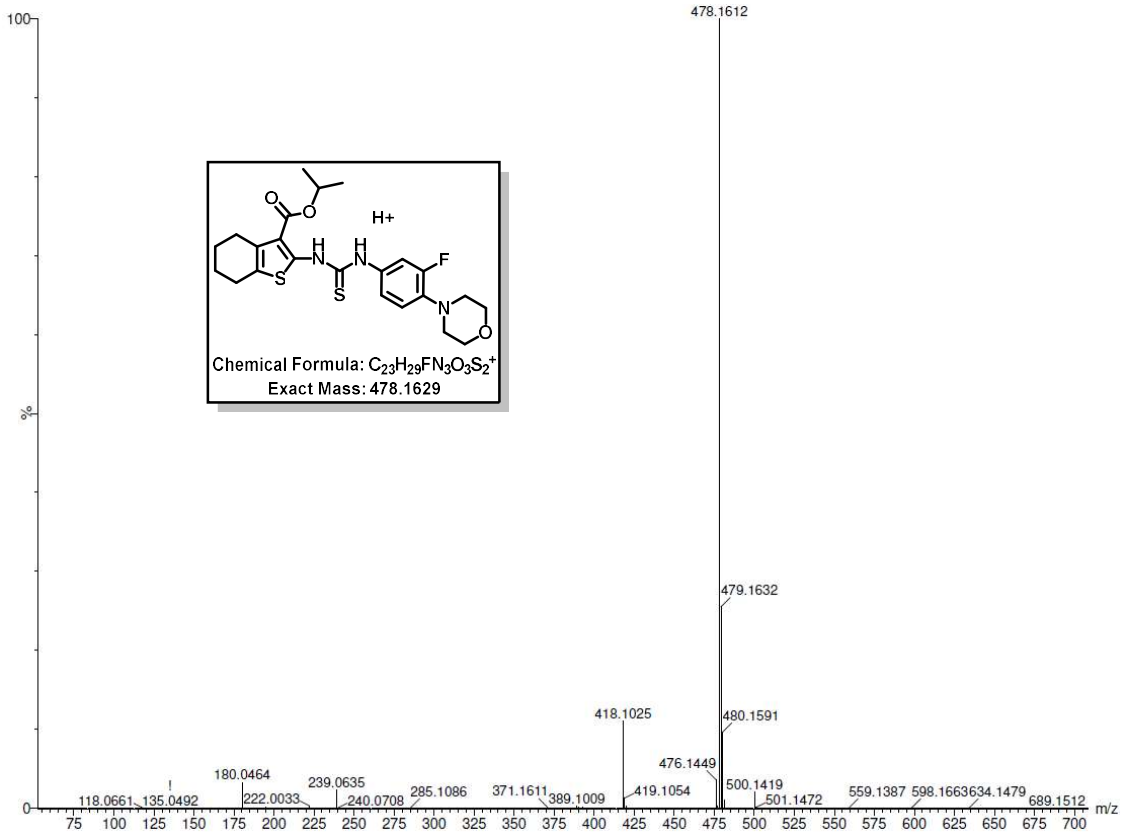

Figure S24. HRMS spectrum of **8h**.

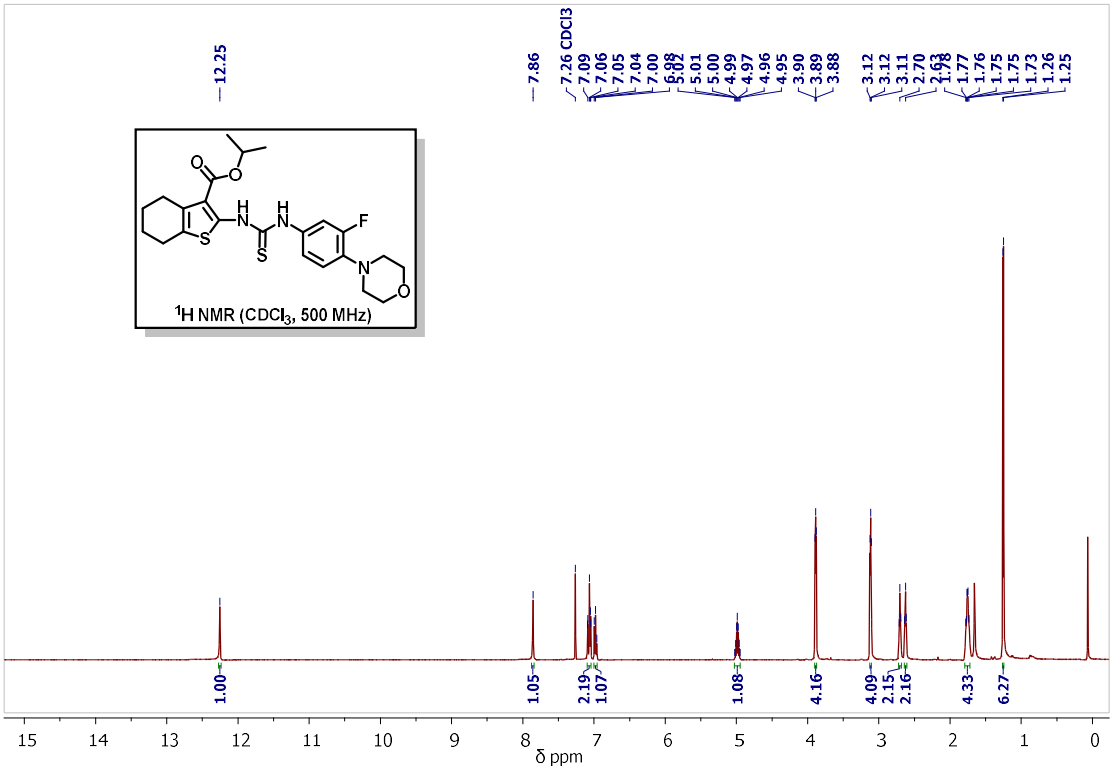

Figure S25. ^{1}H NMR spectra (500 MHz, RT) of compound **8h** in $CDCl_3$.

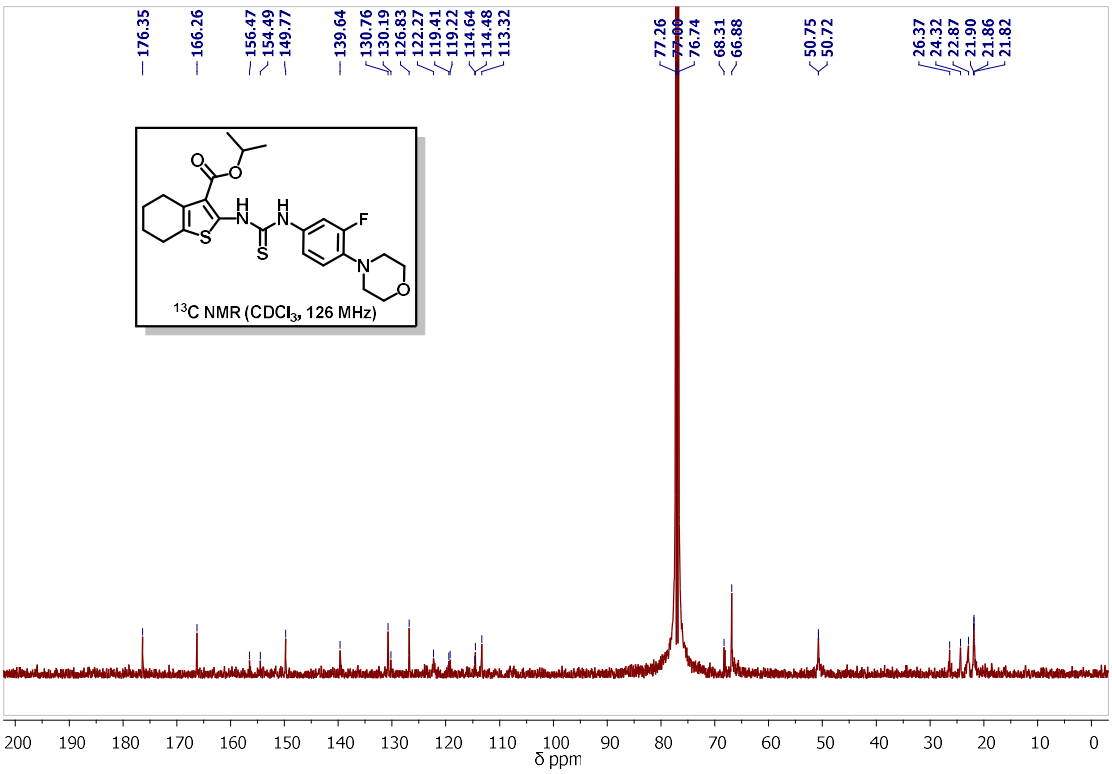

Figure S26. $^{13}C\{^{1}H\}$ NMR spectra (126 MHz, RT) of compound **8h** in $CDCl_3$.

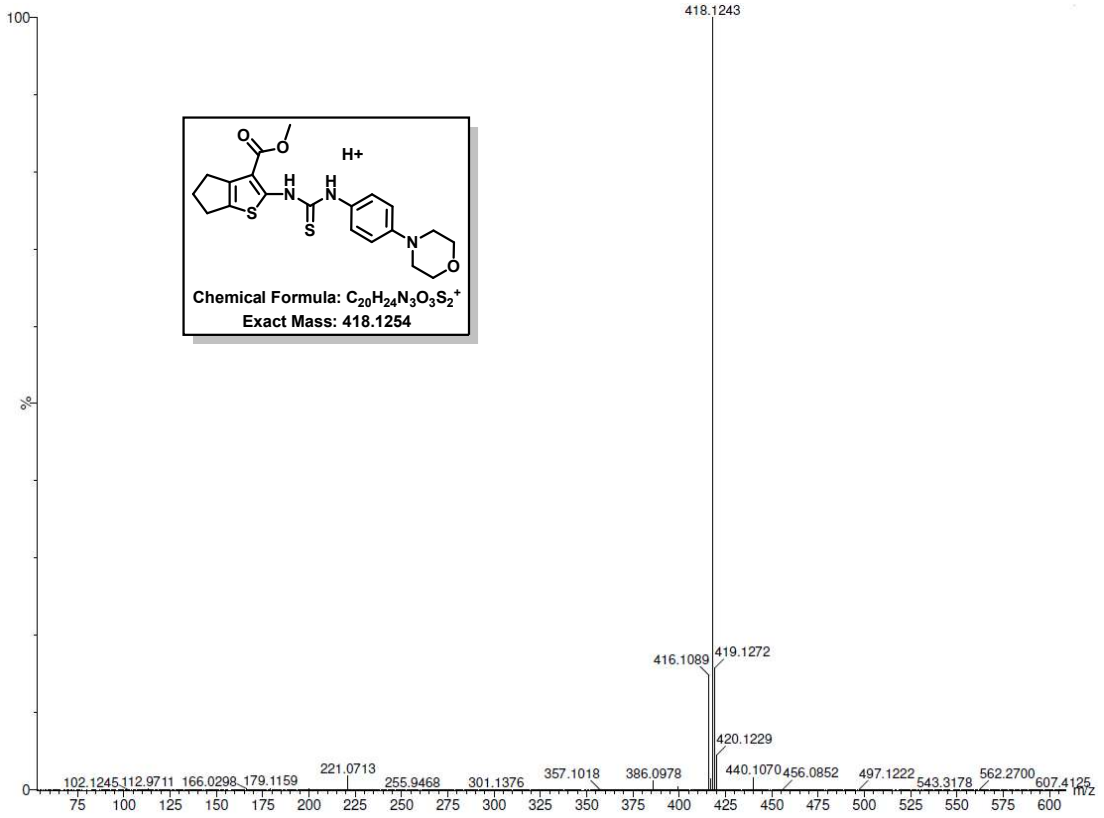

Figure S27. HRMS spectrum of **9a**.

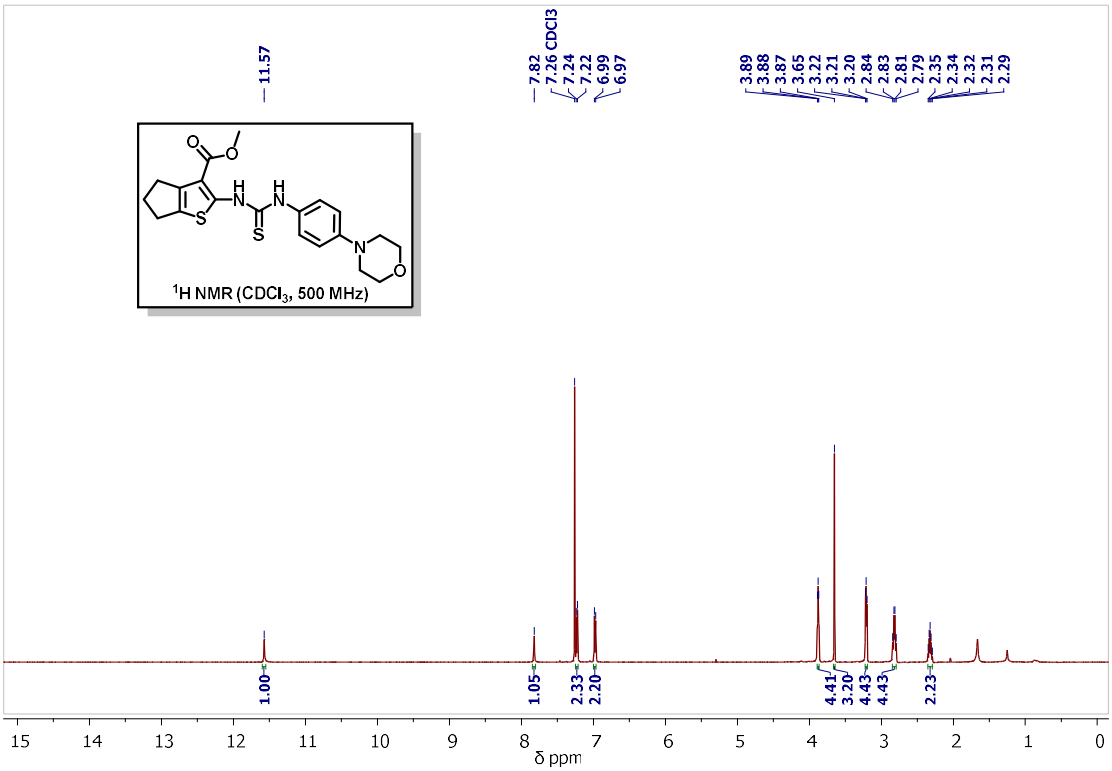

Figure S28. ^{1}H NMR spectra (500 MHz, RT) of compound **9a** in $CDCl_3$.

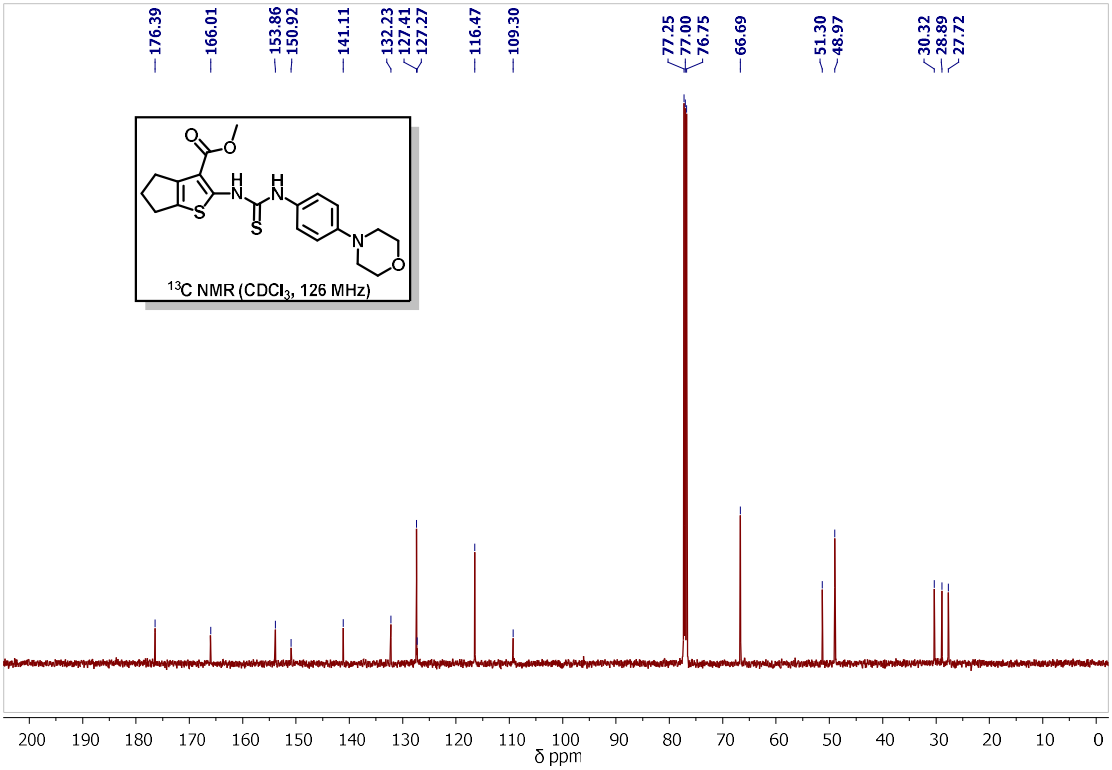

Figure S29. $^{13}C\{^{1}H\}$ NMR spectra (126 MHz, RT) of compound **9a** in $CDCl_3$.

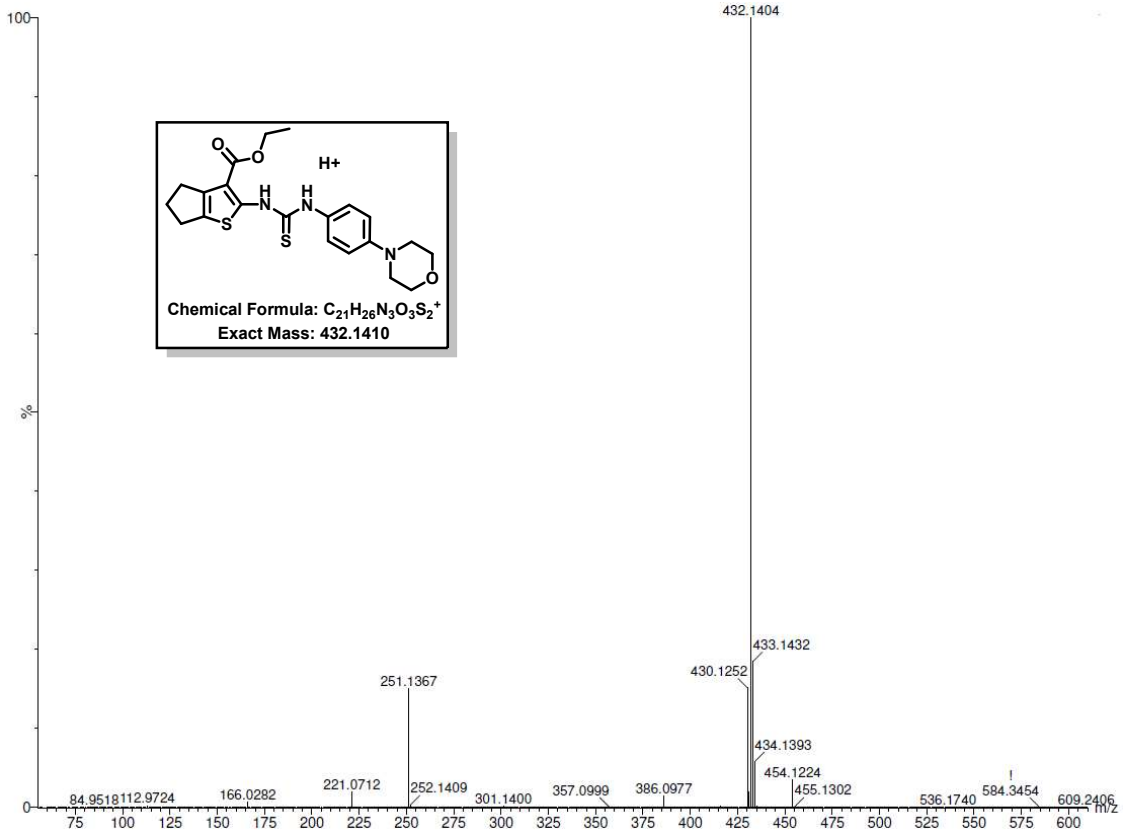

Figure S30. HRMS spectrum of **9b**.

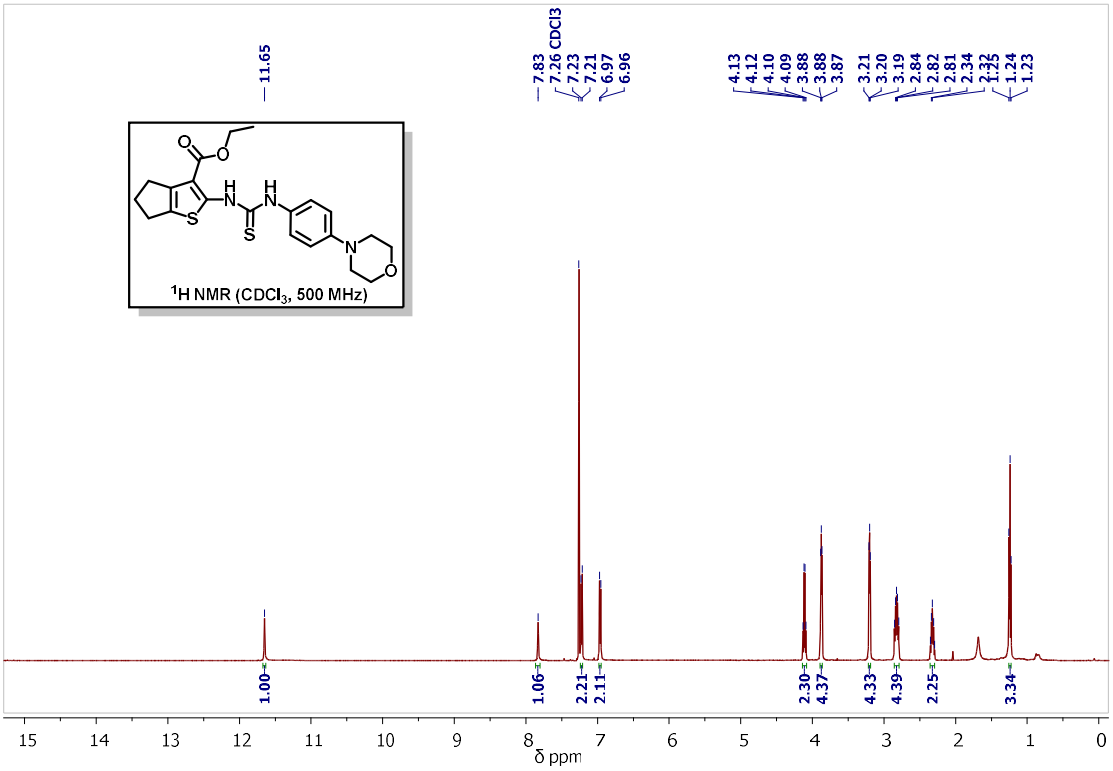

Figure S31. ^{1}H NMR spectra (500 MHz, RT) of compound **9b** in $CDCl_3$.

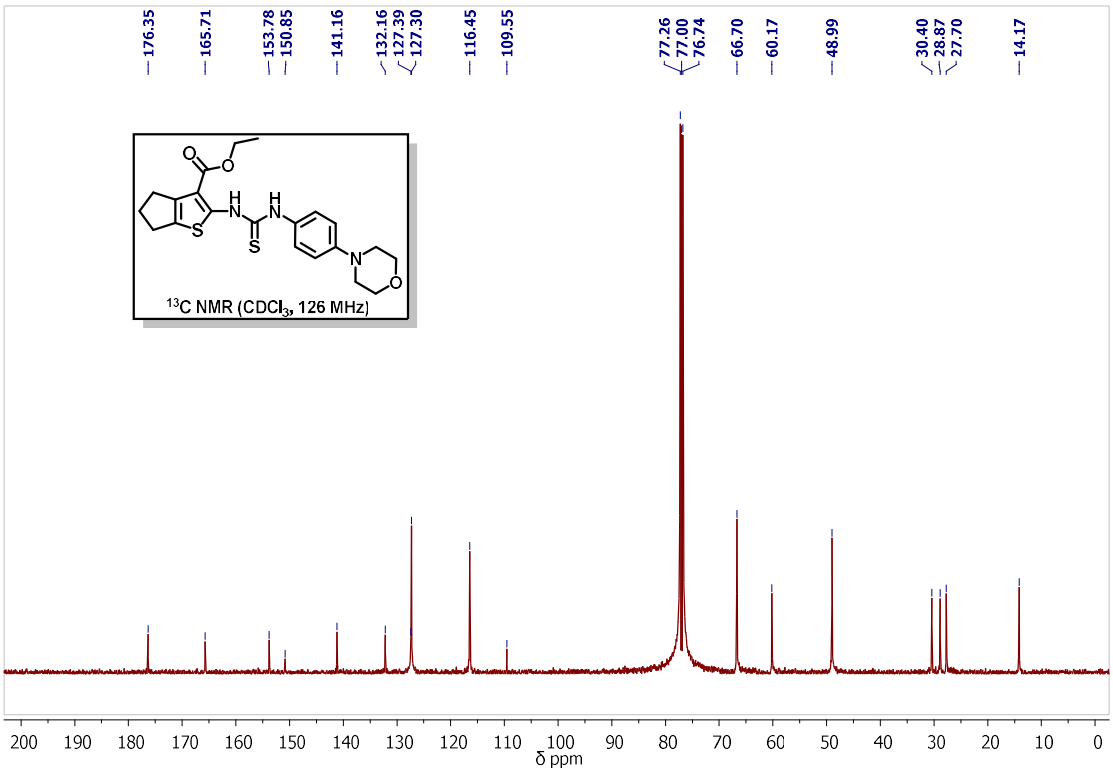

Figure S32. $^{13}C\{^{1}H\}$ NMR spectra (126 MHz, RT) of compound **9b** in $CDCl_3$.

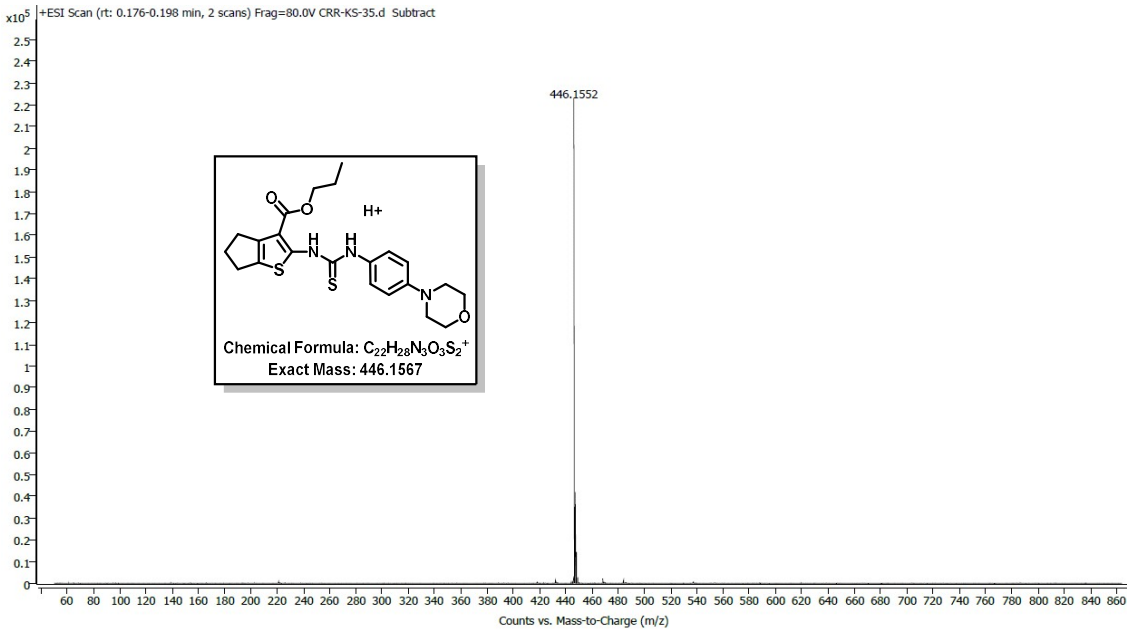

Figure S33. HRMS spectrum of **9c**.

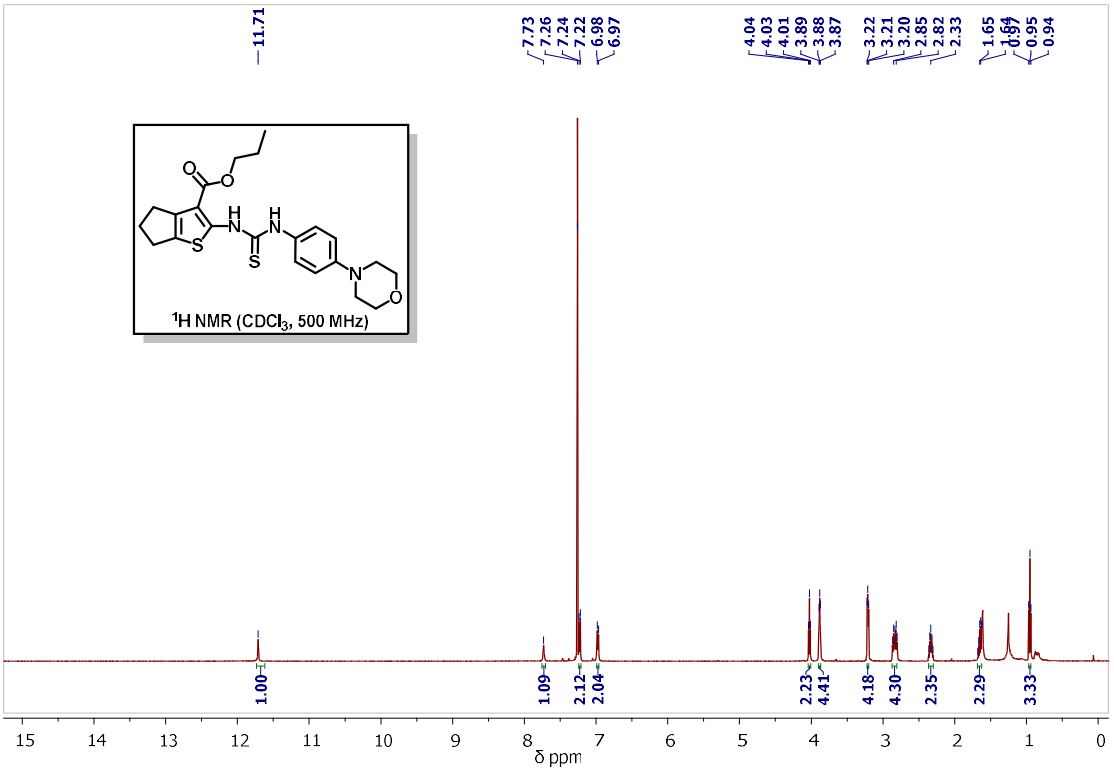

Figure S34. ^{1}H NMR spectra (500 MHz, RT) of compound **9c** in $CDCl_3$.

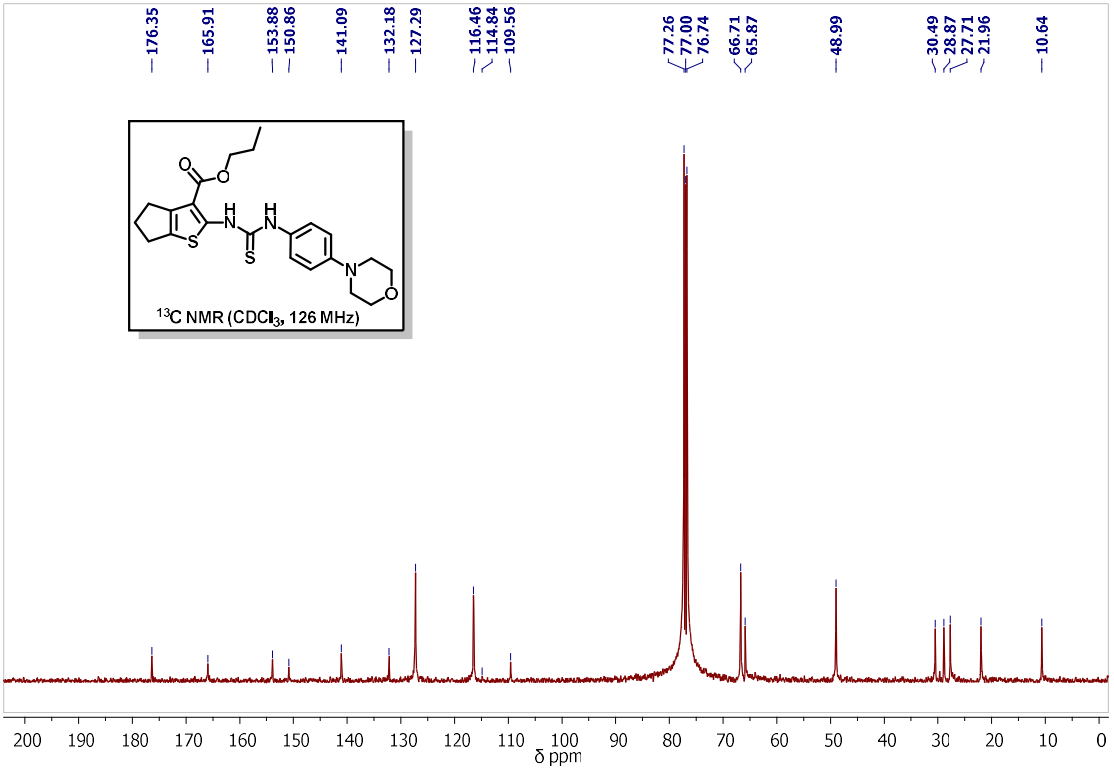

Figure S35. $^{13}C\{^1H\}$ NMR spectra (126 MHz, RT) of compound **9c** in $CDCl_3$.

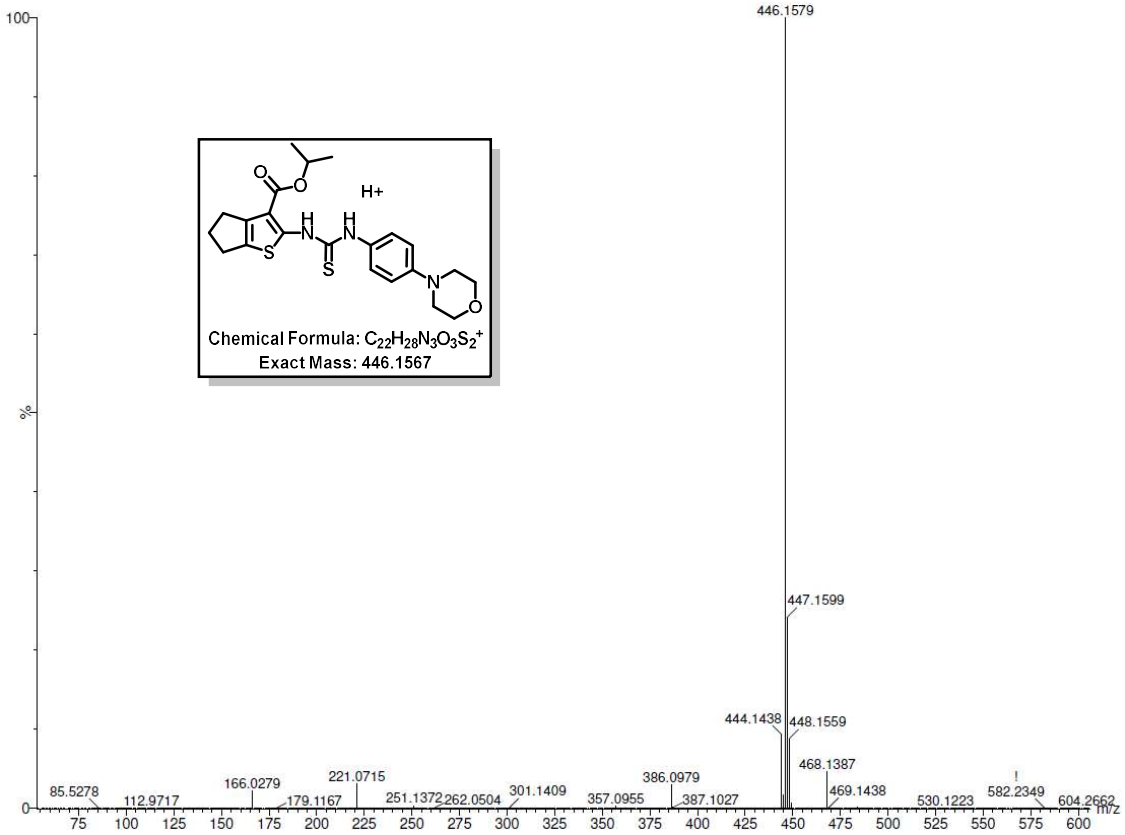

Figure S36. HRMS spectrum of **9d**.

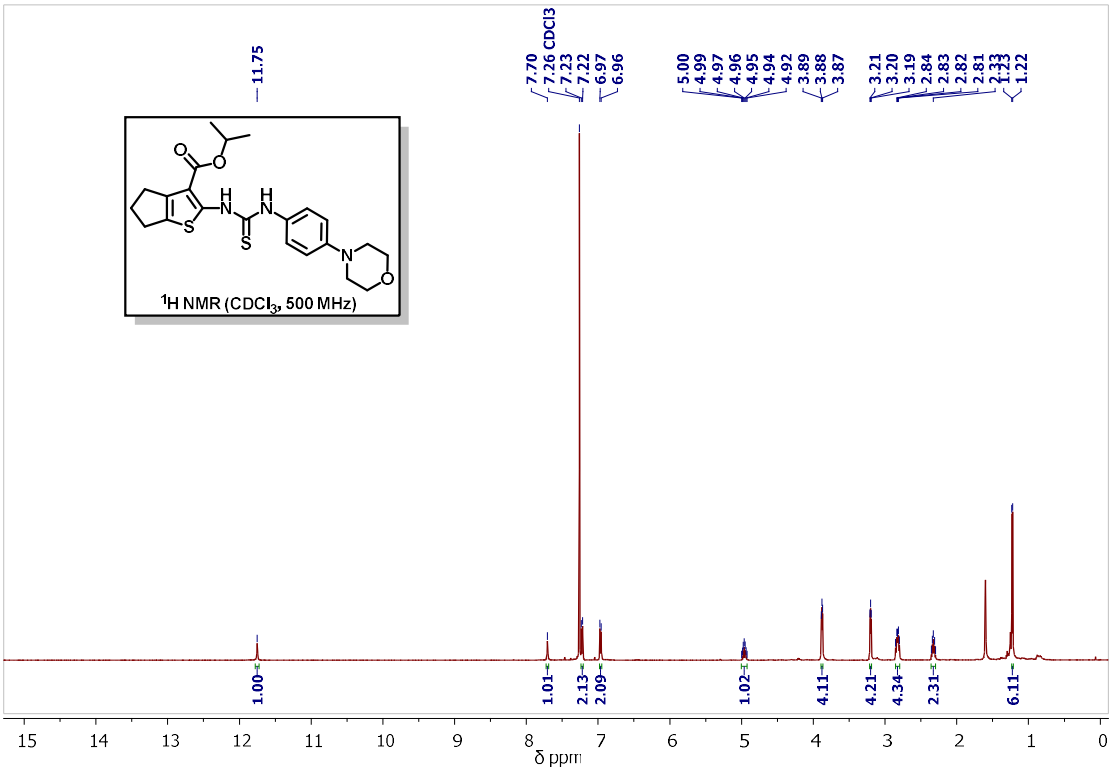

Figure S37. ^{1}H NMR spectra (500 MHz, RT) of compound **9d** in $CDCl_3$.

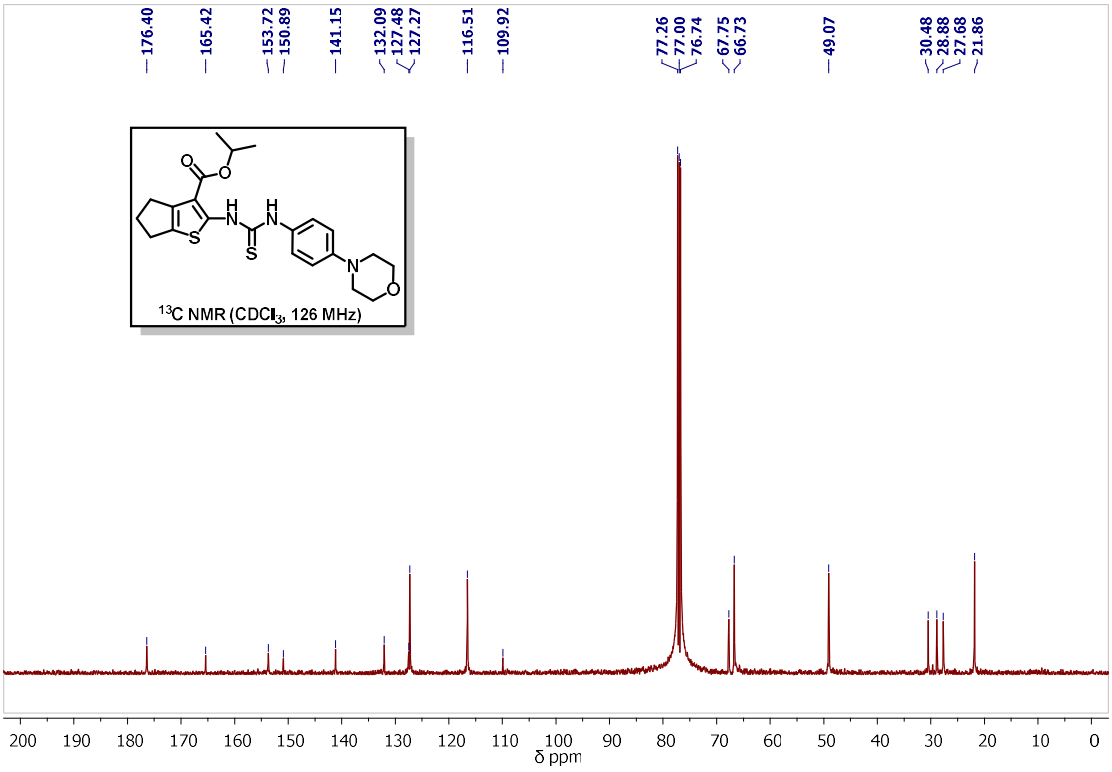

Figure S38. $^{13}C\{^{1}H\}$ NMR spectra (126 MHz, RT) of compound **9d** in $CDCl_3$.

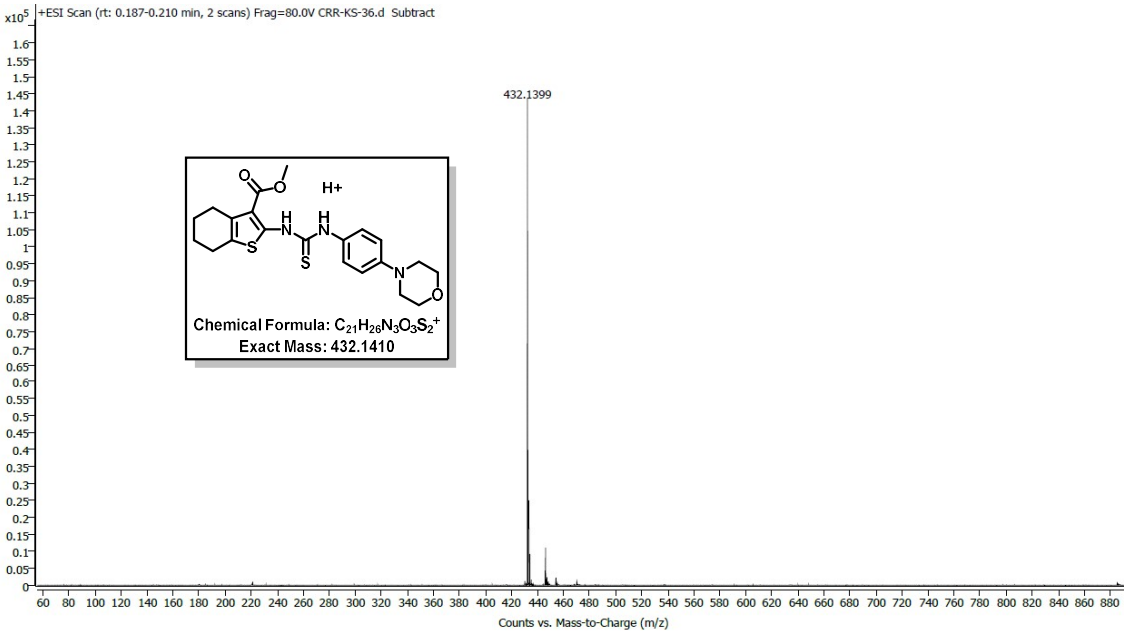

Figure S39. HRMS spectrum of **9e**.

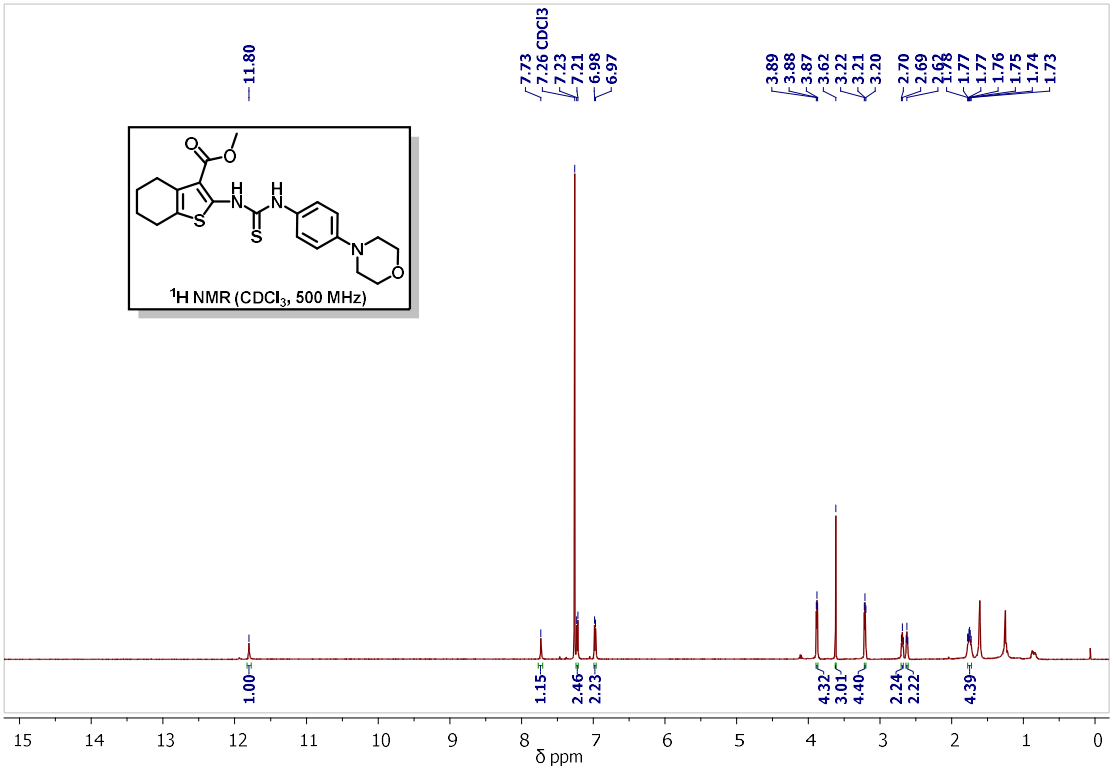

Figure S40. ^{1}H NMR spectra (500 MHz, RT) of compound **9e** in $CDCl_3$.

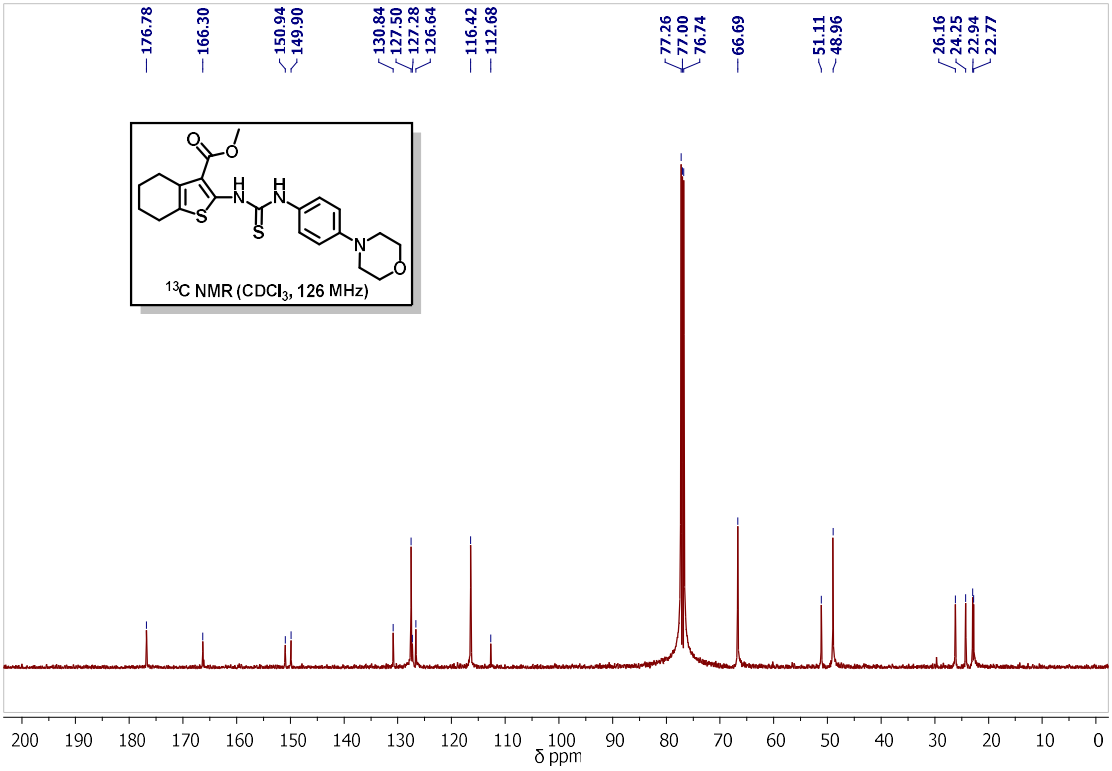

Figure S41. $^{13}C\{^{1}H\}$ NMR spectra (126 MHz, RT) of compound **9e** in $CDCl_3$.

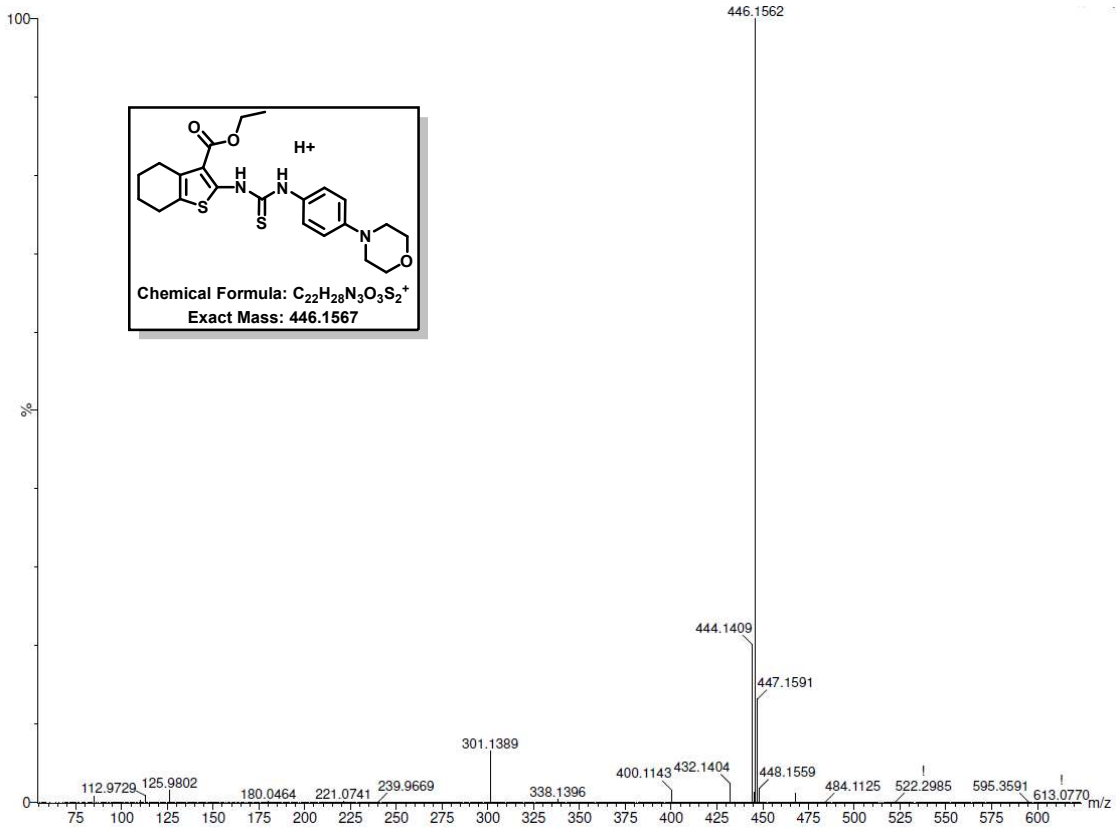

Figure S42. HRMS spectrum of **9f**.

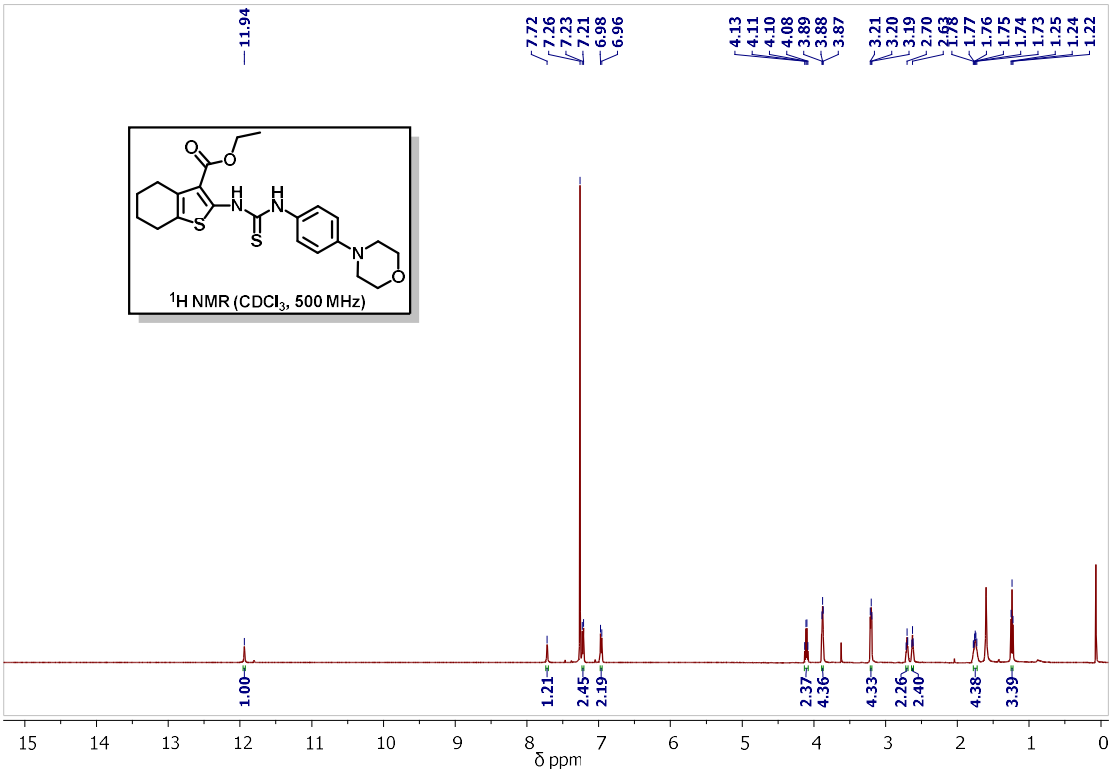

Figure S43. ^{1}H NMR spectra (500 MHz, RT) of compound **9f** in $CDCl_3$.

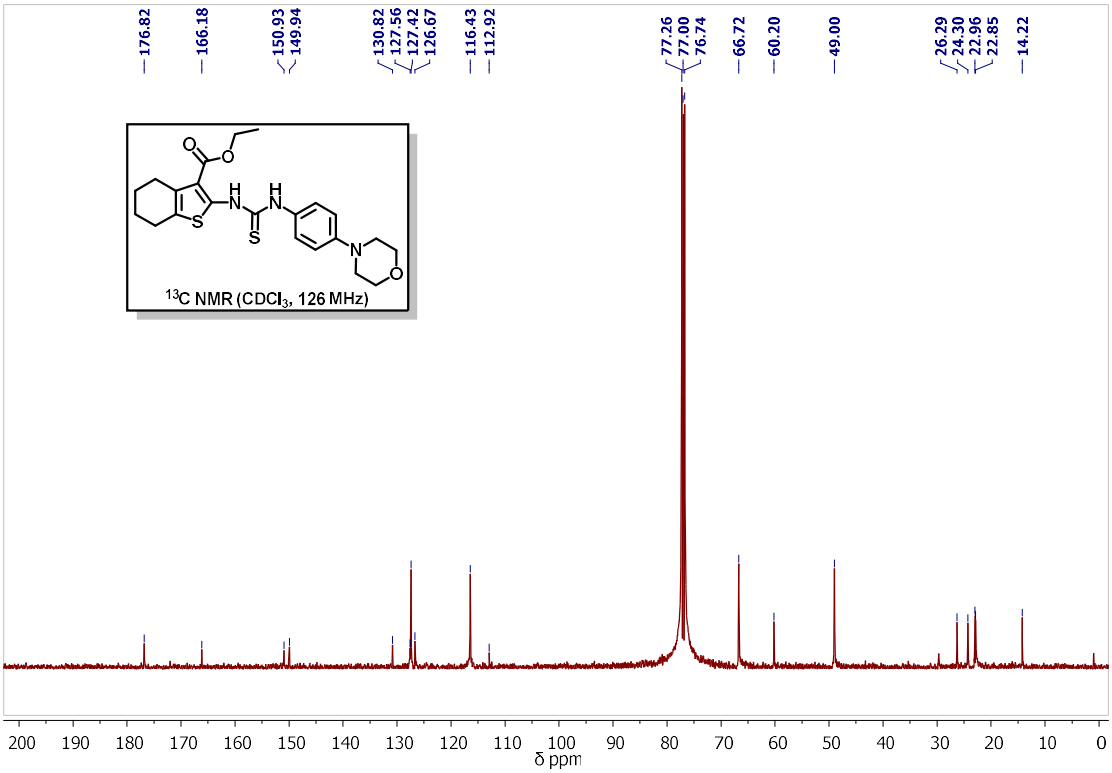

Figure S44. $^{13}C\{^{1}H\}$ NMR spectra (126 MHz, RT) of compound **9f** in $CDCl_3$.

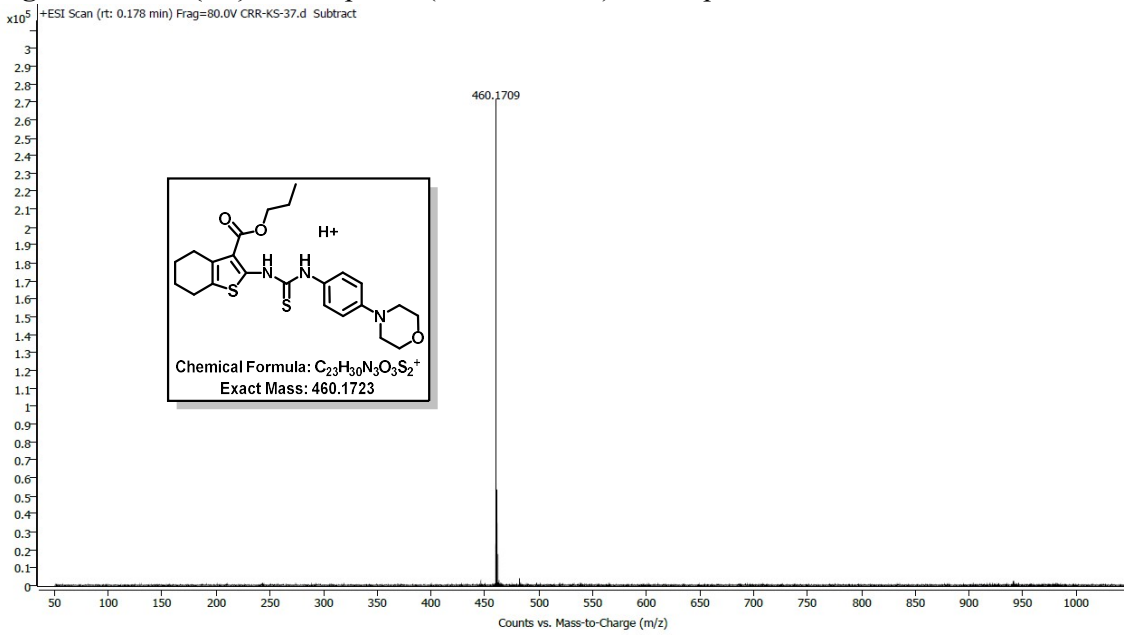

Figure S45. HRMS spectrum of **9g**.

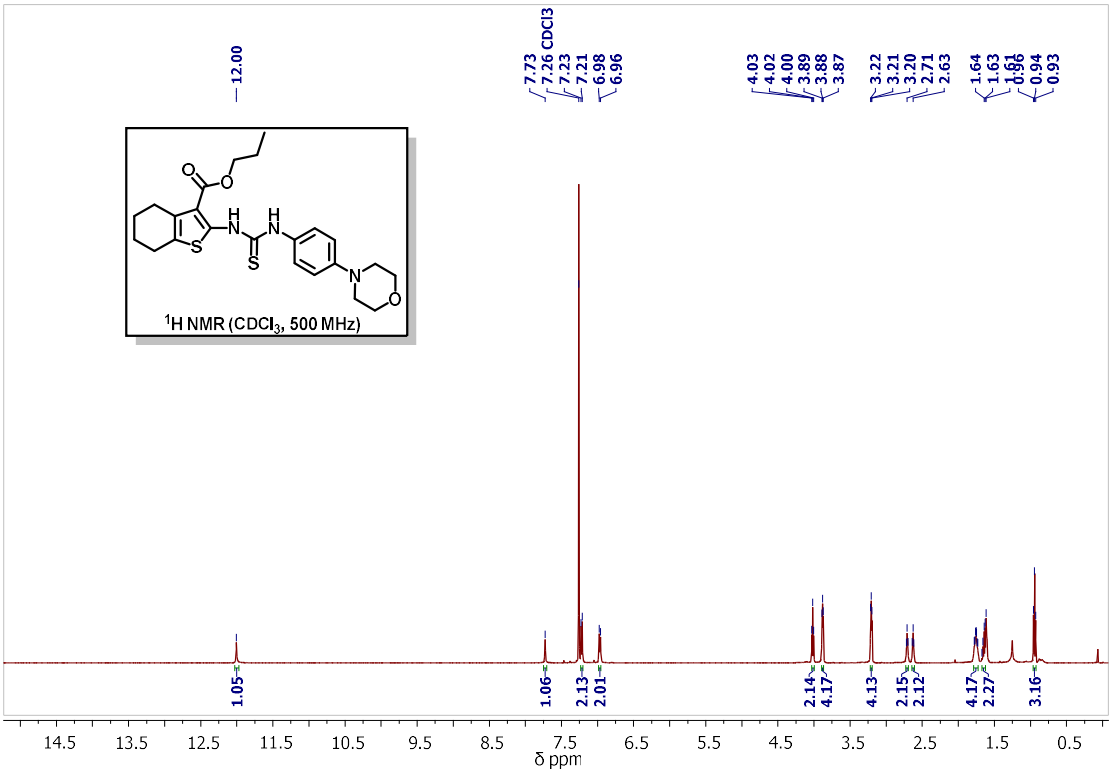

Figure S46. ^{1}H NMR spectra (500 MHz, RT) of compound **9g** in $CDCl_3$.

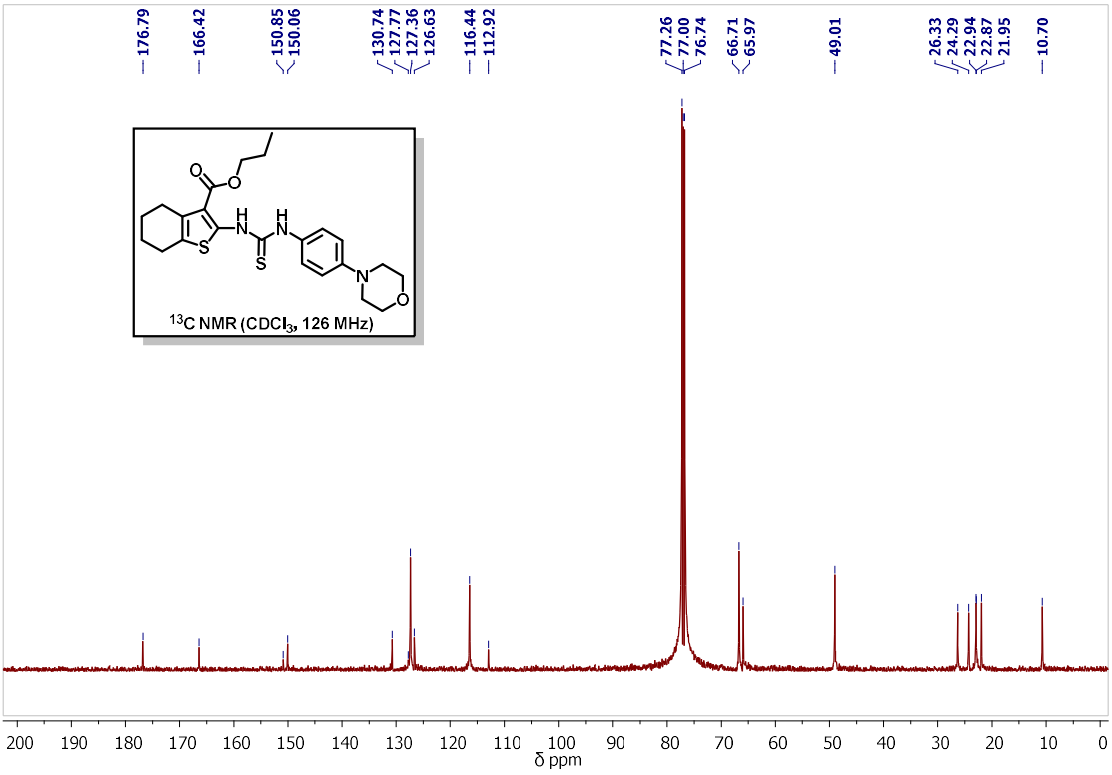

Figure S47. $^{13}C\{^{1}H\}$ NMR spectra (126 MHz, RT) of compound **9g** in $CDCl_3$.

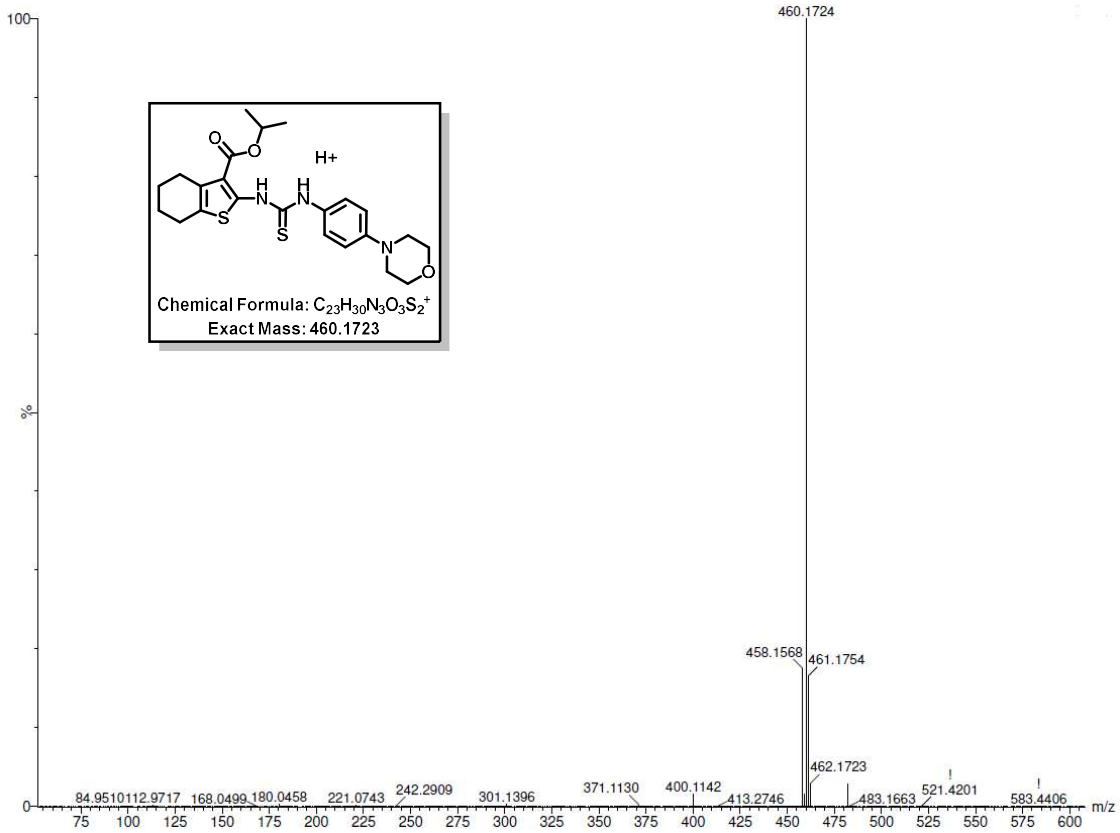

Figure S48. HRMS spectrum of **9h**.

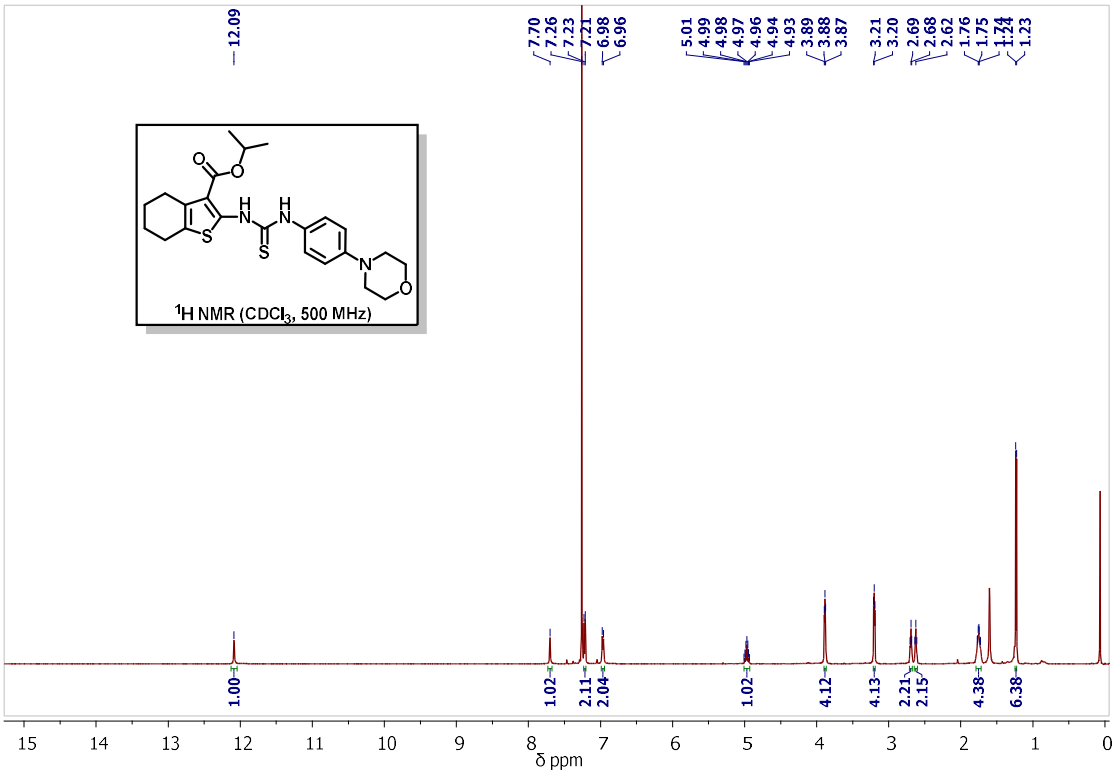

Figure S49. ^{1}H NMR spectra (500 MHz, RT) of compound **9h** in $CDCl_3$.

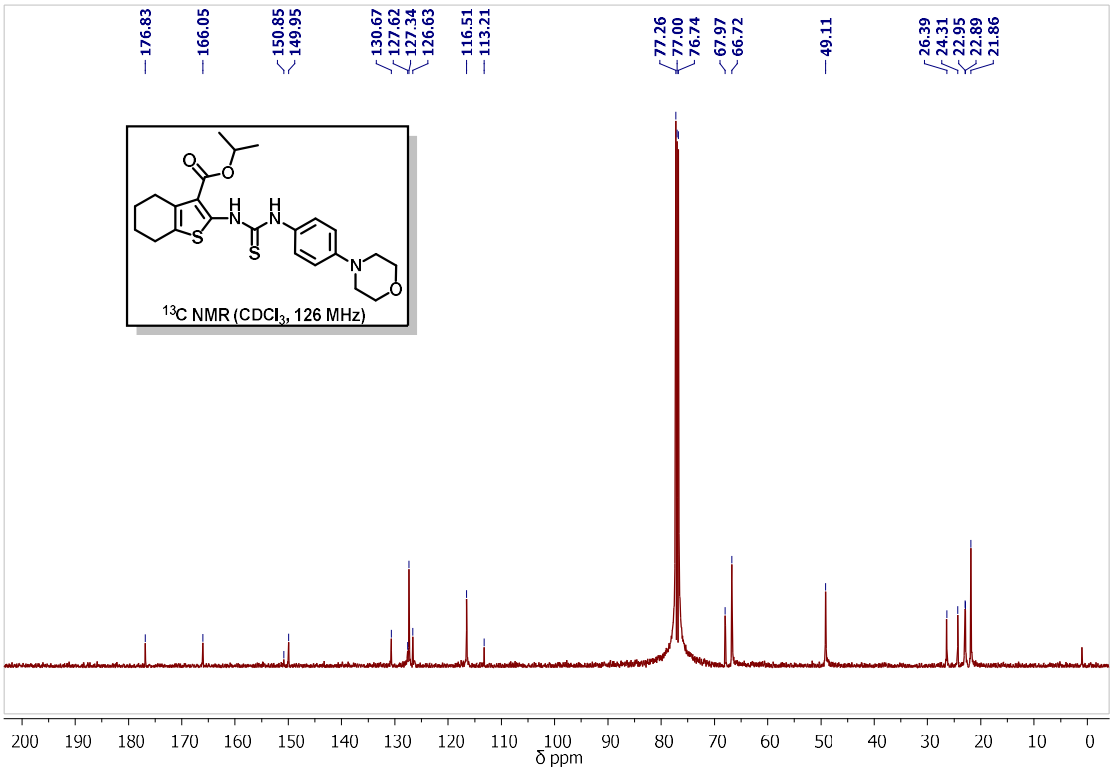

Figure S50. $^{13}C\{^{1}H\}$ NMR spectra (126 MHz, RT) of compound **9h** in $CDCl_3$.

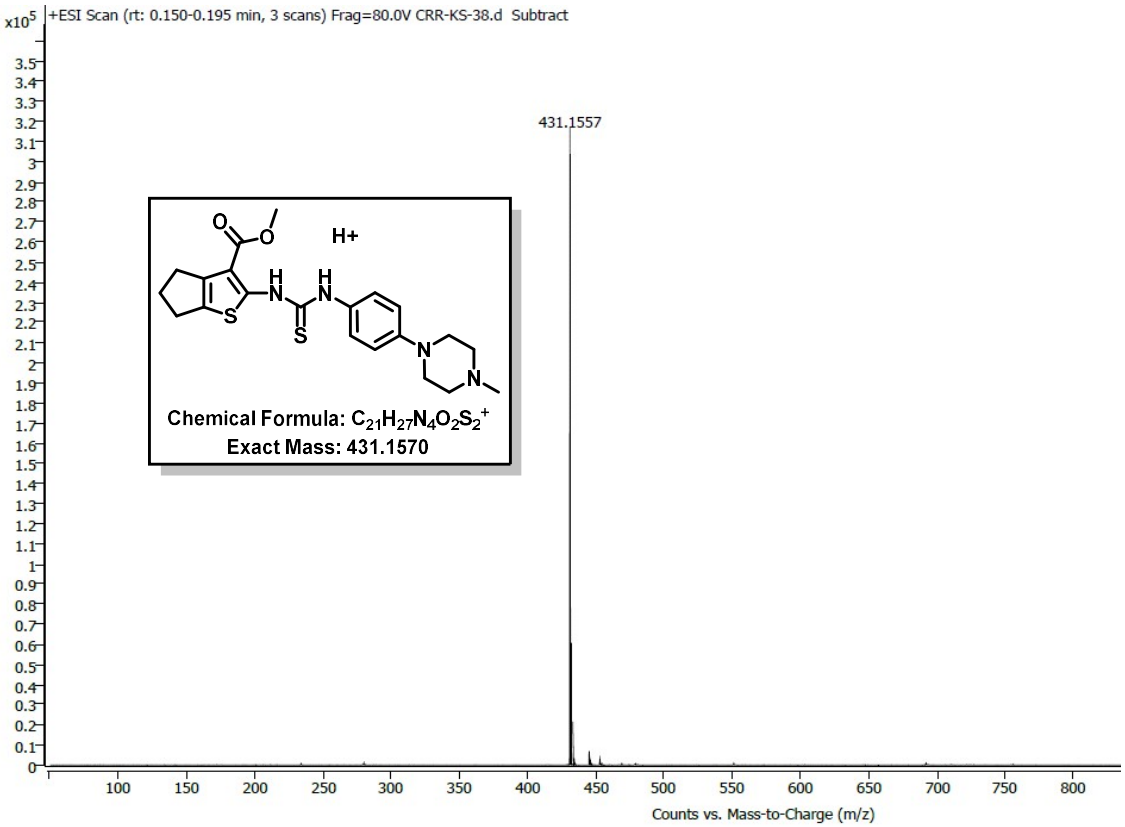

Figure S51. HRMS spectrum of **10a**.

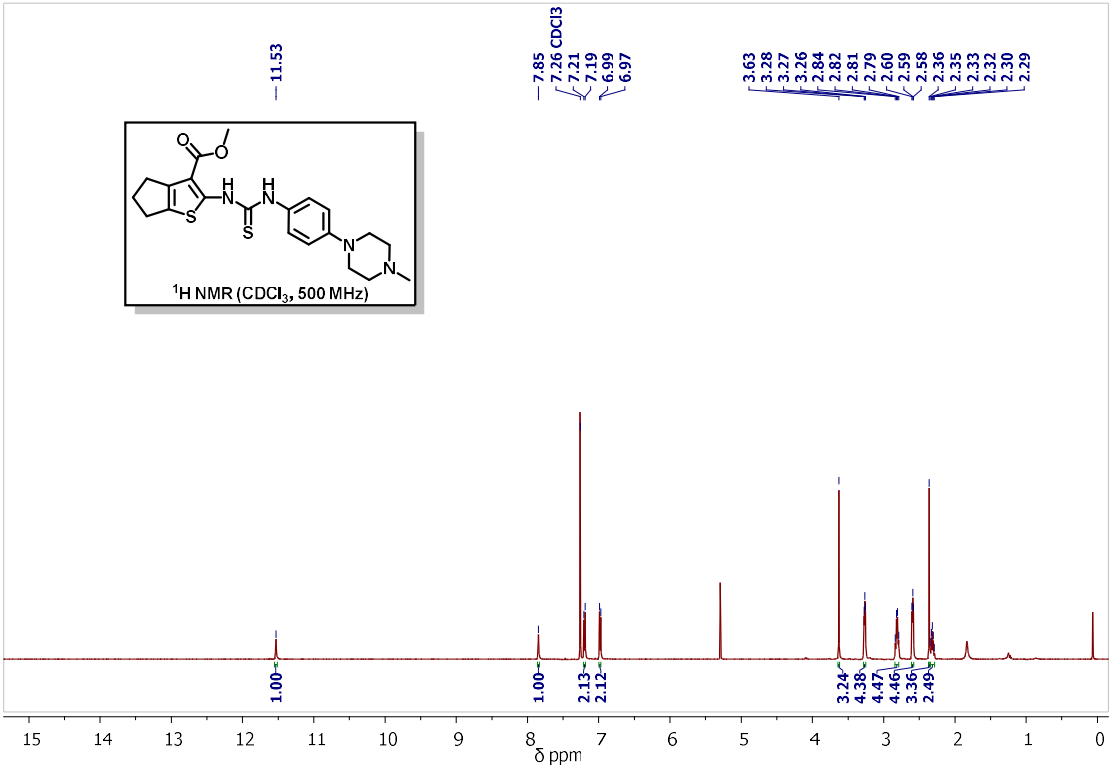

Figure S52. ^{1}H NMR spectra (500 MHz, RT) of compound **10a** in $CDCl_3$.

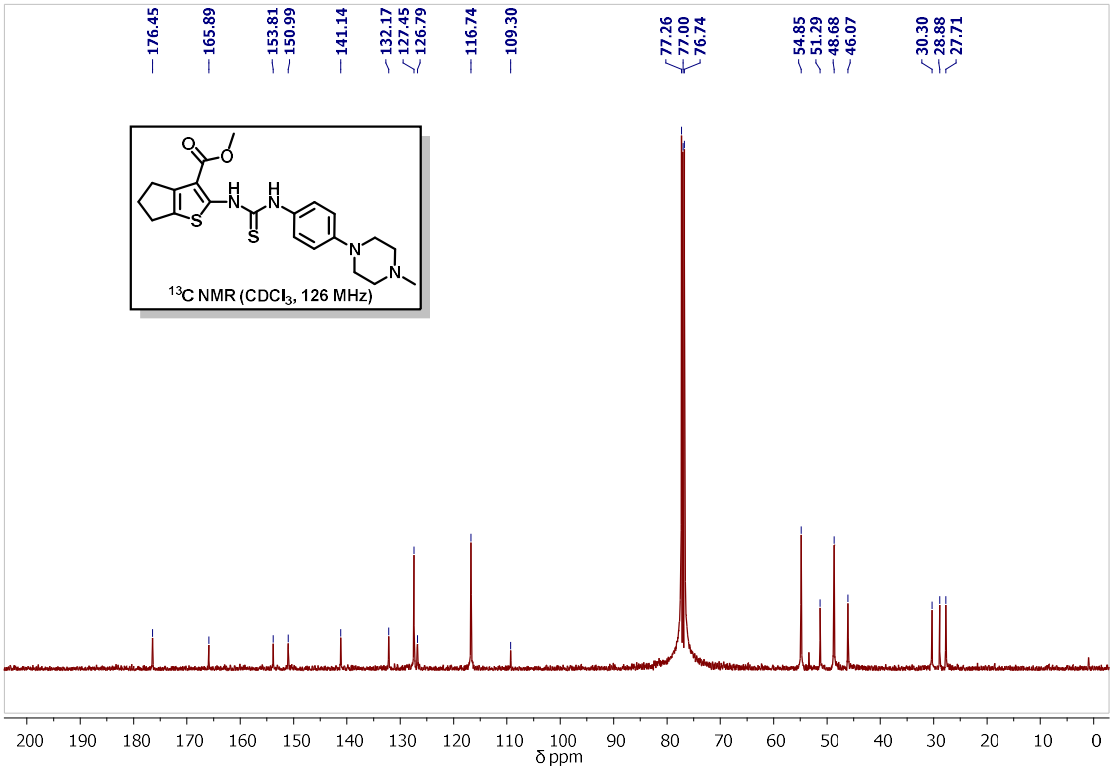

Figure S53. $^{13}C\{^{1}H\}$ NMR spectra (126 MHz, RT) of compound **10a** in $CDCl_3$.

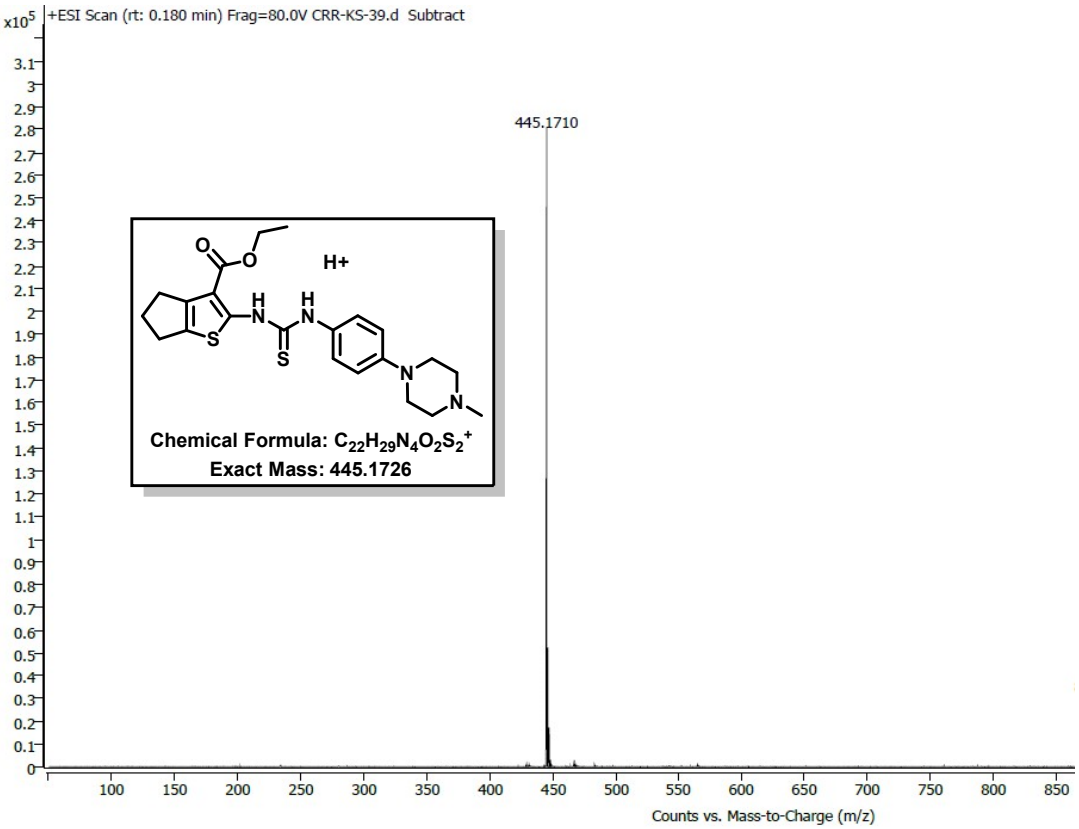

Figure S54. HRMS spectrum of **10b**.

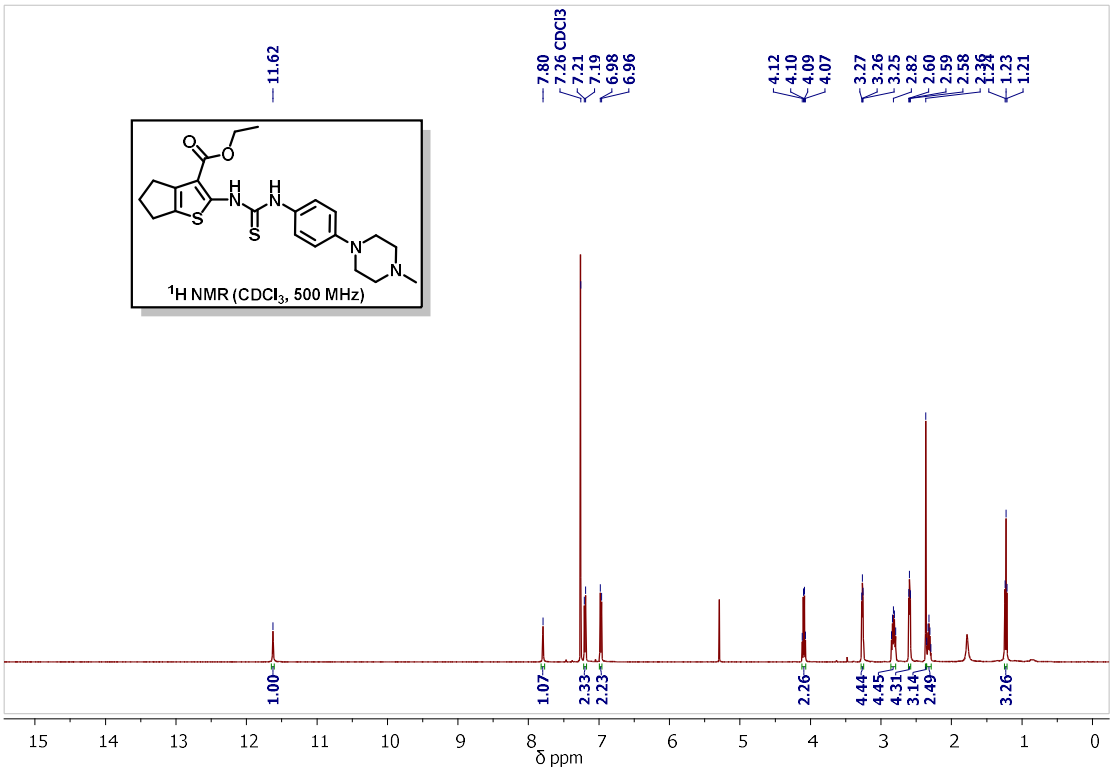

Figure S55. ^{1}H NMR spectra (500 MHz, RT) of compound **10b** in $CDCl_3$.

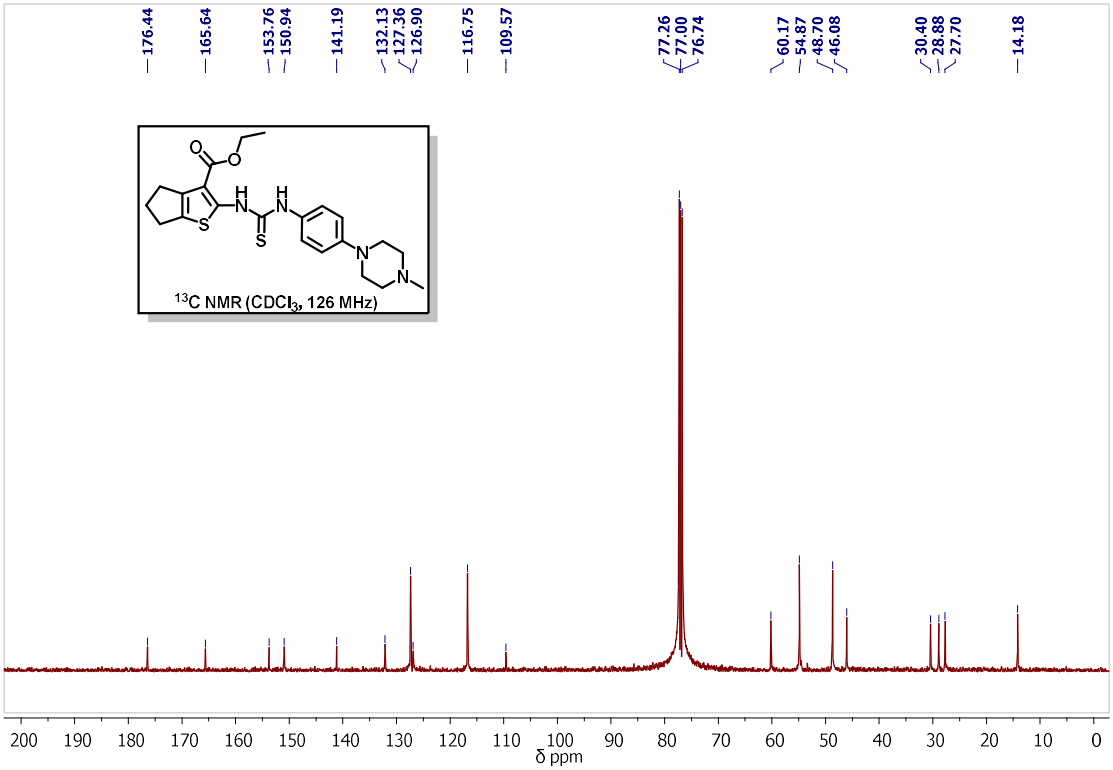

Figure S56. $^{13}C\{^{1}H\}$ NMR spectra (126 MHz, RT) of compound **10b** in $CDCl_3$.

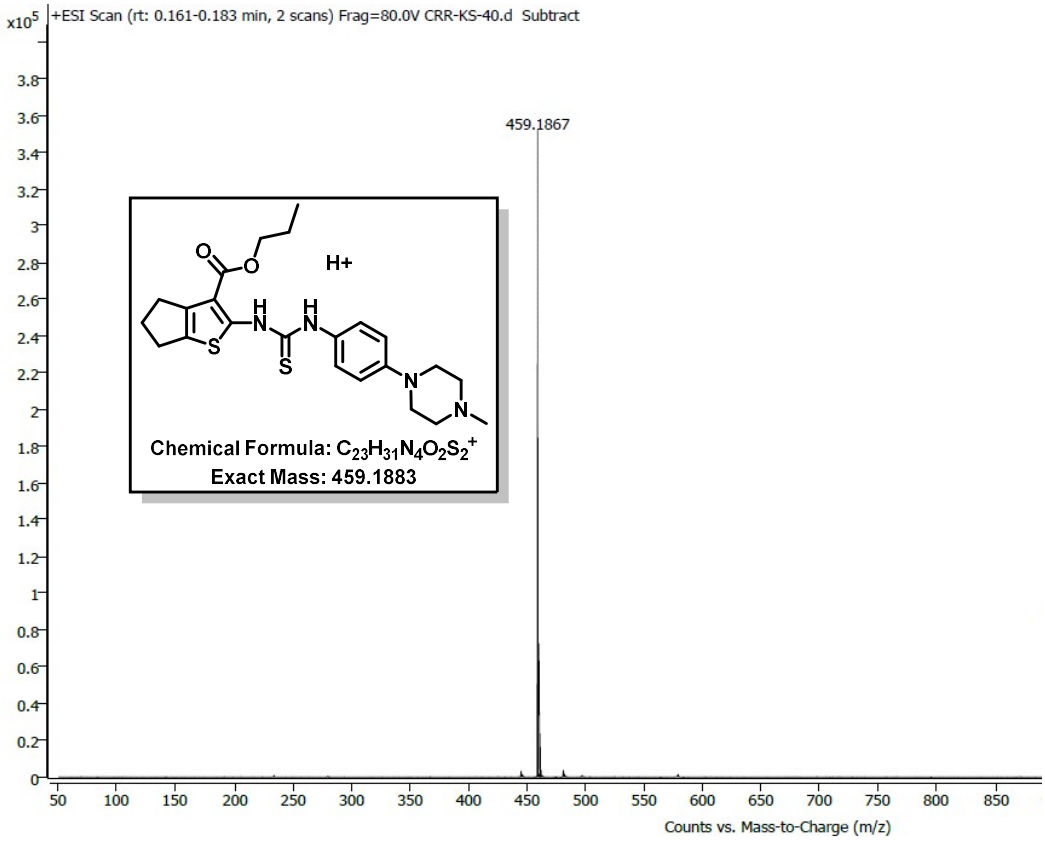

Figure S57. HRMS spectrum of **10c**.

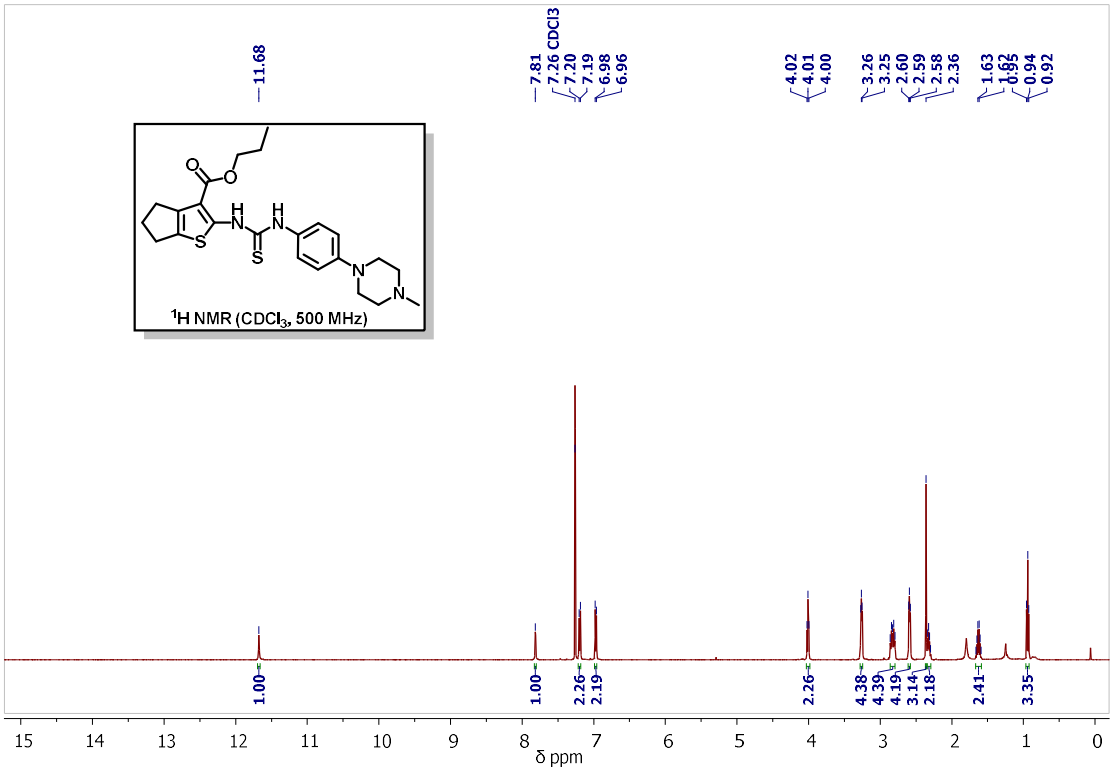

Figure S58. ^{1}H NMR spectra (500 MHz, RT) of compound **10c** in $CDCl_3$.

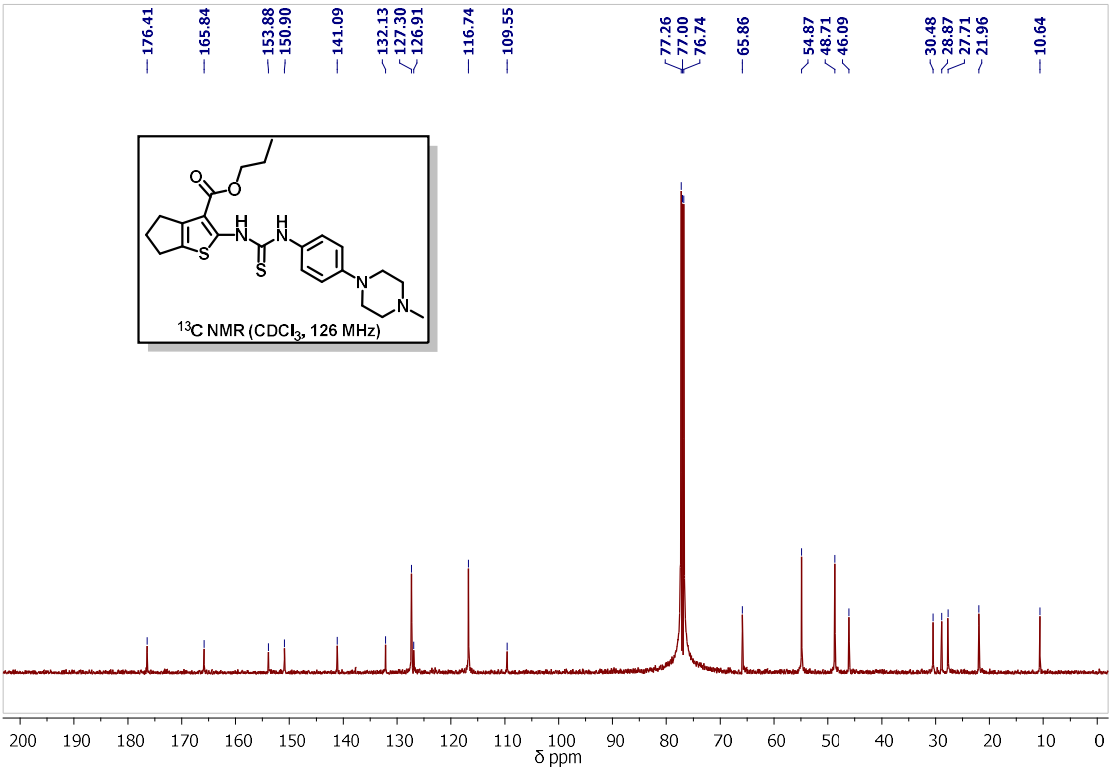

Figure S59. $^{13}C\{^{1}H\}$ NMR spectra (126 MHz, RT) of compound **10c** in $CDCl_3$.

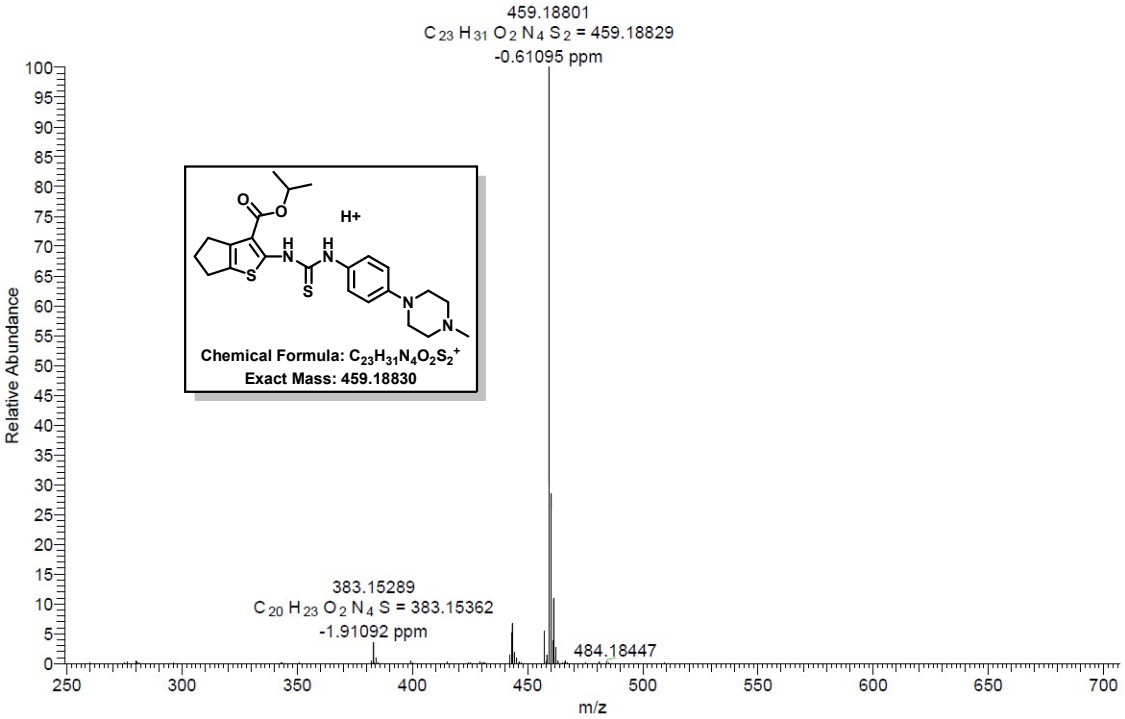

Figure S60. HRMS spectrum of **10d**.

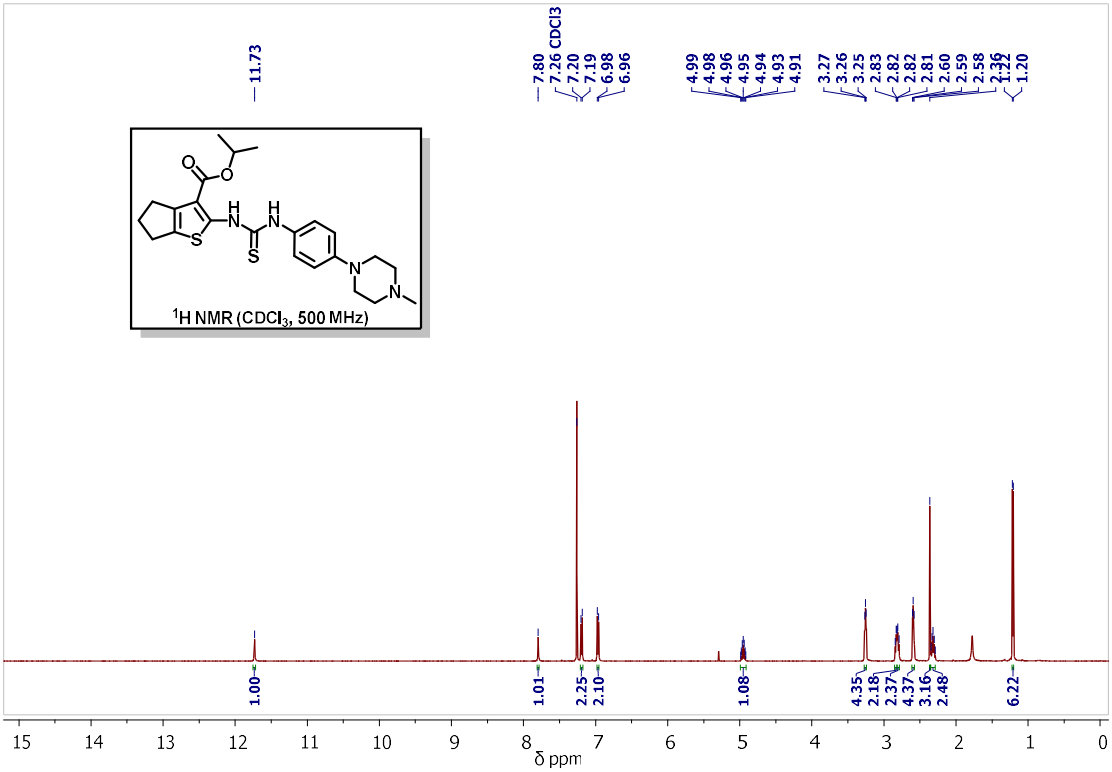

Figure S61. ^{1}H NMR spectra (500 MHz, RT) of compound **10d** in $CDCl_3$.

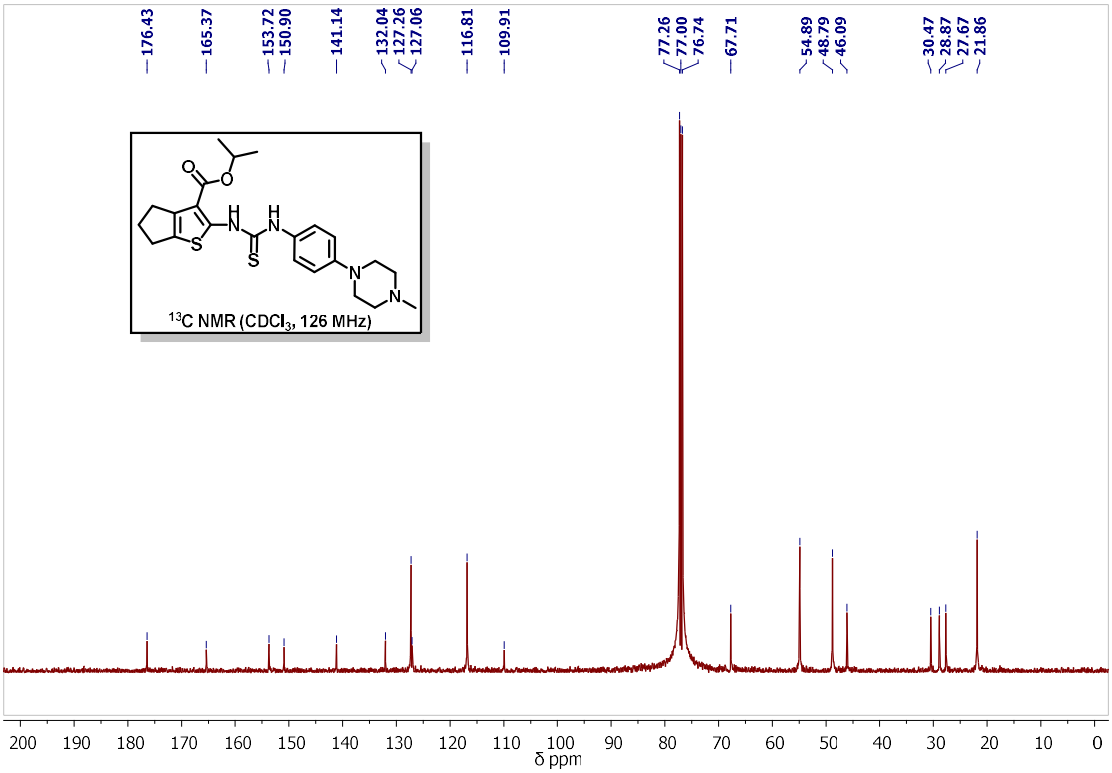

Figure S62. $^{13}C\{^{1}H\}$ NMR spectra (126 MHz, RT) of compound **10d** in $CDCl_3$.

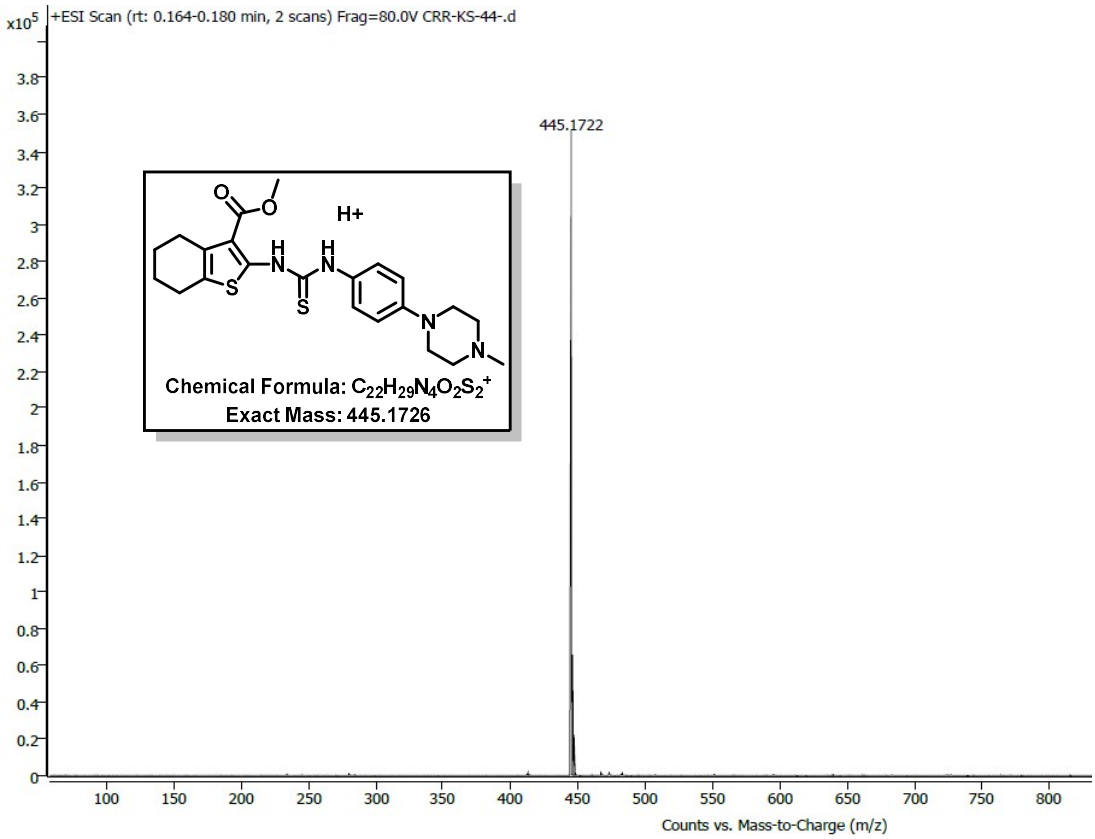

Figure S63. HRMS spectrum of **10e**.

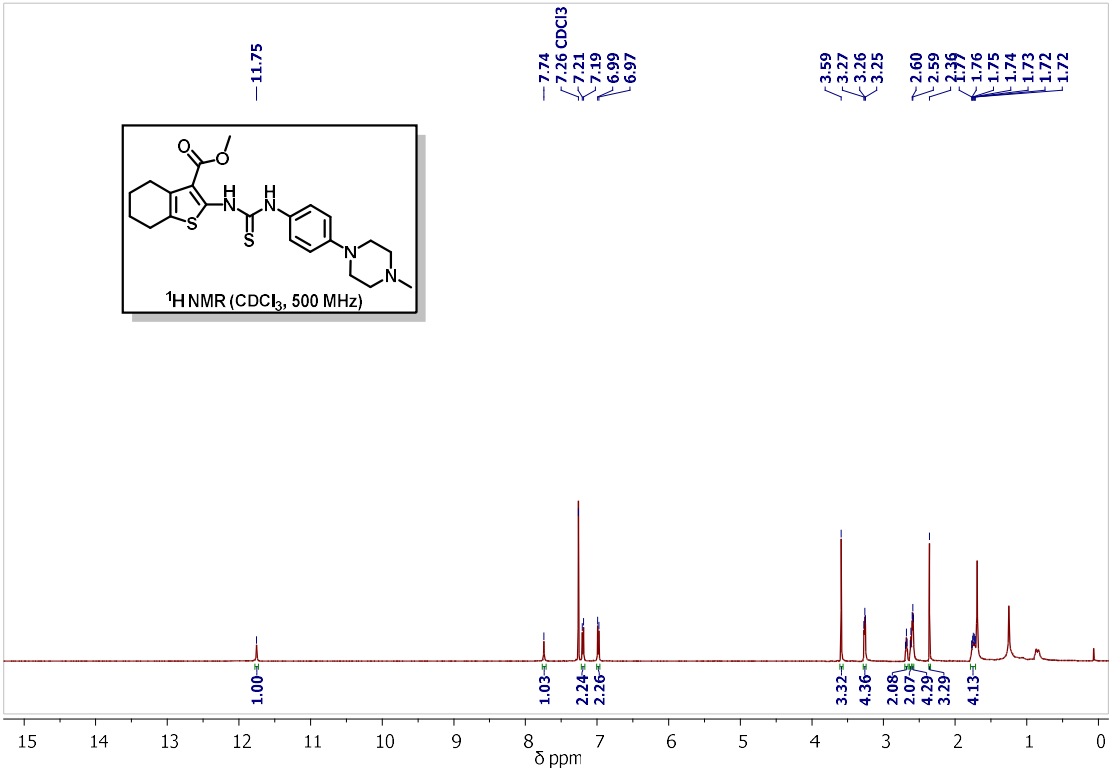

Figure S64. ^{1}H NMR spectra (500 MHz, RT) of compound **10e** in $CDCl_3$.

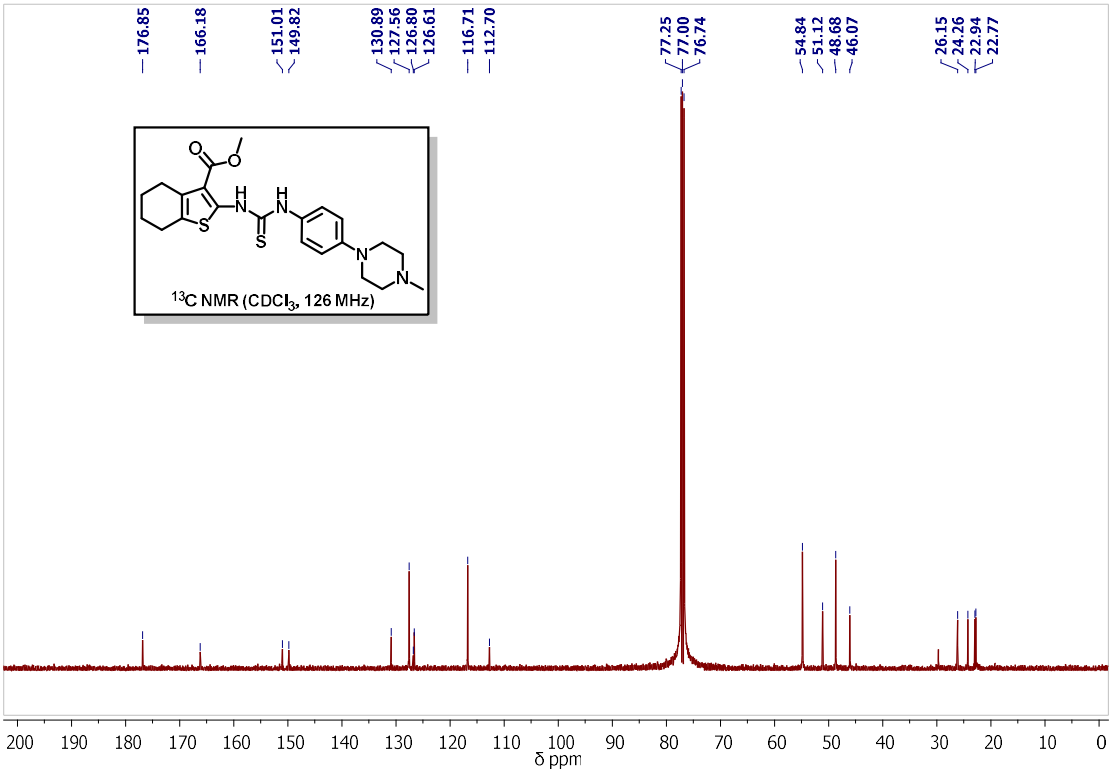

Figure S65. $^{13}C\{^{1}H\}$ NMR spectra (126 MHz, RT) of compound **10e** in $CDCl_3$.

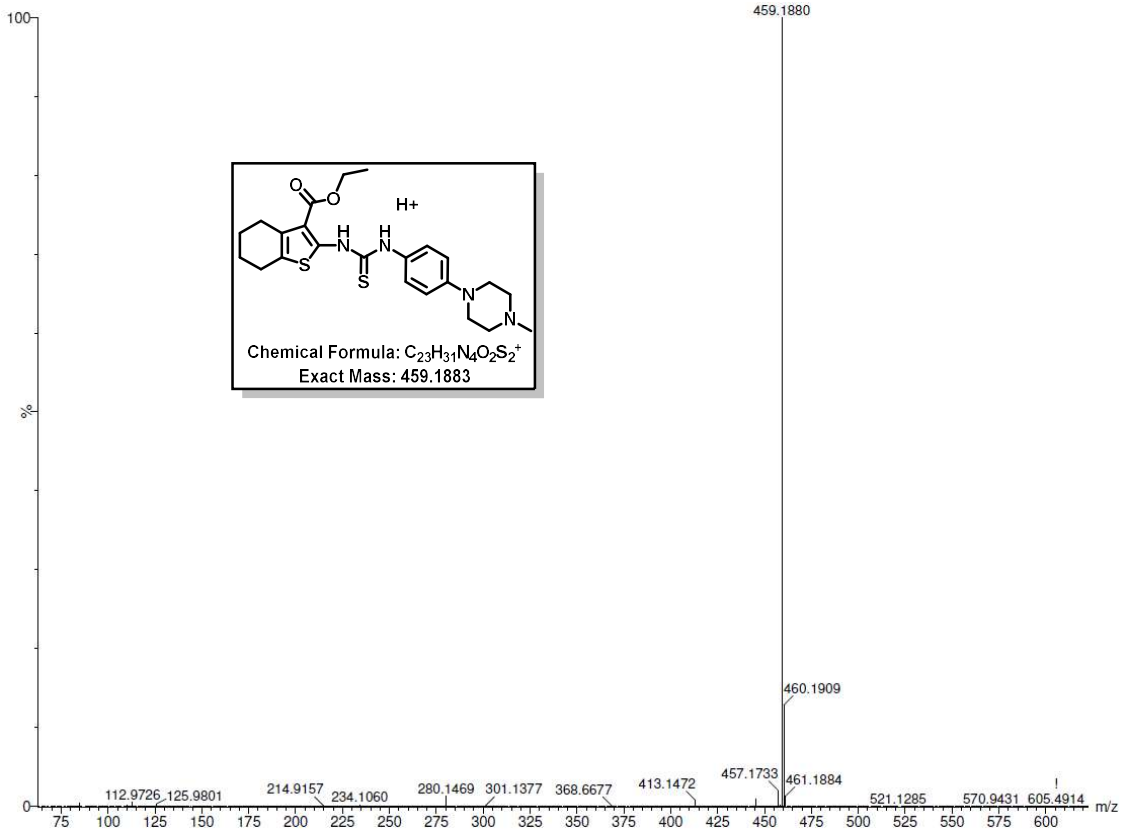

Figure S66. HRMS spectrum of **10f**.

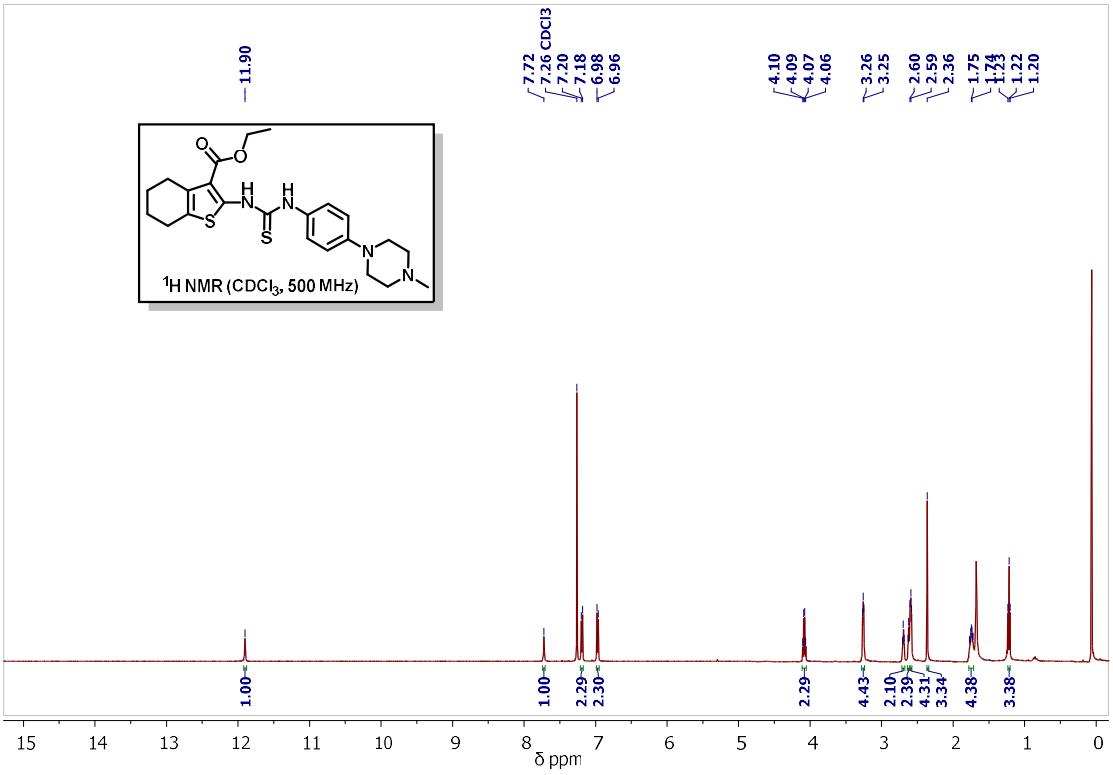

Figure S67. ^{1}H NMR spectra (500 MHz, RT) of compound **10f** in $CDCl_3$.

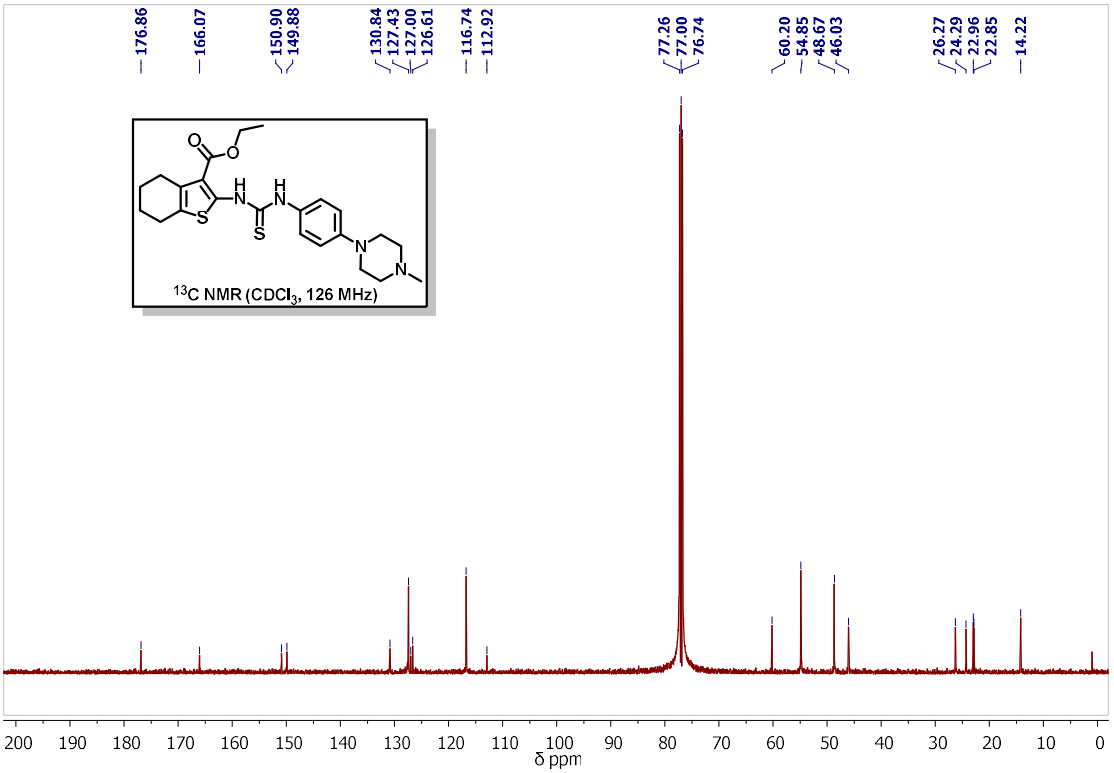

Figure S68. $^{13}C\{^{1}H\}$ NMR spectra (126 MHz, RT) of compound **10f** in $CDCl_3$.

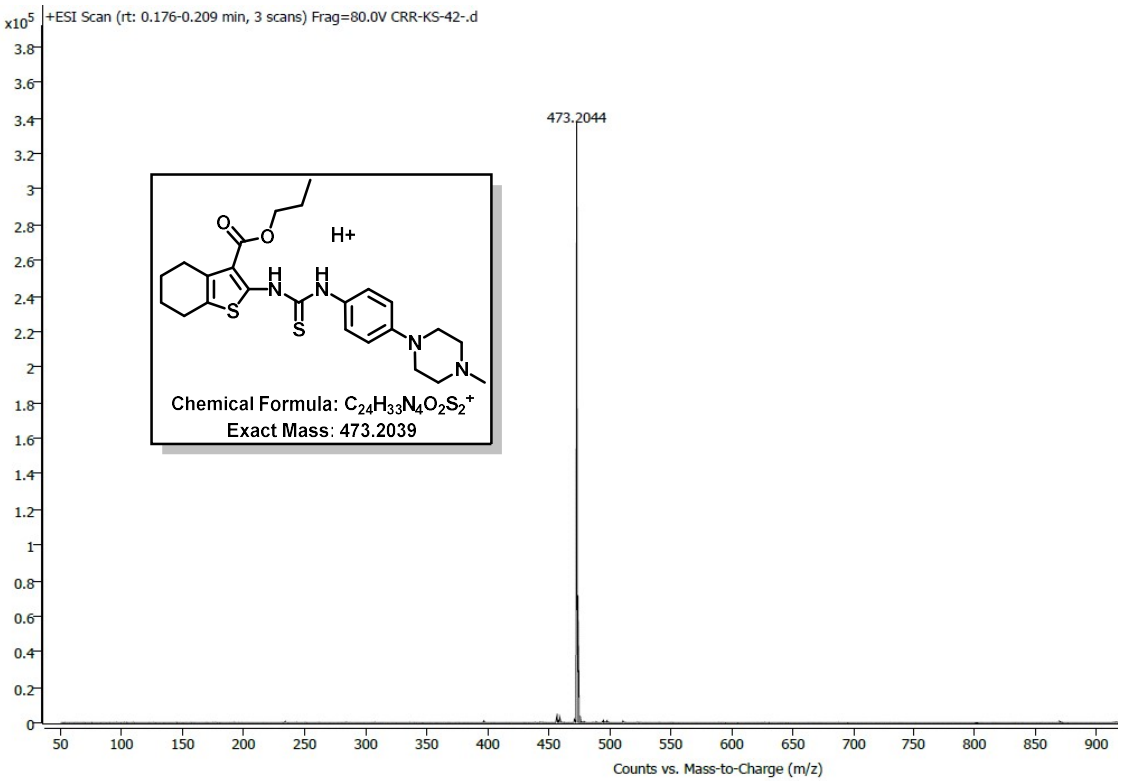

Figure S69. HRMS spectrum of **10g**.

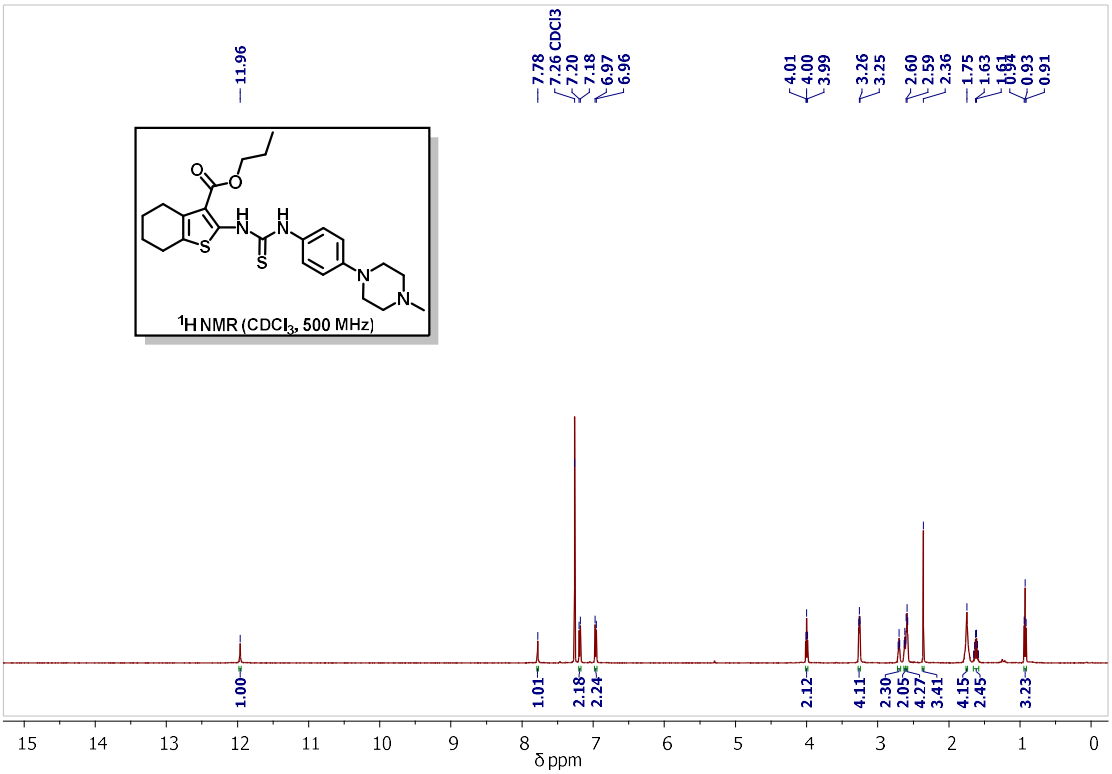

Figure S70. ^{1}H NMR spectra (500 MHz, RT) of compound **10g** in $CDCl_3$.

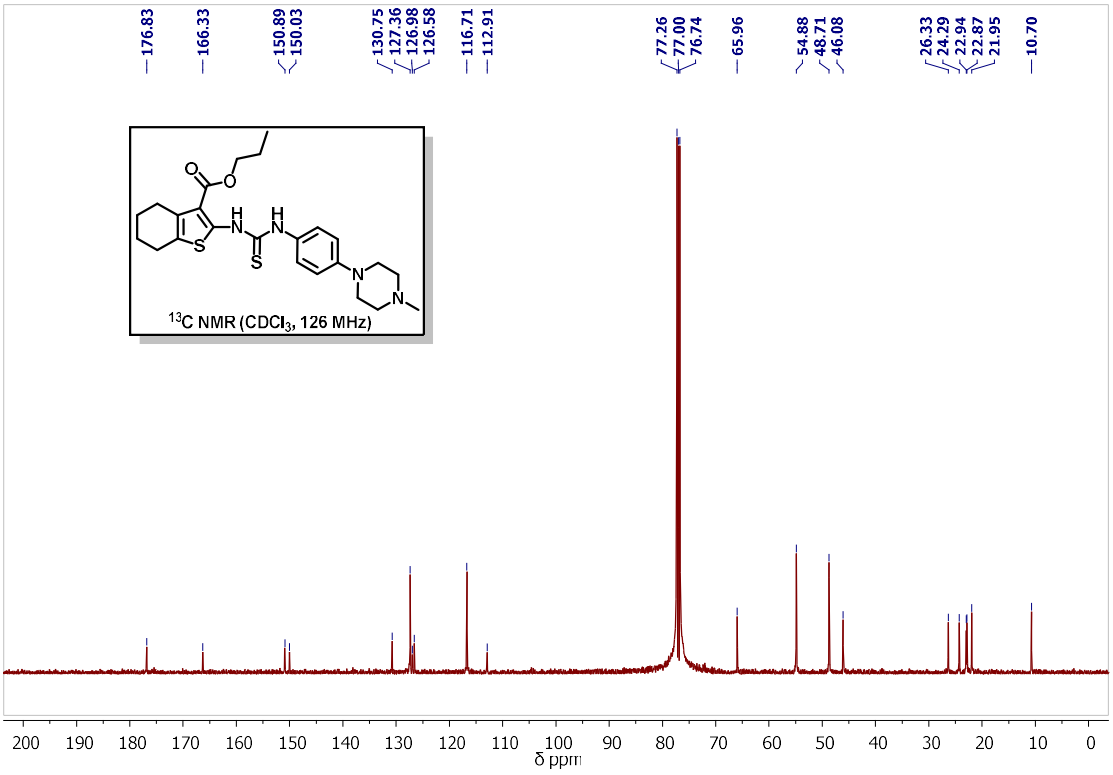

Figure S71. $^{13}C\{^{1}H\}$ NMR spectra (126 MHz, RT) of compound **10g** in $CDCl_3$.

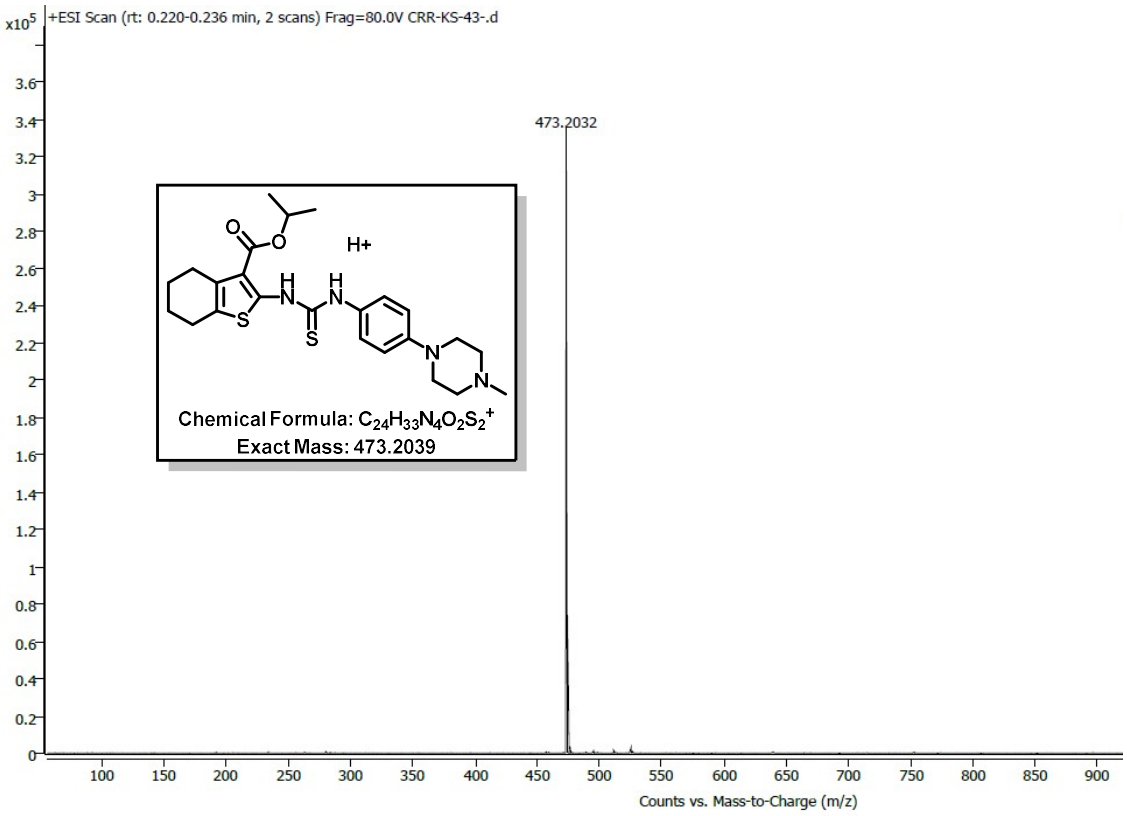

Figure S72. HRMS spectrum of **10h**.

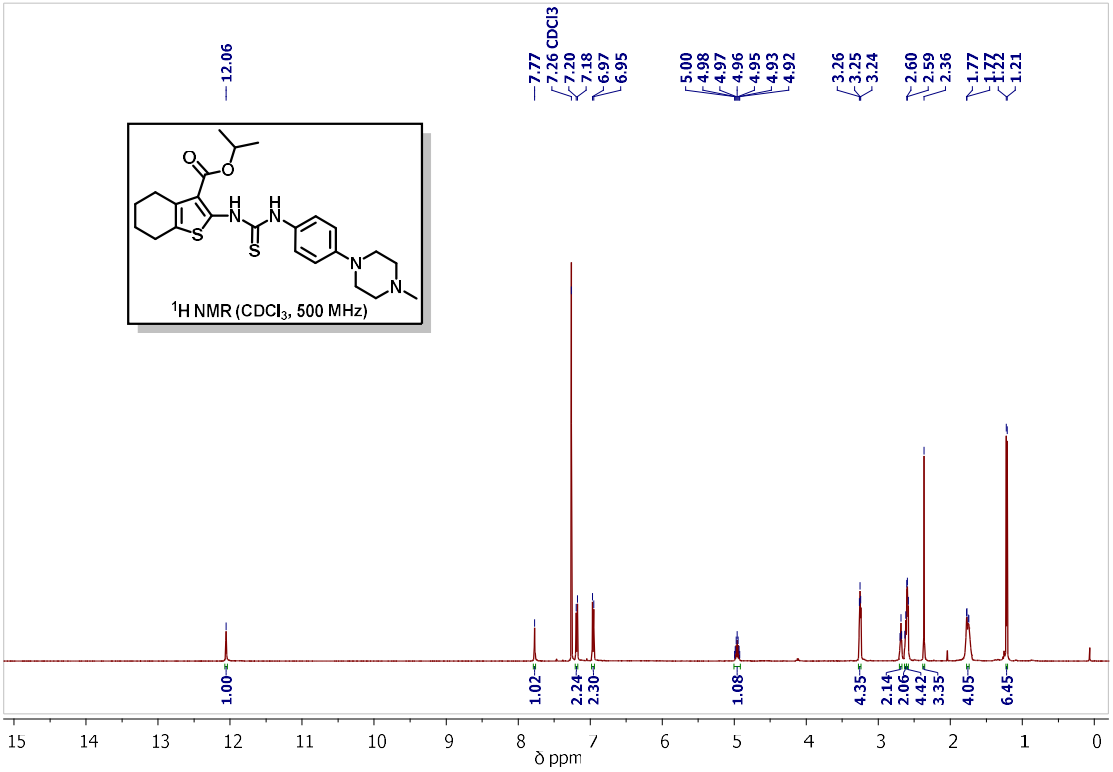

Figure S73. ^{1}H NMR spectra (500 MHz, RT) of compound **10h** in $CDCl_3$.

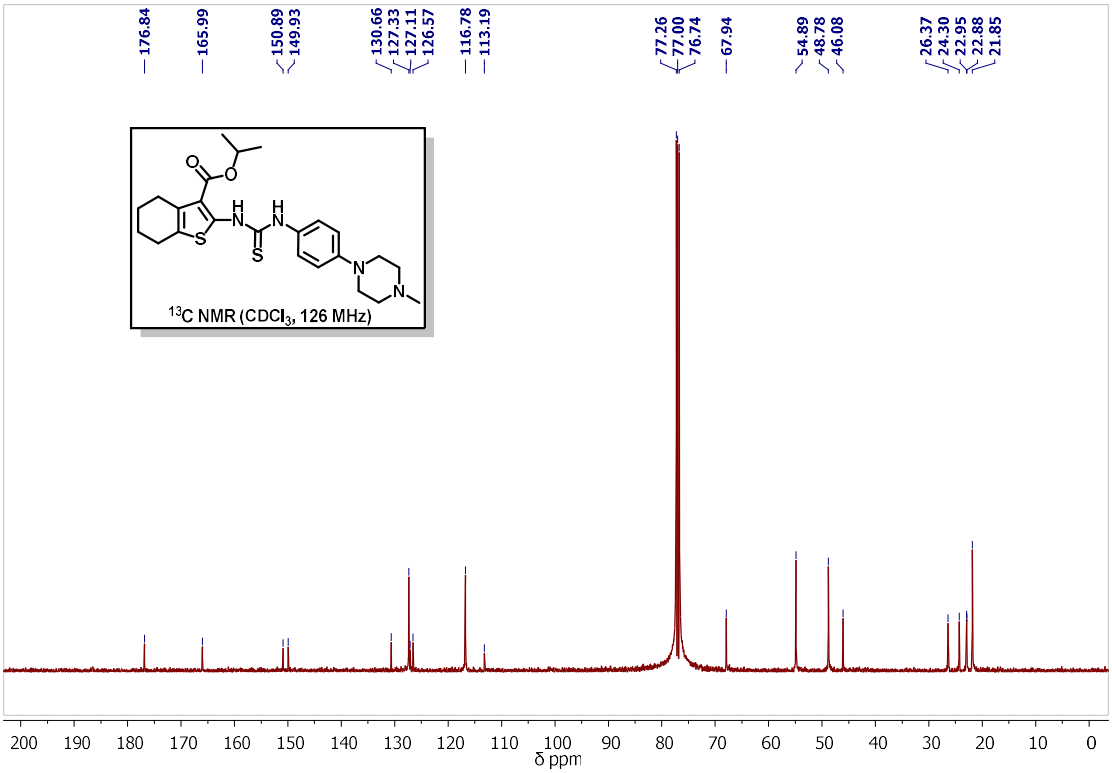

Figure S74. $^{13}C\{^{1}H\}$ NMR spectra (126 MHz, RT) of compound **10h** in $CDCl_3$.

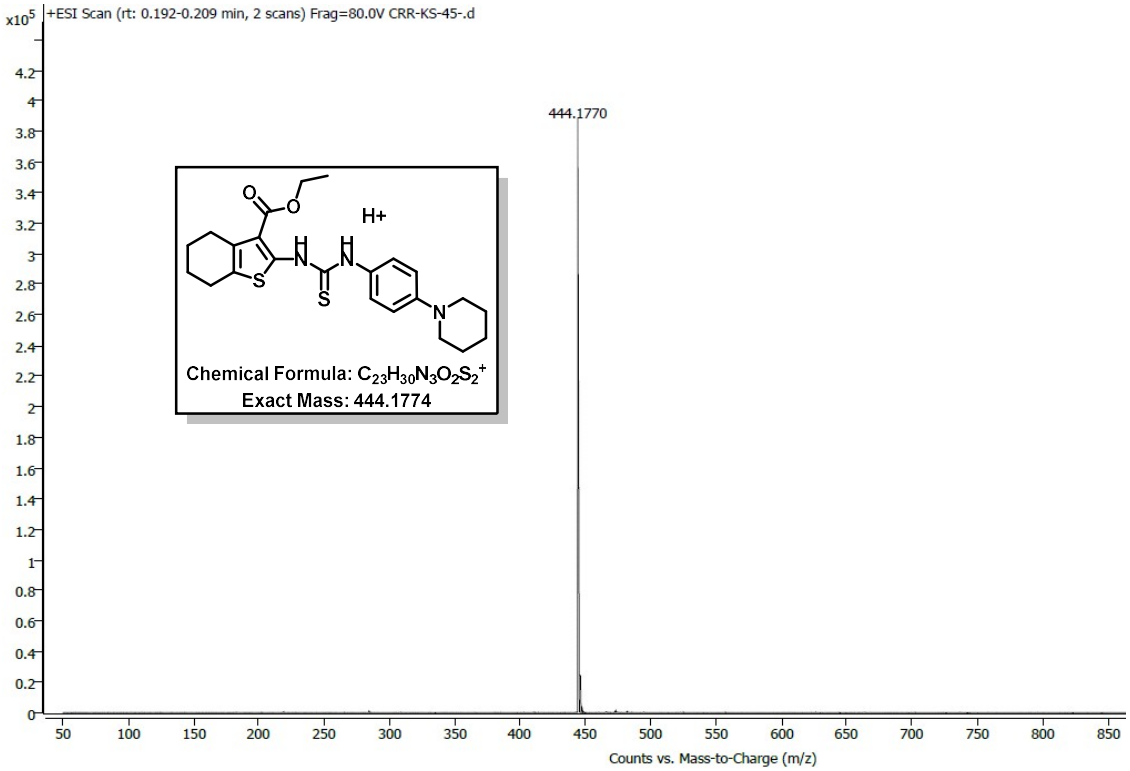

Figure S75. HRMS spectrum of **11a**.

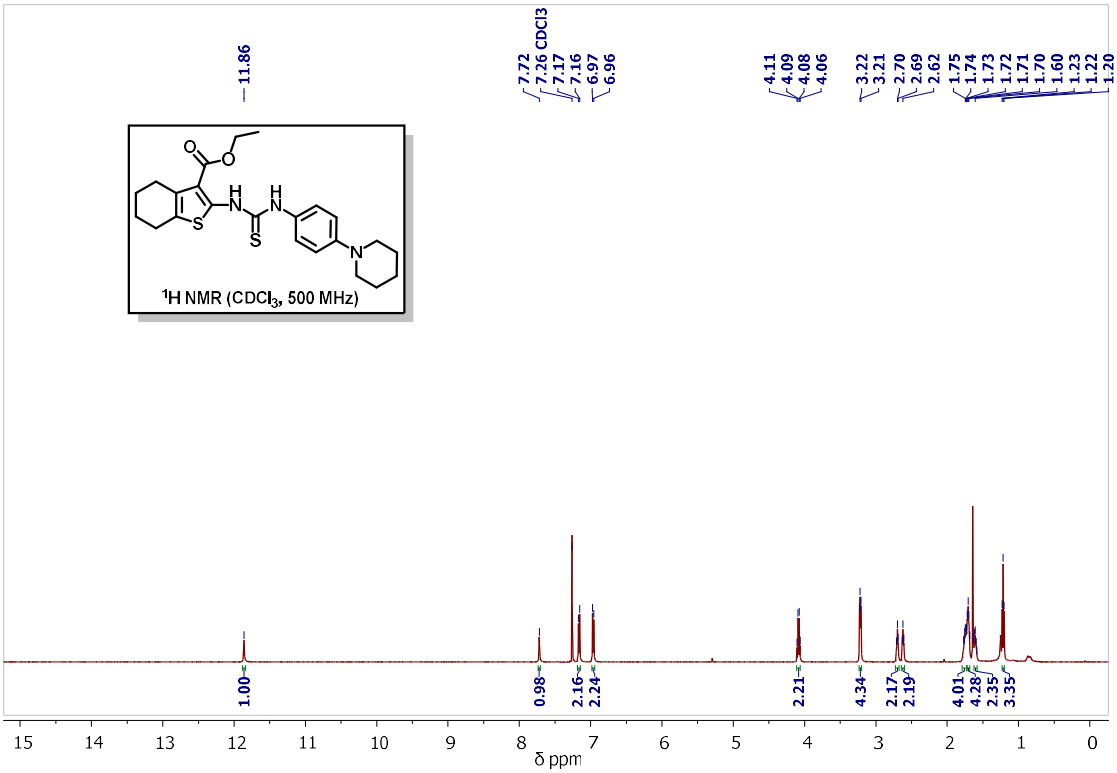

Figure S76. ^{1}H NMR spectra (500 MHz, RT) of compound **11a** in $CDCl_3$.

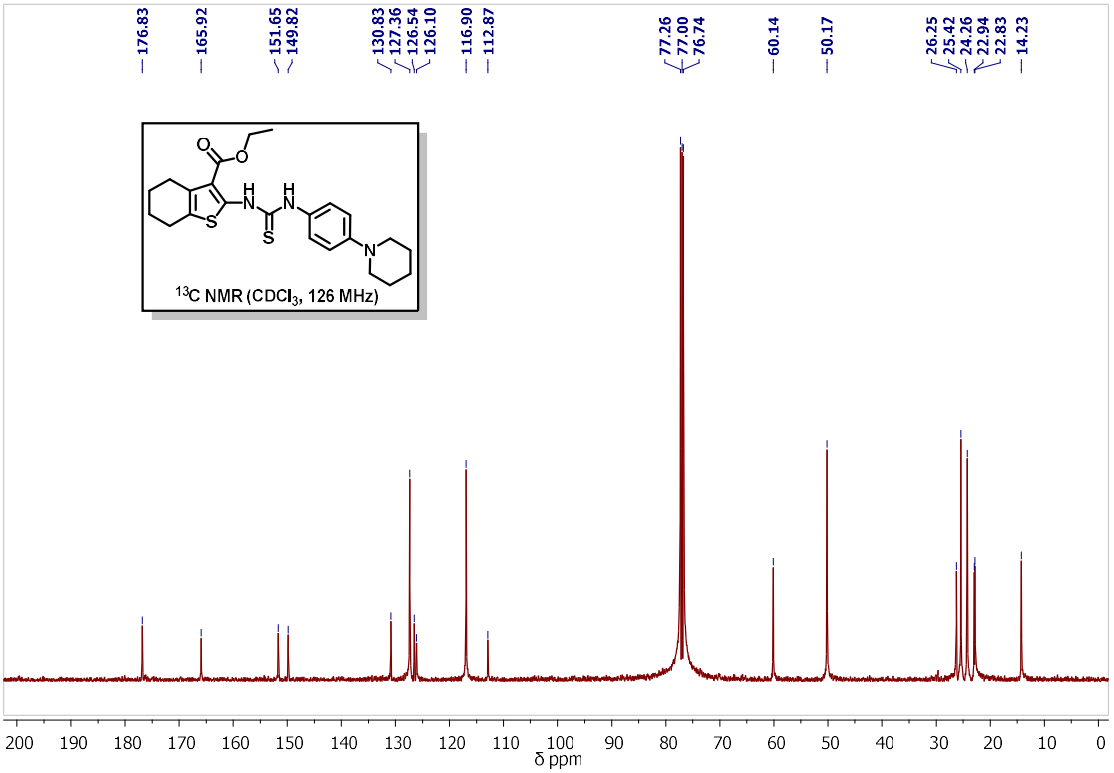

Figure S77. $^{13}C\{^{1}H\}$ NMR spectra (126 MHz, RT) of compound **11a** in $CDCl_3$.

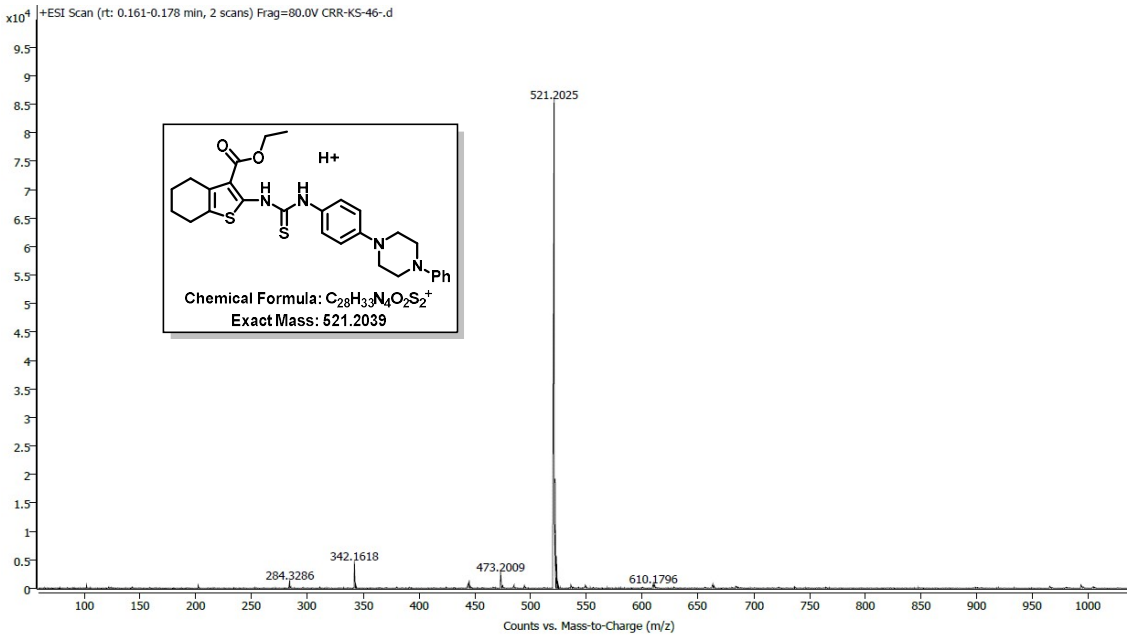

Figure S78. HRMS spectrum of **11b**.

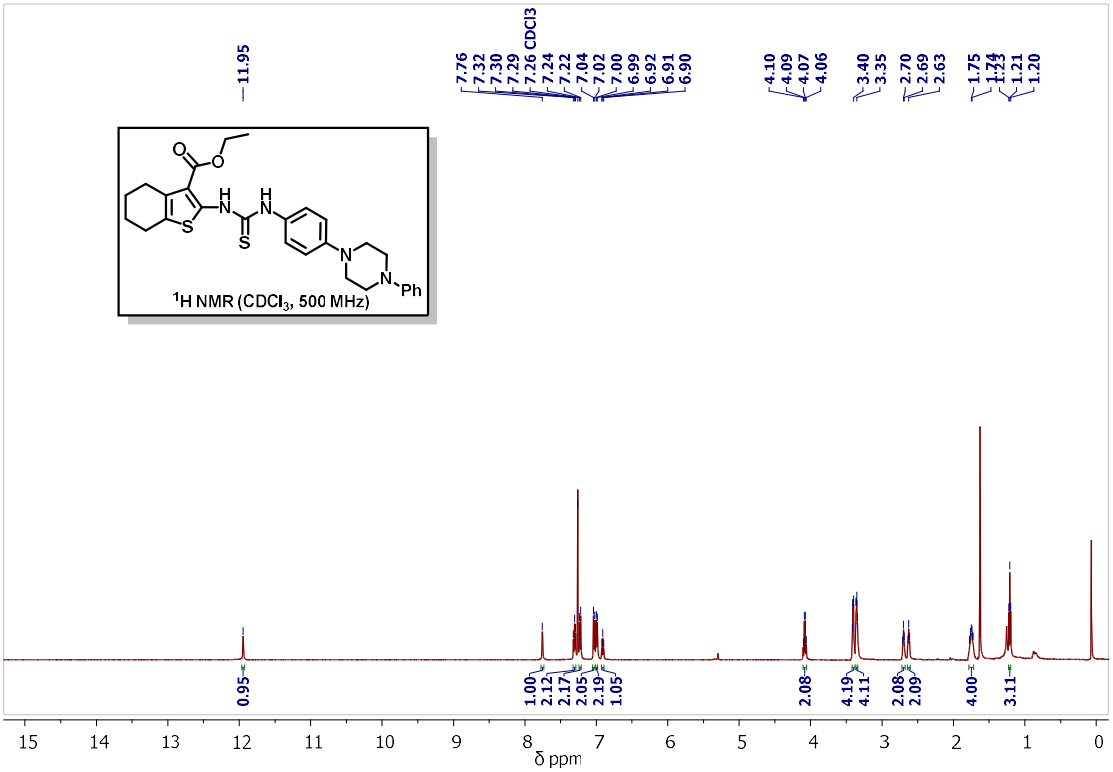

Figure S79. ^{1}H NMR spectra (500 MHz, RT) of compound **11b** in $CDCl_3$.

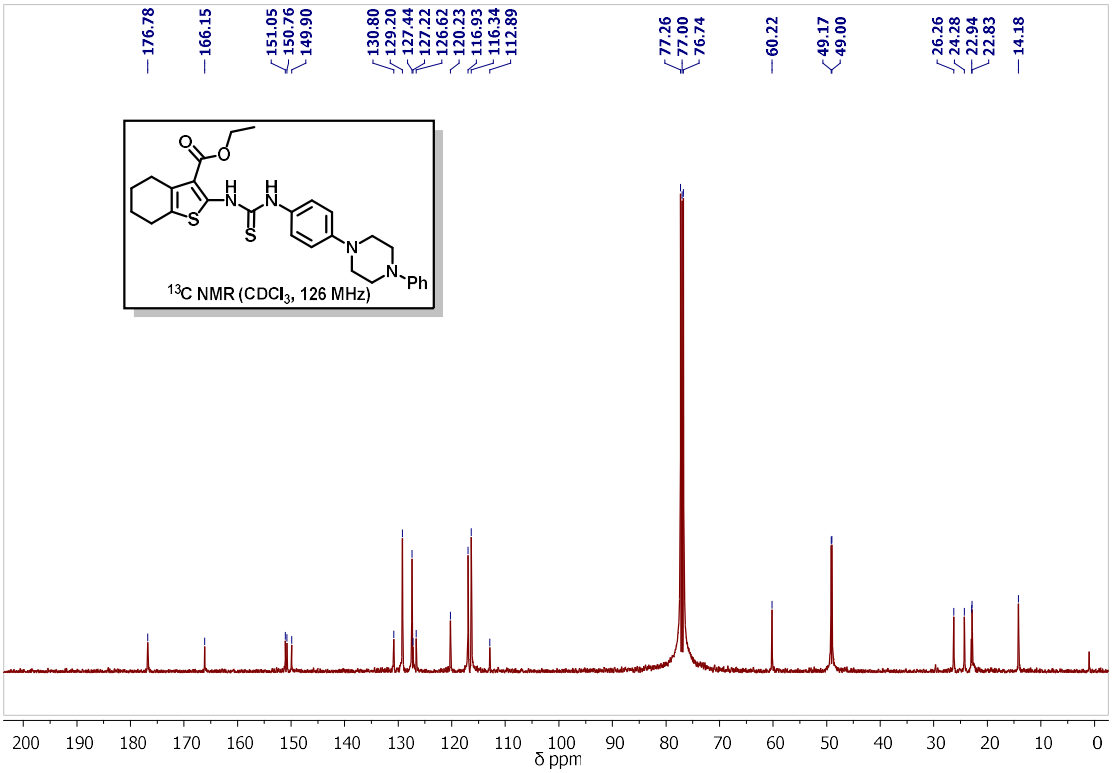

Figure S80. $^{13}C\{^{1}H\}$ NMR spectra (126 MHz, RT) of compound **11b** in $CDCl_3$.

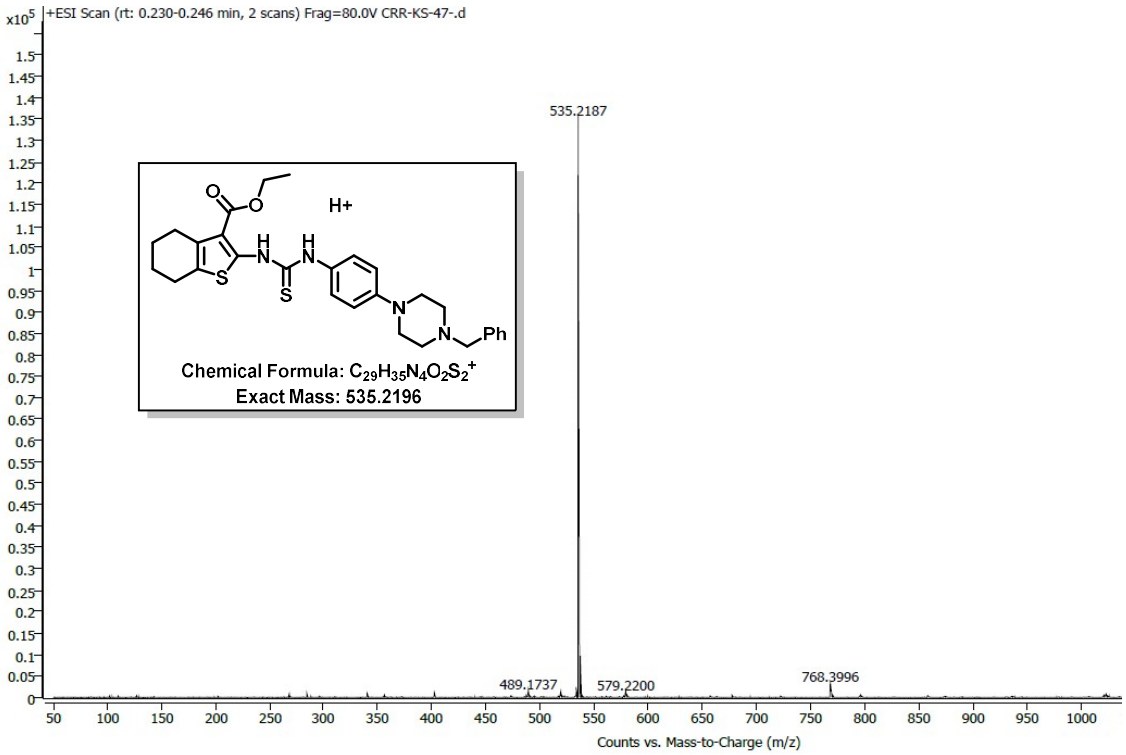

Figure S81. HRMS spectrum of **11c**.

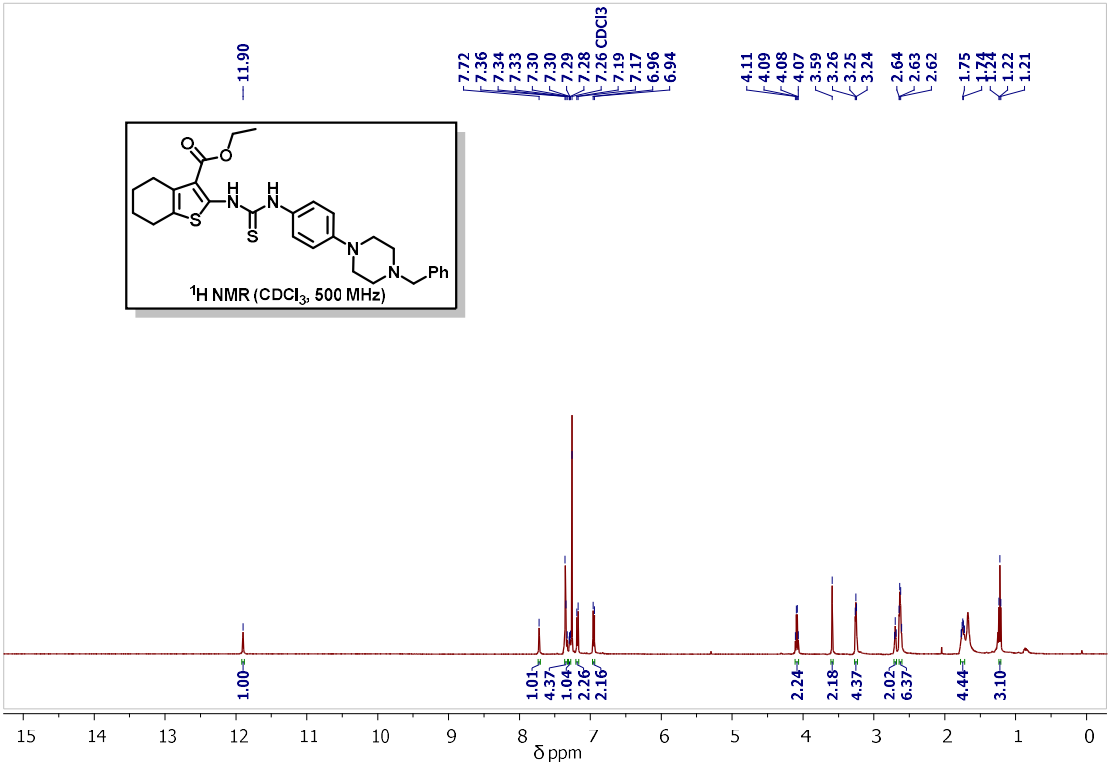

Figure S82. ^{1}H NMR spectra (500 MHz, RT) of compound **11c** in $CDCl_3$.

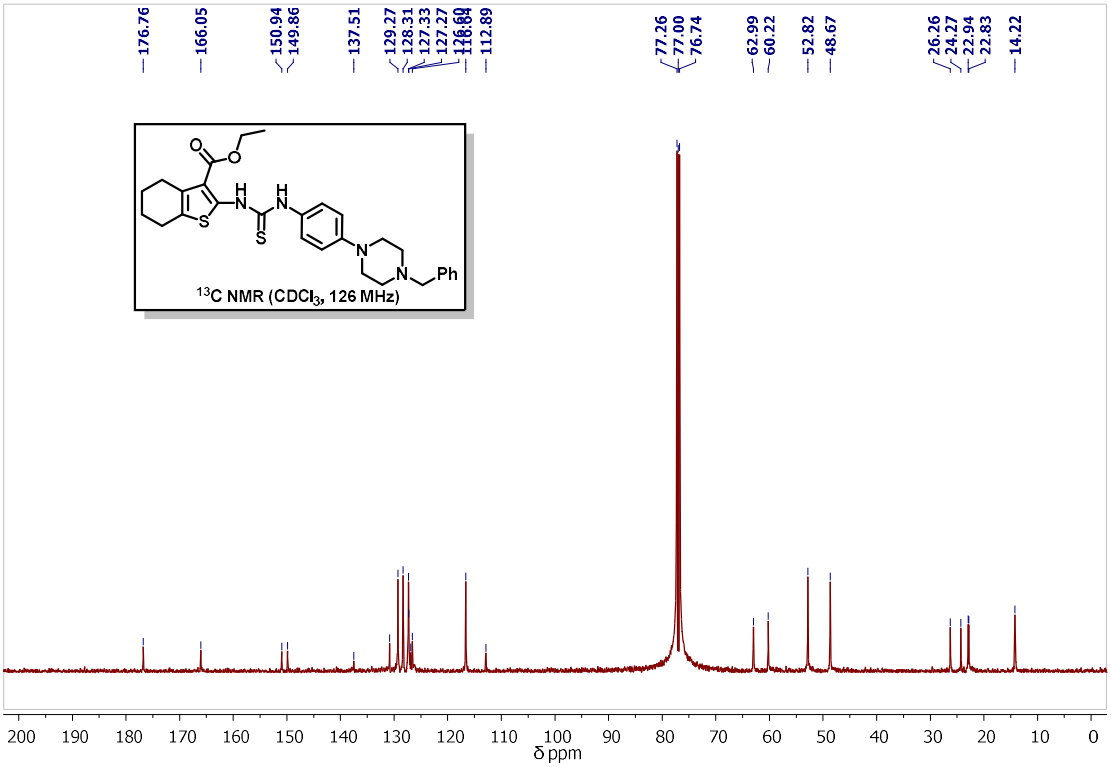

Figure S83. $^{13}C\{^{1}H\}$ NMR spectra (126 MHz, RT) of compound **11c** in $CDCl_3$.

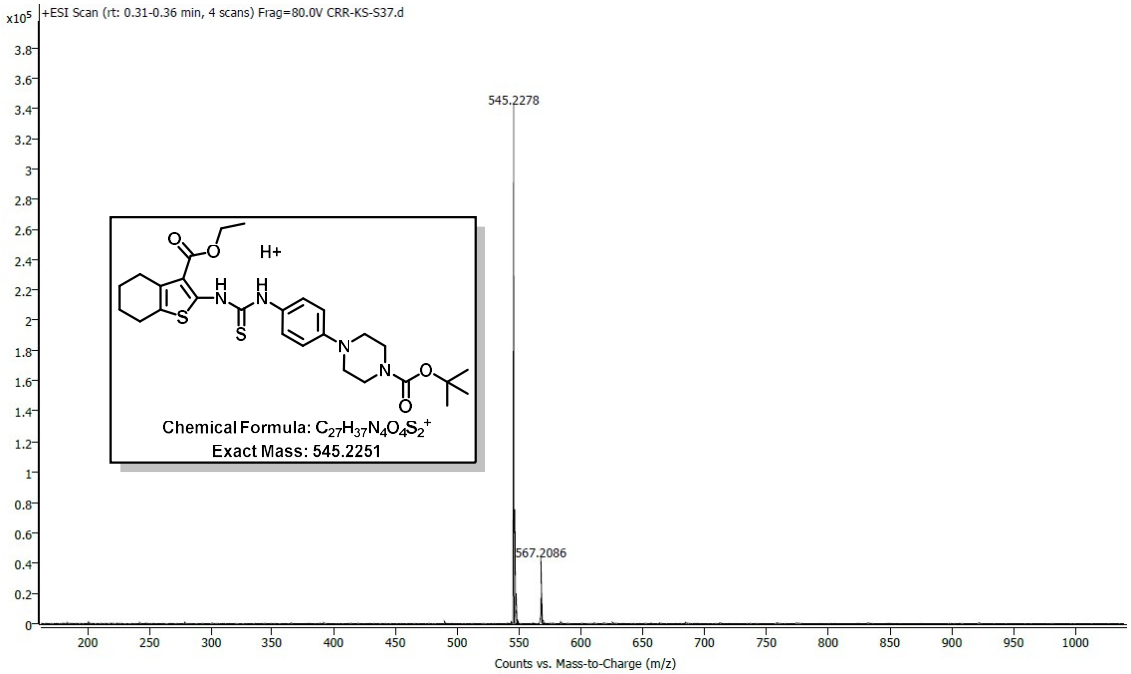

Figure S84. HRMS spectrum of **11d**.

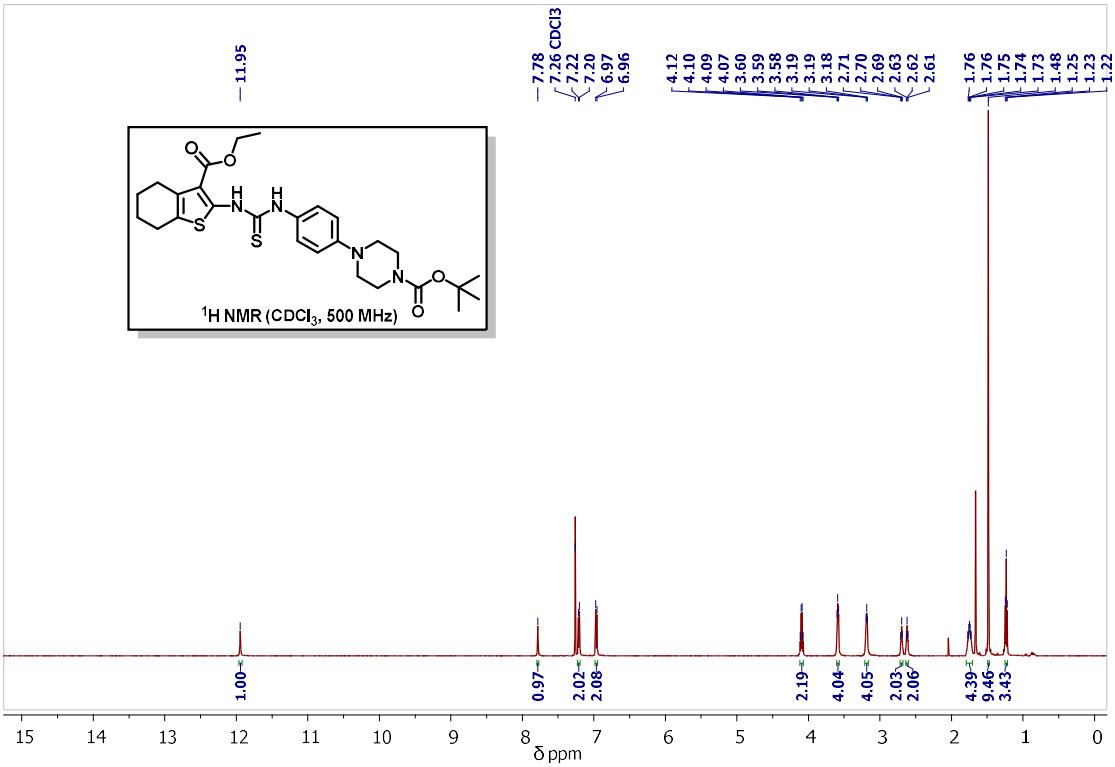

Figure S85. ^{1}H NMR spectra (500 MHz, RT) of compound **11d** in $CDCl_3$.

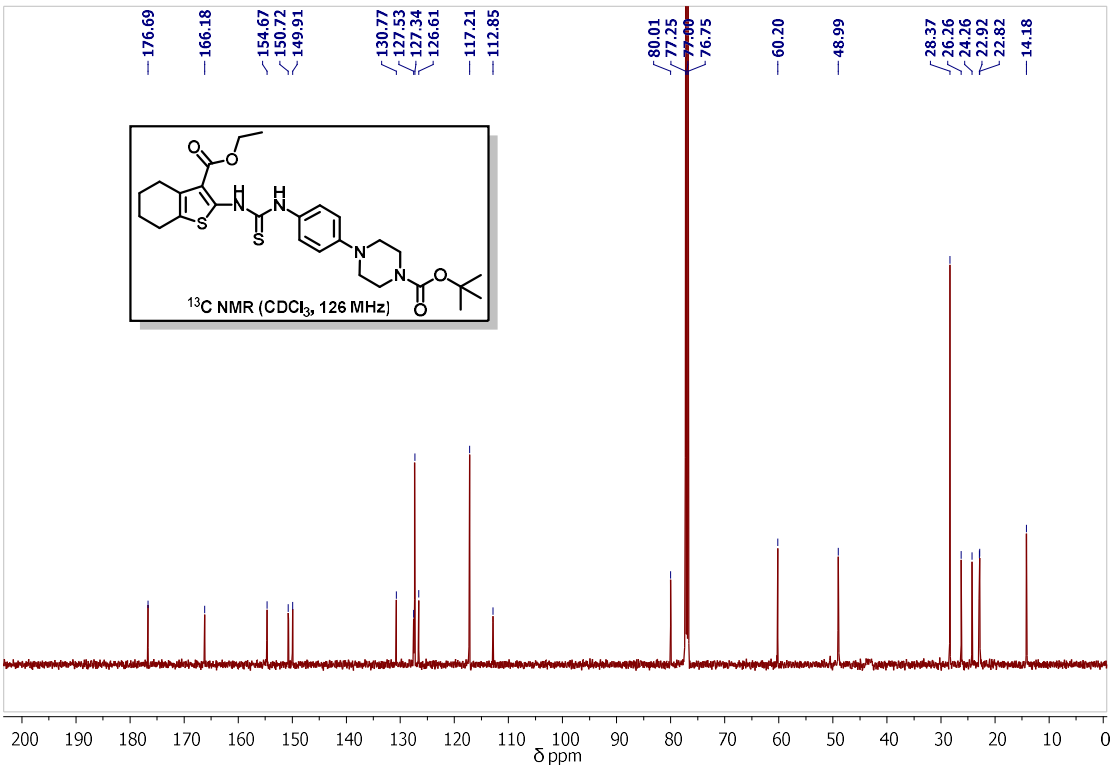

Figure S86. $^{13}C\{^{1}H\}$ NMR spectra (126 MHz, RT) of compound **11d** in $CDCl_3$.

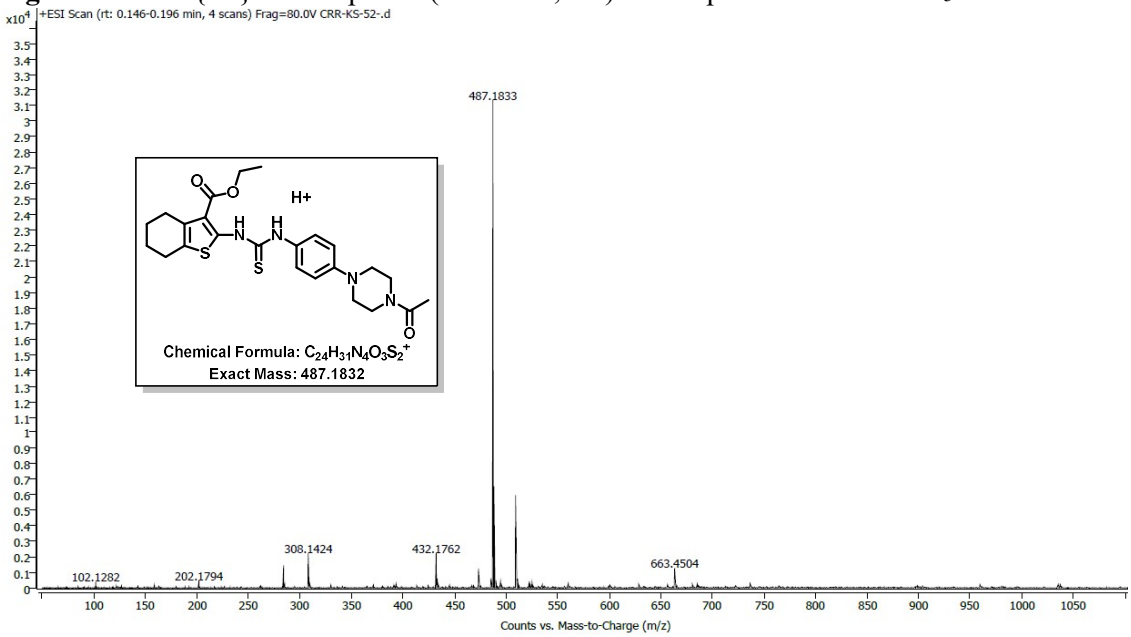

Figure S87. HRMS spectrum of **11e**.

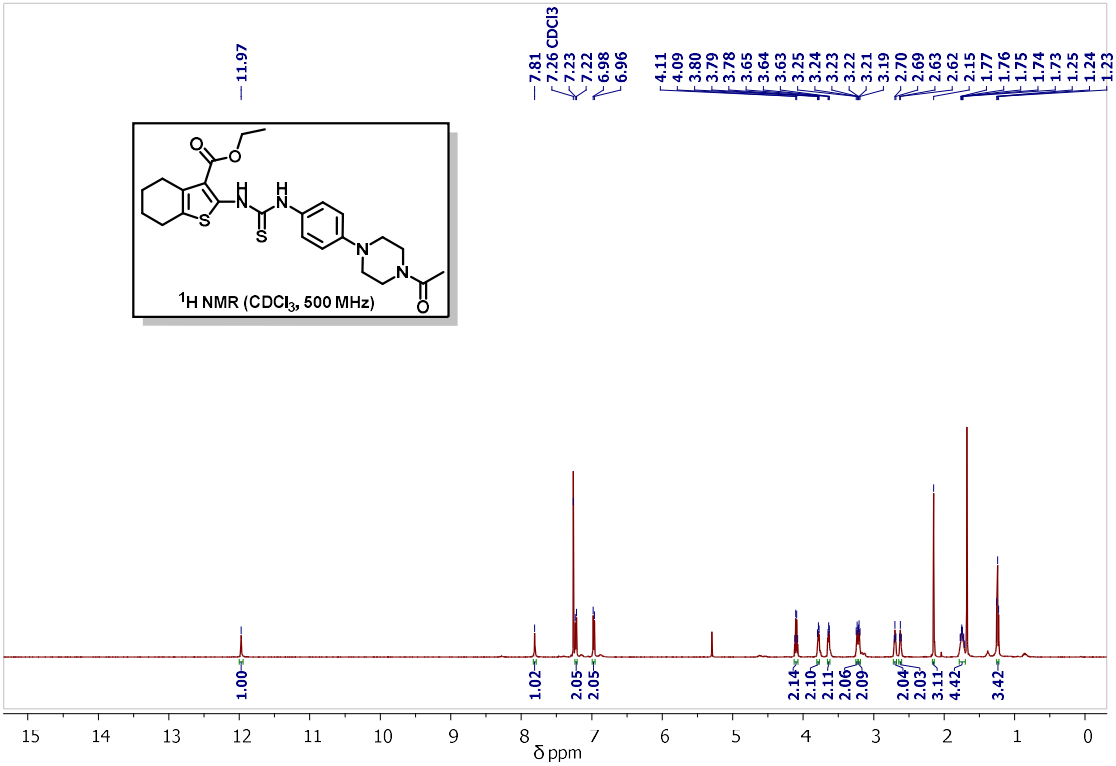

Figure S88. ^{1}H NMR spectra (500 MHz, RT) of compound **11e** in $CDCl_3$.

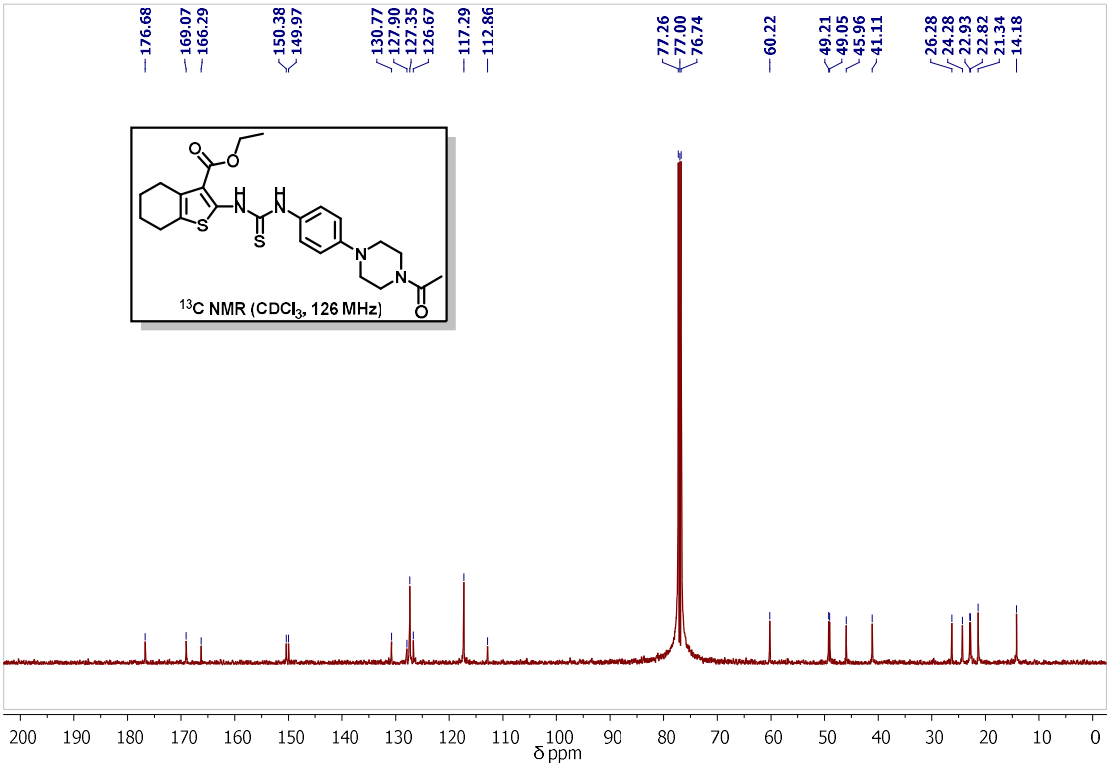

Figure S89. $^{13}C\{^{1}H\}$ NMR spectra (126 MHz, RT) of compound **11e** in $CDCl_3$.

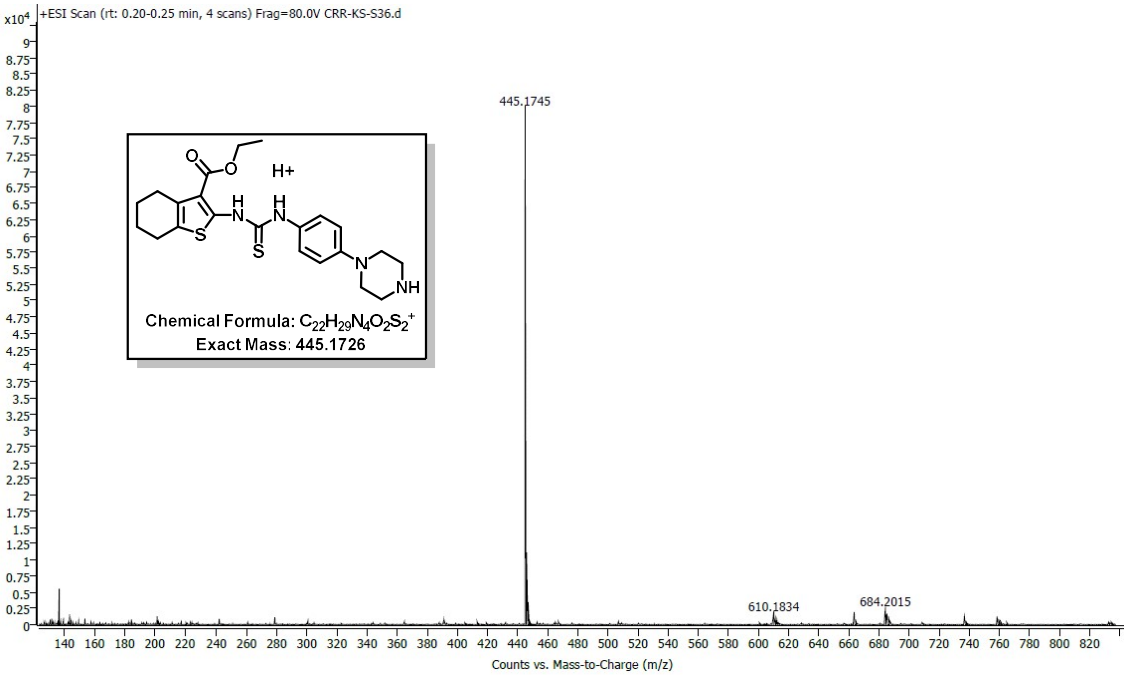

Figure S90. HRMS spectrum of **11f**.

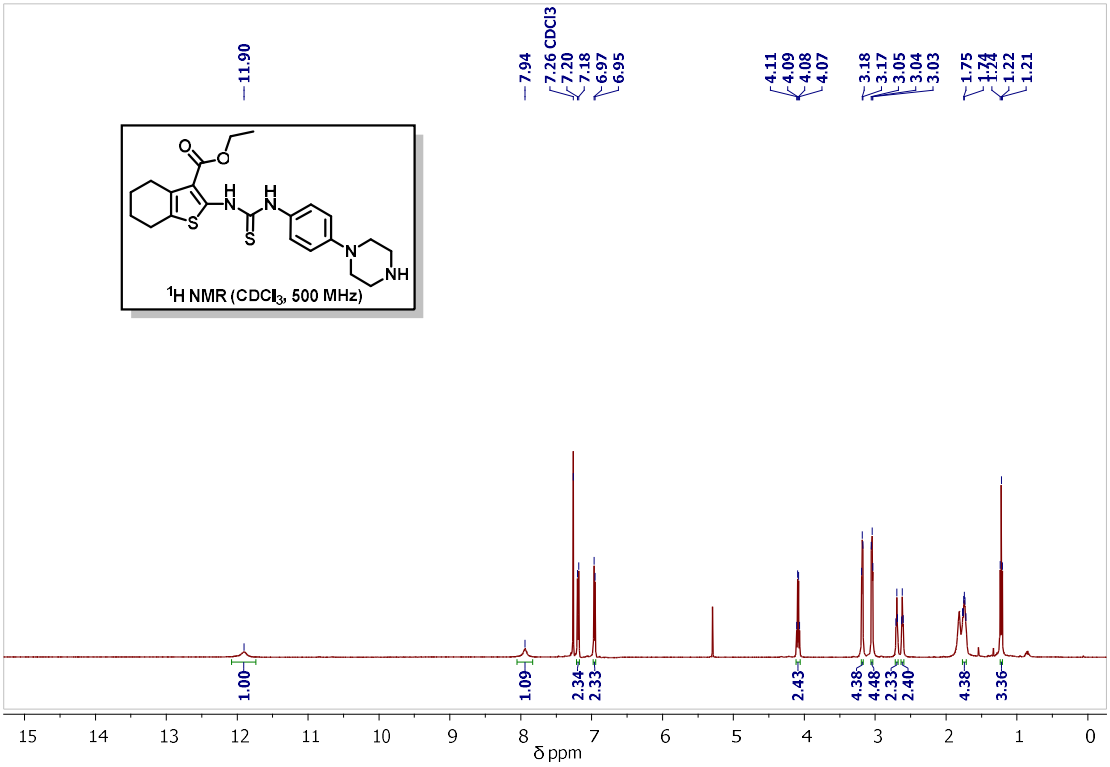

Figure S91. ^{1}H NMR spectra (500 MHz, RT) of compound **11f** in $CDCl_3$.

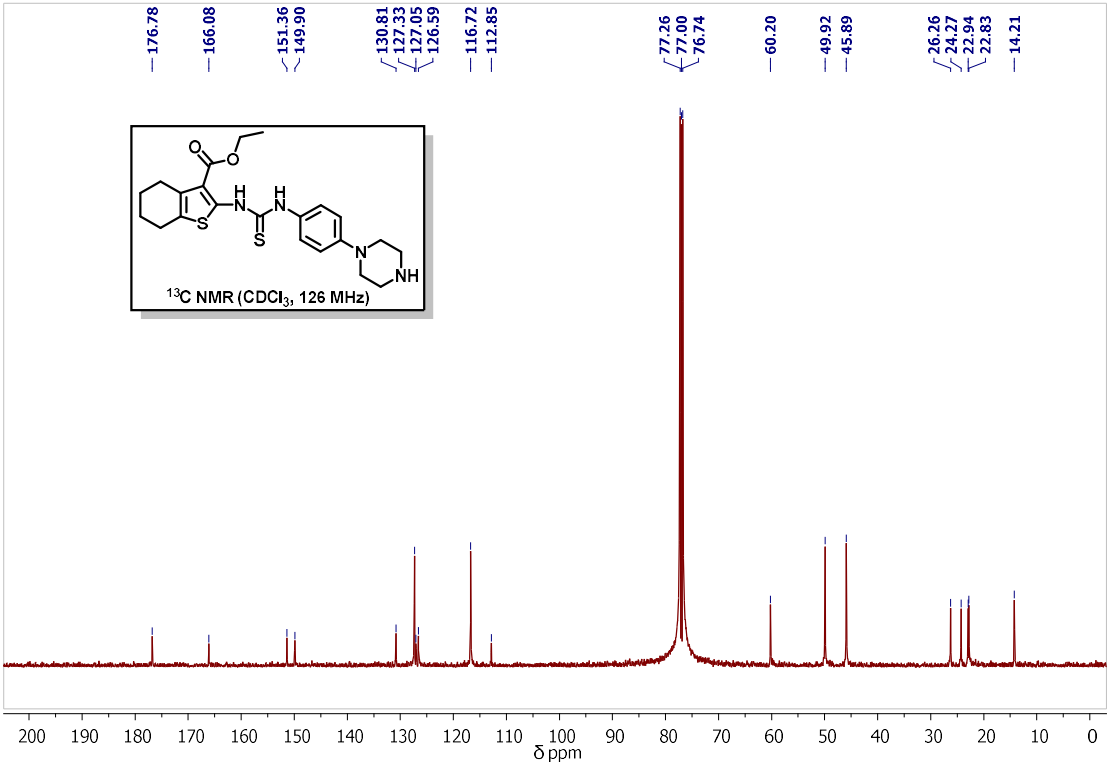

Figure S92. $^{13}C\{^{1}H\}$ NMR spectra (126 MHz, RT) of compound **11f** in $CDCl_3$.

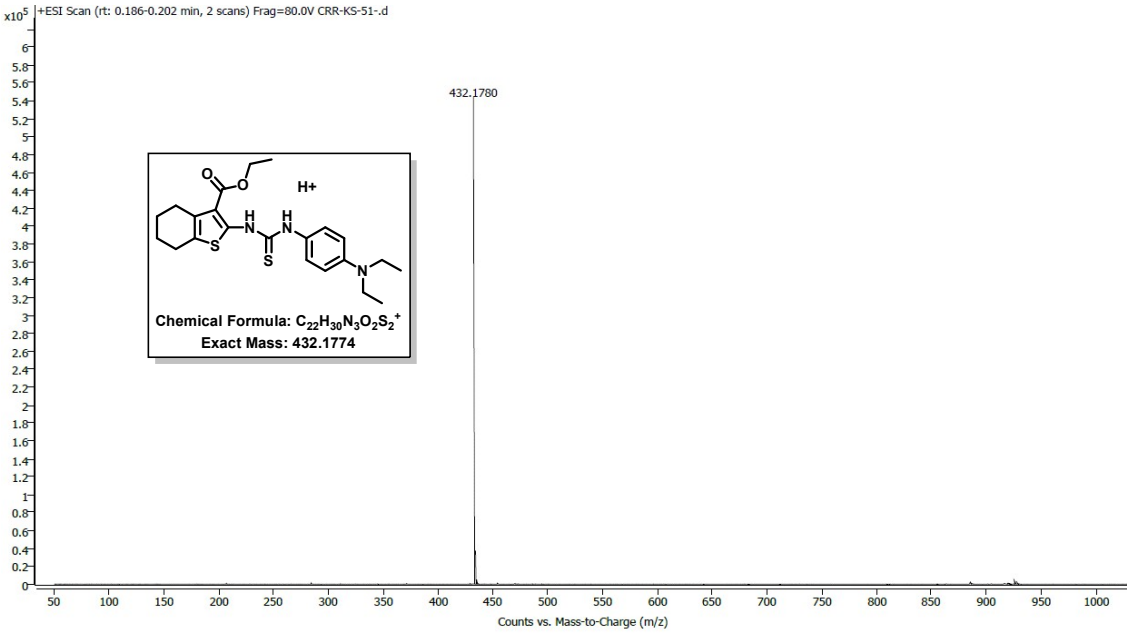

Figure S93. HRMS spectrum of **12a**.

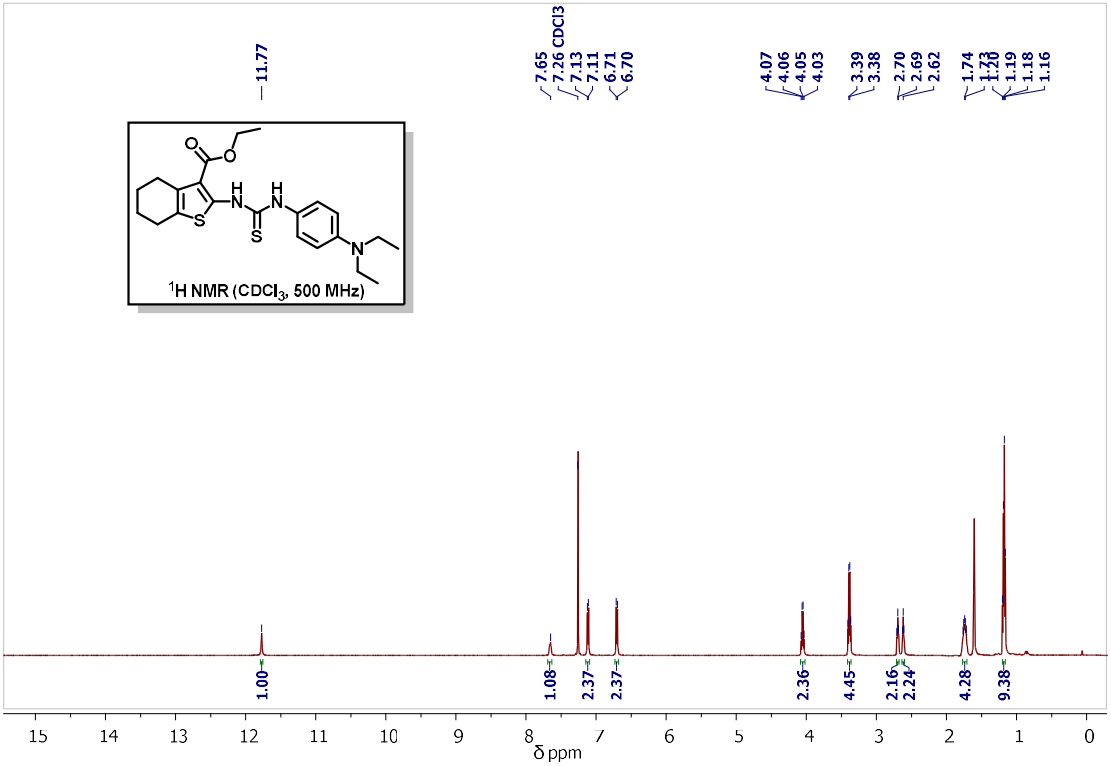

Figure S94. ^{1}H NMR spectra (500 MHz, RT) of compound **12a** in $CDCl_3$.

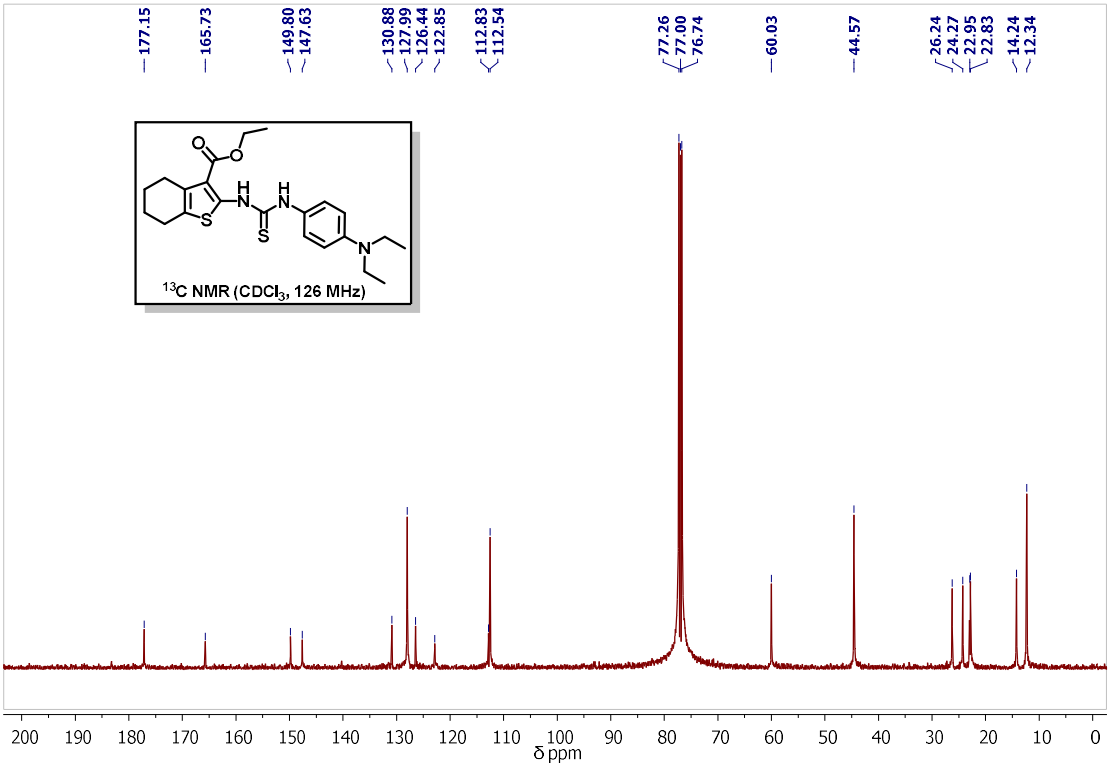

Figure S95. $^{13}C\{^{1}H\}$ NMR spectra (126 MHz, RT) of compound **12a** in $CDCl_3$.

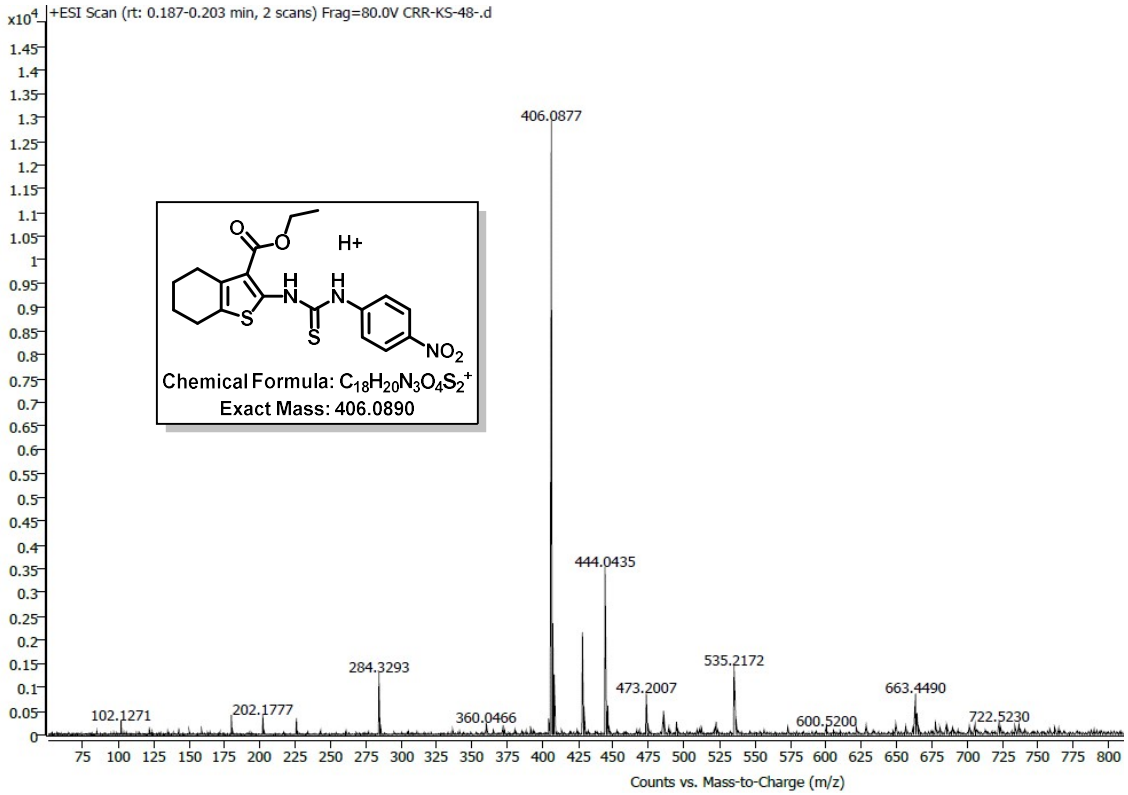

Figure S96. HRMS spectrum of **12b**.

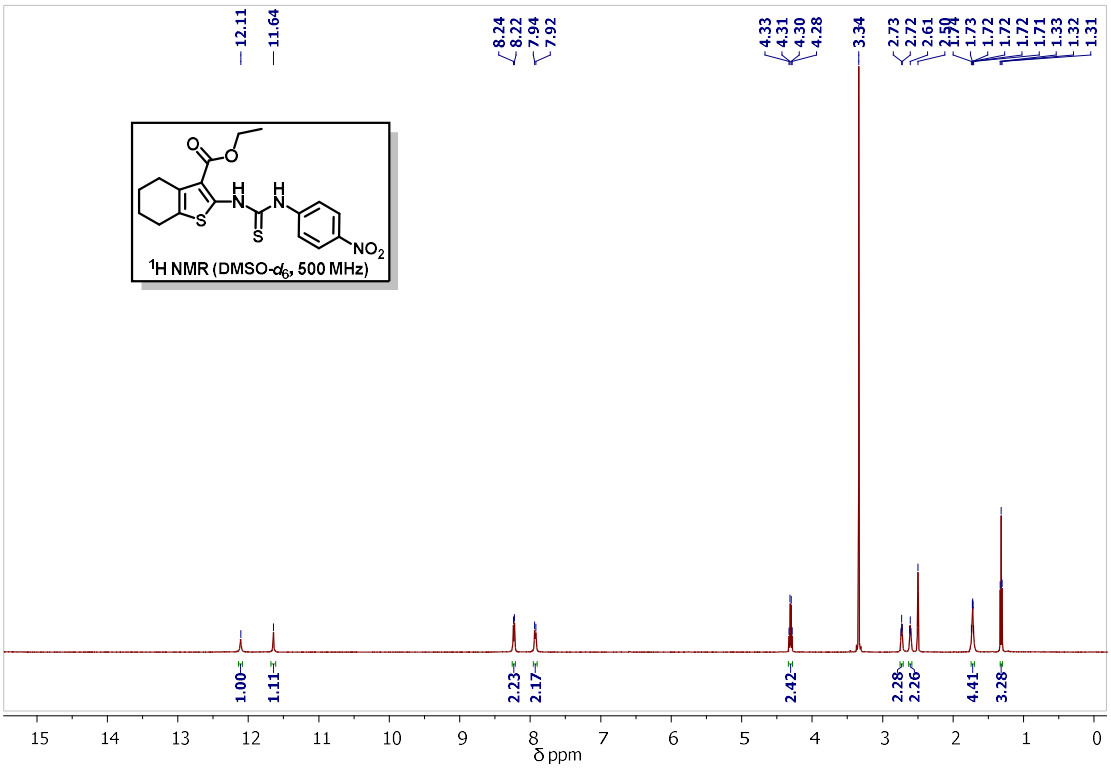

Figure S97. ^{1}H NMR spectra (500 MHz, RT) of compound **12b** in DMSO-d_6.

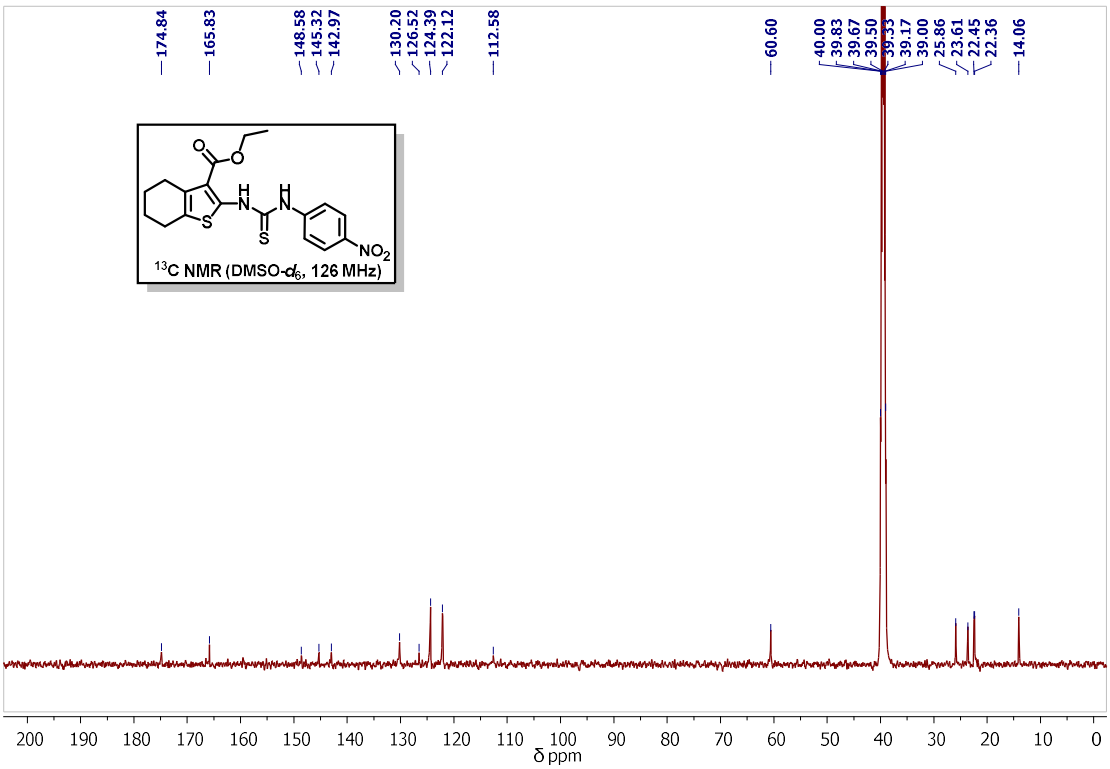

Figure S98. $^{13}C\{^{1}H\}$ NMR spectra (126 MHz, RT) of compound **12b** in DMSO-d_6.

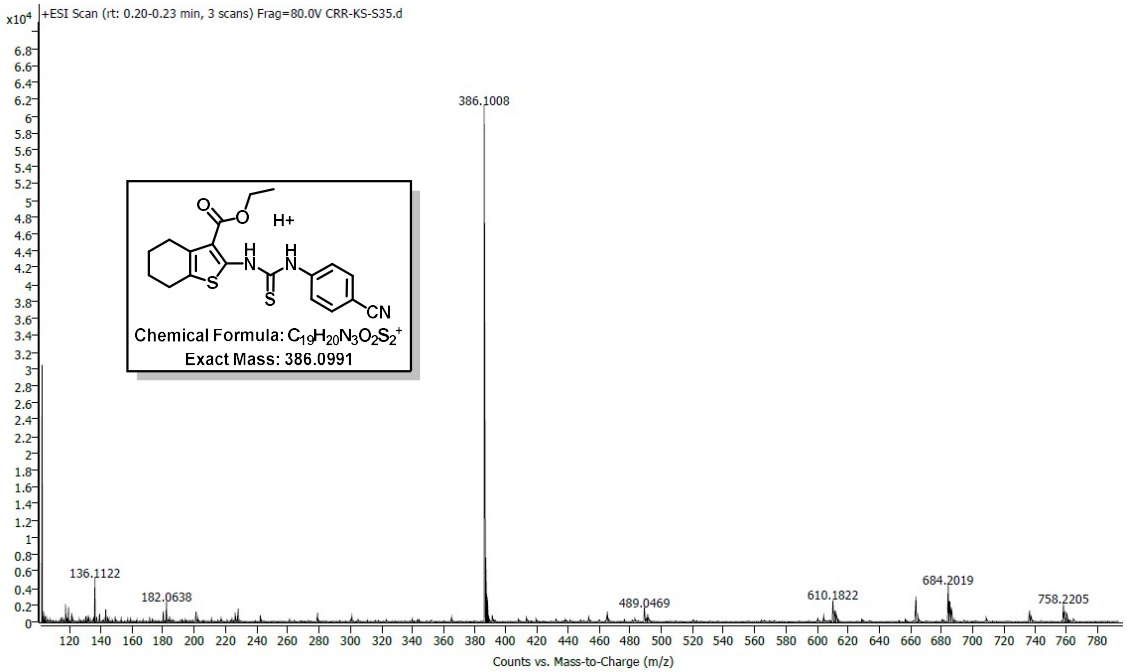

Figure S99. HRMS spectrum of **12c**.

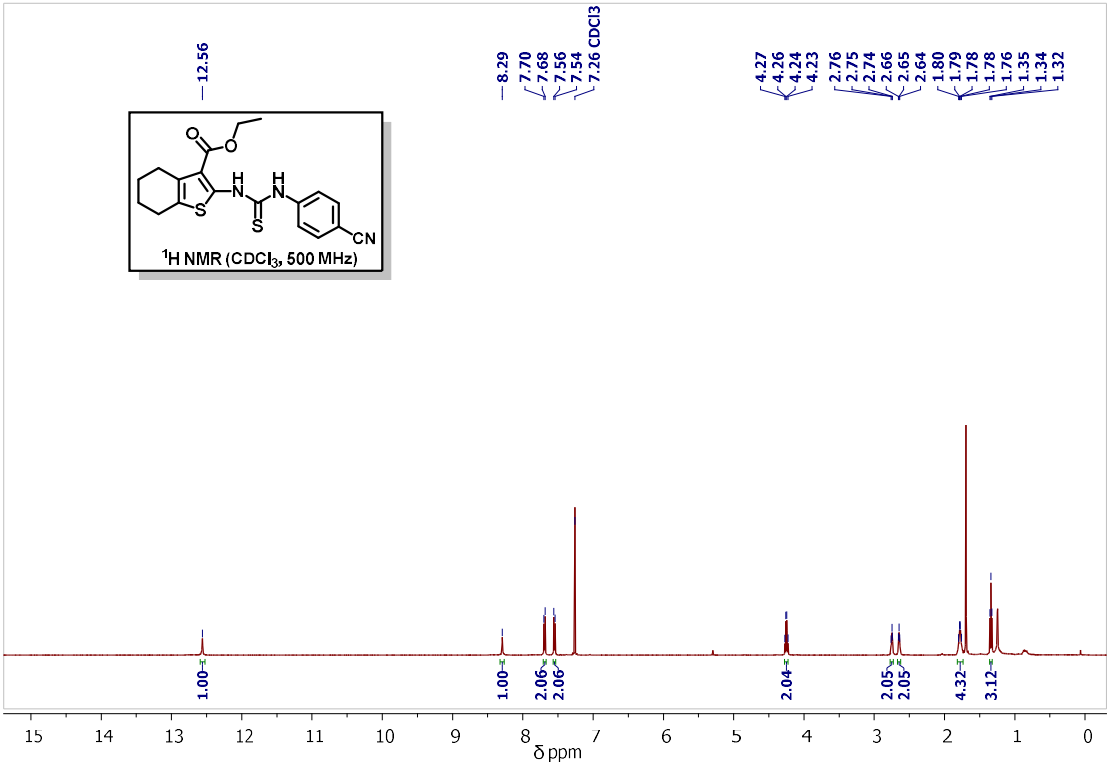

Figure S100. ^{1}H NMR spectra (500 MHz, RT) of compound **12c** in $CDCl_3$.

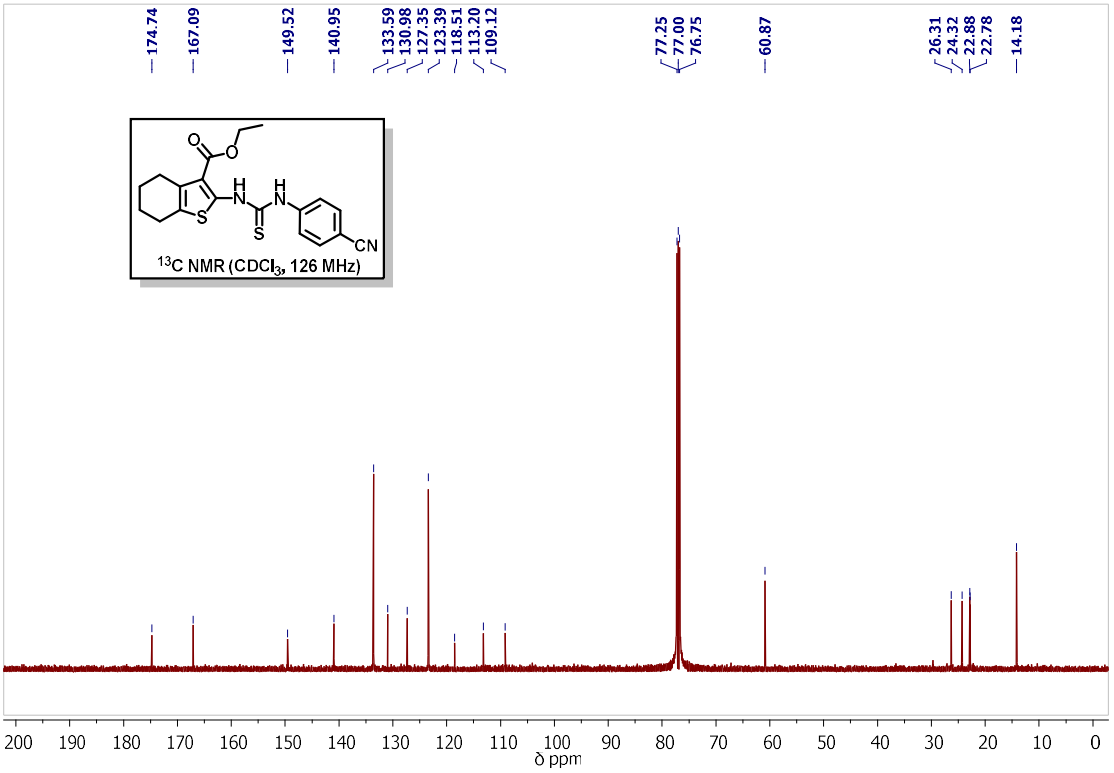

Figure S101. $^{13}C\{^{1}H\}$ NMR spectra (126 MHz, RT) of compound **12c** in $CDCl_3$.

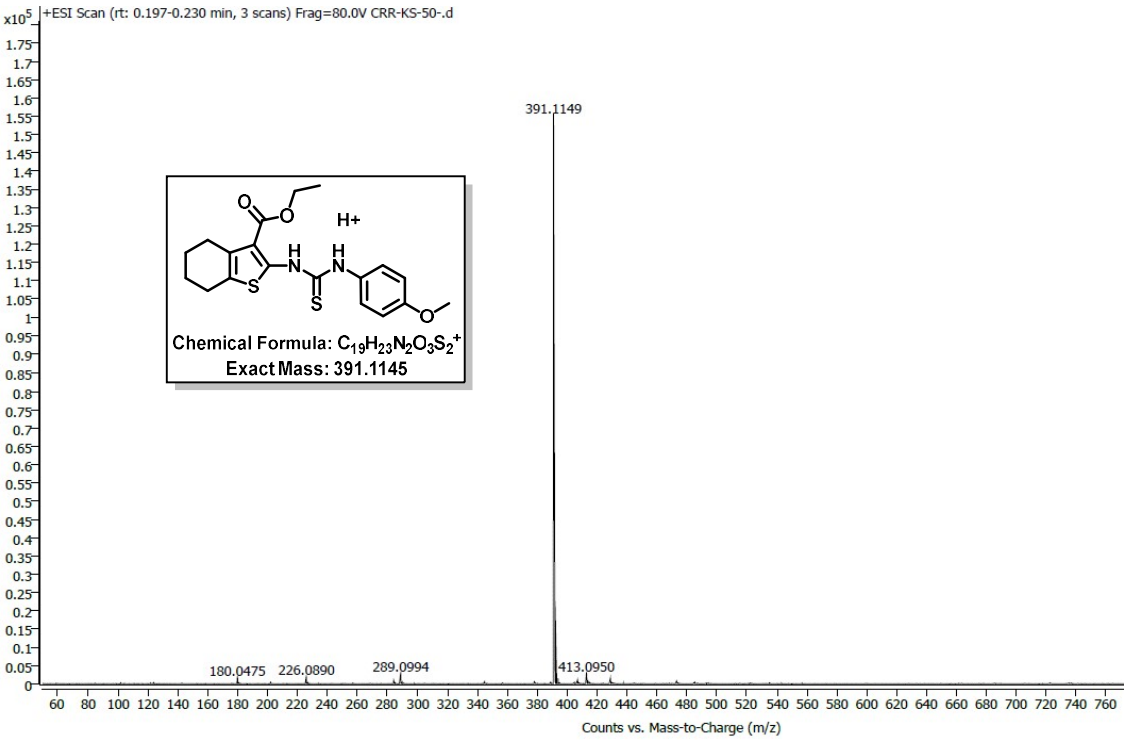

Figure S102. HRMS spectrum of **12d**.

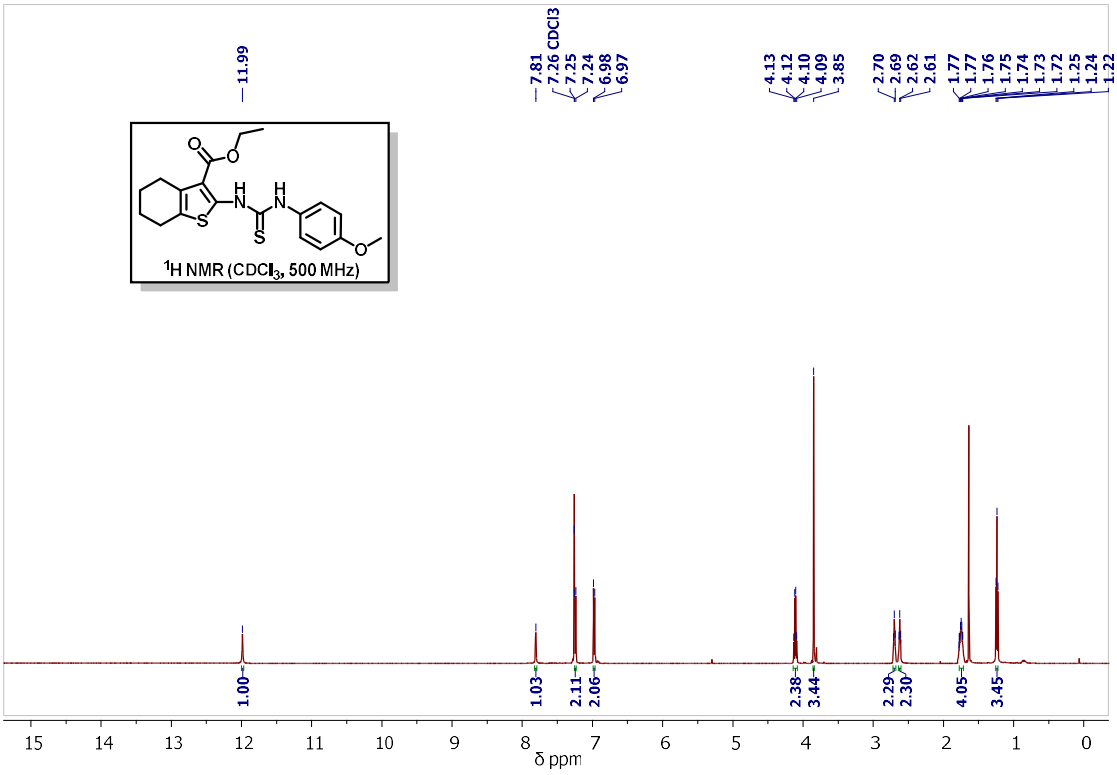

Figure S103. ^{1}H NMR spectra (500 MHz, RT) of compound **12d** in $CDCl_3$.

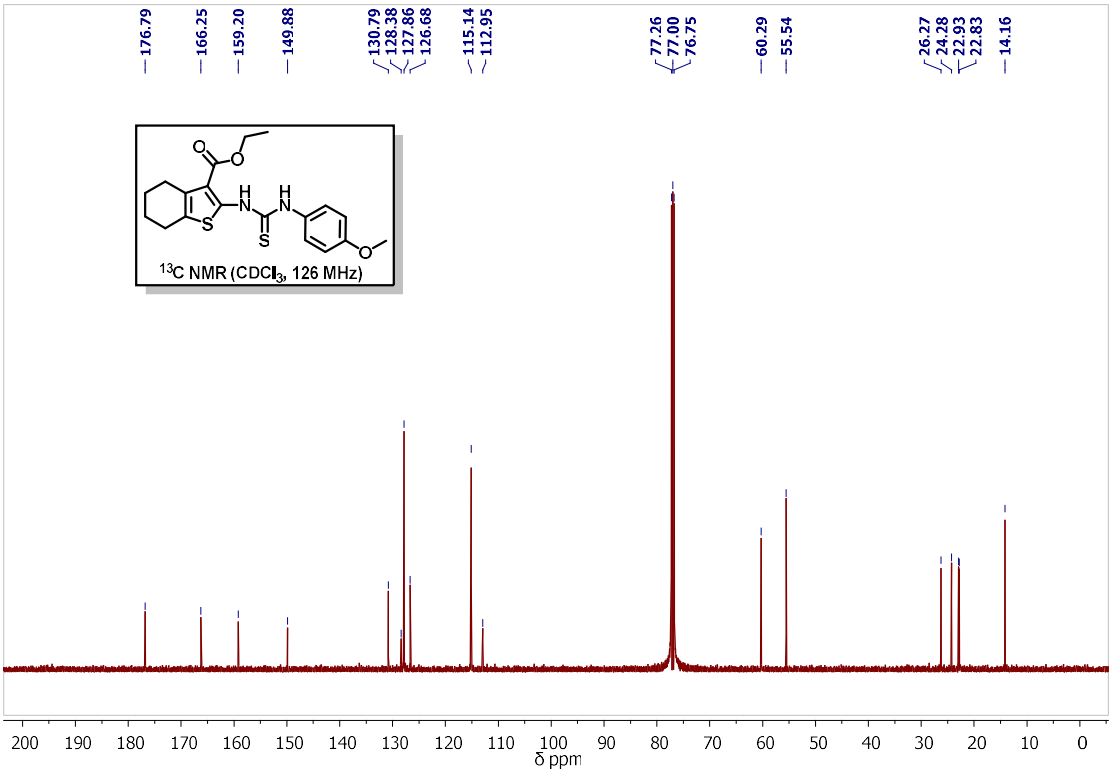

Figure S104. $^{13}C\{^{1}H\}$ NMR spectra (126 MHz, RT) of compound **12d** in $CDCl_3$.

3. References

1 Bruker, APEX3, SAINT and SADABS. Bruker AXS, Inc., Madison, Wisconsin, USA, 2016.

2 G. M. Sheldrick, A Short History of SHELX, *Acta Crystallogr. A, Found. Crystallogr.*, 2008, **64**, 112–122.

3 L. J. Farrugia, WinGX and ORTEP for Windows: An Update, *J. Appl. Cryst.*, 2012, **45**, 849–854.